KU LEUVEN

ARENBERG DOCTORAL SCHOOL
Faculty of Engineering Science

Event-Driven Demand Response for Electric Vehicles in Multi-aggregator Distribution Grid Settings

Klaas De Craemer

Dissertation presented in partial fulfillment of the requirements for the degree of Doctor in Engineering

July 2014

Event-Driven Demand Response for Electric Vehicles in Multi-aggregator Distribution Grid Settings

Klaas DE CRAEMER

Examination committee:
Prof. dr. Adhemar Bultheel, chair
Prof. dr. ir. G. Deconinck, supervisor
Prof. dr. ir. R. Belmans
Prof. dr. ir. Y. Berbers
Prof. dr. ir. C. Develder
(Ghent University)
Prof. dr. I.G. R. Kamphuis
(University of Technology Eindhoven)
dr. ir. B. Claessens
(VITO)

Dissertation presented in partial fulfillment of the requirements for the degree of Doctor in Engineering

July 2014

ISBN 978-94-6018-862-6

D/2014/7515/85

Abstract

In recent years, demand response has come under renewed research attention, as a tool to facilitate the integration of an increasing share of renewable but intermittent energy sources into today's electricity system. Intelligent demand response systems that manage flexible loads are able to aggregate consumers so that they can be represented collectively on the energy markets.

At the same time, there is the looming prospect of the electrification of transport, as car manufacturers are faced with stricter emission regulations. However, the introduction of charging electric vehicles at residential locations brings its own challenges, since distribution grids were never dimensioned for the coinciding activation of such large loads. Solutions are needed that safeguard the state of distribution grids and at the same time allow demand response using market objectives.

Following a description of the state of the art regarding intelligent charging of electric vehicles, an overview of existing algorithms that facilitate demand response is given. In a second part, situations where demand response poses problems for the distribution grid and ways to mitigate them using distribution grid congestion management and voltage droop control are elaborated on.

To be able to assess several such scenarios, a simulator has been developed that can simulate large groups of flexible loads, modeled as a multi-agent system, in a demand response setting. The simulator integrates with a load-flow analyzer, so that both the collective behavior at the energy markets and the technical limits occurring in distribution grids can be taken into account.

One demand response algorithm in particular, inspired by microeconomic principles, has favorable trade-offs between complexity, communication and optimality of control. This multi-agent market based control algorithm is applied to the problem of coordinated charging of electric vehicles. Several alterations are introduced. Besides adding scheduling functionality, the algorithm is implemented using events instead of time slots, while the use of caching reduces

the exchange of messages.

Eventually, two realistic scenarios are studied in more detail. First a Time-of-Use setting during which electric vehicles are coordinated by an aggregator that aims to find the lowest cost of charging for its fleet, and secondly a case where an aggregator manages a portfolio consisting of electric vehicles and wind generator, with the goal of minimizing 15 minute imbalance with nominated volumes under unpredictable wind output. To evaluate the impact on the distribution grid, vehicles charge along households inside several weak urban test grids. Consequently, the effect on the market objectives is tested by varying shares of vehicles located inside weak distribution grids in an aggregator's fleet, with or without voltage droop controllers. Eventually, the scenarios are extended to the case where multiple completing aggregators are active in the same distribution grids.

The results show that event-driven demand response for electric vehicles provides a suitable method for solving future demand response problems in a multi-aggregator distribution grid setting. An aggregate & dispatch-type algorithm may be suboptimal compared to some other solutions, but provides very good scalability and low complexity, which is beneficial for large-scale demand response implementations. Furthermore, considering the weak grid settings used here, the need for additional grid congestion management mechanisms beyond voltage droop control can be challenged.

Beknopte Samenvatting

In de laatste jaren is de toepassing van vraagsturing onder hernieuwde onderzoeksaandacht gekomen, als een middel om de integratie van moeilijk voorspelbare hernieuwbare energiebronnen in het electriciteitsnetwerk te verbeteren. Intelligente vraagsturingssystemen die flexibele lasten kunnen aansturen zijn in staat om een groep consumenten te aggregeren zodat ze collectief vertegenwoordigd kunnen worden op de energiemarkt.

Tegelijkertijd is er de opkomende elektrificatie van mobiliteit en transport, omdat autofabrikanten geconfronteerd worden met steeds stricter wordende emissienormen. De introductie van elektrische wagens die thuis opladen brengt uitdagingen met zich mee, aangezien distributienetwerken nooit gedimensioneerd werden op de samenvallende aanschakeling van dergelijk grote lasten. Daarom is er nood aan oplossingen die de goede werking van het distributienetwerk waarborgen en tegelijkertijd vraagsturing op basis van marktobjectieven mogelijk maken.

Na een beschrijving van de stand van zaken en de trends omtrent het intelligent laden van elektrische voertuigen, wordt een overzicht gegeven van bestaande algoritmes die intelligente vraagsturing mogelijk maken. In een tweede deel worden situaties besproken waarin vraagsturing problemen oplevert voor de werking van het distributienetwerk, samen met de mogelijkheden om dergelijke problemen tegemoet te komen. Er wordt kort ingegaan op het gebruik van netwerkcongestie beheer en spannings droop-controle.

Om een aantal situaties in detail te kunnen bestuderen werd een omgeving ontwikkeld die grote groepen van flexibele lasten onder vraagsturing kan simuleren als multi-agent systeem. De omgeving integreert ook met een load-flow implementatie, zodat tegelijkertijd de marktobjectieven van een aggregator en de technische limieten die optreden binnen een distributienetwerk in rekening gebracht kunnen worden.

Een algoritme voor vraagsturing in het bijzonder, dat is geïnspireerd op

microeconomische principes, heeft een interessante afweging tussen complexiteit, communicatie en de optimaliteit van de controle-acties. Dit multi-agent en marktgebaseerde controlealgoritme wordt toegepast op het aansturen van opladende elektrische voertuigen. Verschillende aanpassingen worden voorgesteld, en naast het toevoegen van planningsfunctionaliteit, wordt een event-gebaseerde implementatie uiteengezet in plaats van een benadering gebaseerd op tijdstappen. Het gebruik van caching laat verder toe om het aantal berichten dat wordt uitgewisseld met de ladende voertuigen drastisch te reduceren.

Uiteindelijk worden twee realistische scenarios in detail bekeken. Bij een 'Time-of-Use' objectief probeert de aggregator via vraagsturing de laagste energiekost te vinden om de voertuigen onder zijn beheer op te laden. Vervolgens wordt een situatie behandeld waarbij de aggregator een portfolio beheert bestaande uit ladende elektrische voertuigen en een windpark. Het doel van de aggregator is om de onbalans op kwartierbasis, die ontstaat door het verschil tussen voorspellingen en de realiteit zo goed mogelijk op te vangen. Om de effecten op het distributienetwerk te kwantificeren, laden de wagens op temidden huishoudelijke lasten en binnen enkele zwakke stedelijke netwerkconfiguraties. Het effect op de marktobjectieven met en zonder spanningsdroop-controle en voor verschillende gradaties van elektrische wagens in zwakke netten wordt nader bekeken. In een laatste stuk worden de scenarios uitgebreid met het geval waarbij concurrerende aggregators actief zijn in hetzelfde distributienetwerk.

Acknowledgements

Gedurende de laatste 5 jaar is mijn doctoraat een boeiende tocht geweest in de academische wereld. In het bijzonder heb ik de kans gehad om samen te werken met motiverende en enthousiaste mensen, die ik hier even wil vermelden.

Eerst en vooral wil ik mijn promotor en begeleider prof. Geert Deconinck bedanken voor de mogelijkheid dit doctoraatswerk te starten, eind 2009. Vertrekkend van een aantal relatief kleine onderzoeksprojecten in samenwerking met de industrie, kreeg ik de vrijheid om onderwerpen naar eigen en groeiend inzicht verder uit te diepen. Dit bracht mij niet veel later in contact met het onderwerp van gecoördineerd laden van elektrische voertuigen en het Intelligator-algoritme.

Verder wil ik ook de leden van de jury, Ronnie Belmans, Yolande Berbers, Chris Develder, René Kamphuis en Bert Claessens, bedanken voor hun interesse in mijn werk, het reviewen ervan, en het commentaar die de kwaliteit van de tekst ten goede kwam. Mijn dank gaat ook uit naar prof. Adhemar Bultheel, om de preliminaire en publieke verdediging voor te zitten.

Speciale dank gaat naar Bert Claessens van het VITO, voor de vele meetings in EnergyVille, zijn opbouwende kritiek, suggesties en de bereidheid om over alles en nog wat van gedachten te wisselen.

Ook mijn collega's en de professoren op ELECTA wil ik bedanken. ELECTA is een erg gedreven groep met bekwame onderzoekers. De ontspannen sfeer die er hangt en de discussies, tips en grappen tijdens pauzes hebben op hun manier ook bijgedragen tot het volmaken van dit doctoraatswerk. Iedereen apart bedanken zou een te lange lijst opleveren en de kans bestaat dat er iemand onterecht overgeslaan wordt. Bij mijn bureaugenoten wil ik mij excuseren voor de hoeveelheid onderdelen en allerhande die er in de werkomgeving rondslingerde.

Dit brengt mij bij het 'Soiree Pratique' team van de IEEE Student Branch Leuven. Het organiseren en opbouwen van de activiteiten was een welgekomen

afwisseling van de eindeloze reeks simulaties.

Als laatste bedank ik ook vrienden en familie. Mijn ouders zijn altijd een onzichtbare steun geweest en hebben mij alle kansen gegeven. Ook mijn vrienden mag ik niet vergeten, voor het onderhouden van een leven naast het onderzoek.

List of Abbreviations

AS	Ancillary Services
AMI	Automated Metering Infrastructure
ARP	Access Responsible Party
BEV	Battery Electric Vehicle
BMS	Battery Management System
CHP	Combined Heat and Power
EV	Electric Vehicle
EVSE	Electric Vehicle Supply Equipment
DC	Direct Current
DOD	Depth Of Discharge
DR	Demand Response
DSO	Distribution System Operator
ICE	Internal Combustion Engine
LP	Linear Programming
LMP	Locational Marginal Pricing
MAS	Multi Agent System
MBC	Market-Based Control
MPC	Model Predictive Control
MILP	Mixed Integer Linear Programming
PHEV	Plug-in Hybrid Electric Vehicle
PWM	Pulse Width Modulation
RTP	Real Time Pricing
SOC	State Of Charge
TCL	Thermostatically Controlled Load
ToU	Time-of-Use
TSO	Transmission System Operator
V2G	Vehicle To Grid
VUF	Voltage Unbalance Factor

Contents

List of Figures

List of Tables

Chapter 1

Introduction

1.1 Smart grids

Because of growing concerns about the environment, decreasing reserves of fossil fuels and government policies, the share of renewable electricity generation, such as wind and photovoltaic power, is steadily increasing. The International Energy Agency (IEA) predicts that by 2035, renewable sources will be responsible for 18% of the worldwide energy production [1]. However, most renewable sources are greatly affected by variability and limited predictability. Complicating matters further is the trend of *distributed generation*, and a shift towards the electrification of transport due to increasingly tighter emissions regulations, both of which strain the limits of distribution grids.

In response to aforementioned trends and problems, electricity networks are moving towards the concept of a smart grid. Central to a smart grid is the integration of modern communication technologies with power electronics, which enables extensive automation and monitoring of grid assets, beyond the possibilities of classic SCADA systems.

1.2 Demand Response

A smart grid infrastructure, besides other aspects, makes it possible for consumers to communicate with each other, energy suppliers and other parties. By exchanging information, consumption can be shifted or reshaped if this is

beneficial. Such use is commonly referred to as Demand Response (DR), which, according to [2, 3], is defined as:

> Demand response can be defined as the changes in electricity usage by end-use customers from their normal consumption patterns in response to changes in the price of electricity over time. Further, DR can be also defined as the incentive payments designed to induce lower electricity use at times of high wholesale market prices or when system reliability is jeopardized. DR includes all intentional electricity consumption pattern modifications by end-use customers that are intended to alter the timing, level of instantaneous demand, or total electricity consumption.

According to this definition, DR can be achieved using either price-based or incentive-based mechanisms:

- Incentive based mechanisms motivate participants to change their consumption pattern using rewards or discounts. Depending on the terms of the program, penalties could also apply if there is no response by the consumer or loads are not curtailed.
- Price-based mechanisms use a fluctuating rate instead of the currently common flat-rate tariffs. This variable price reflects the utility's cost of generating or purchasing electricity at a wholesale level at that specific time of the day. An example of real-time pricing is the usage of smart meters in California, where prices vary by season and time of day [4]. In its most simple shape, there are two time-of-use (ToU) blocks, peak and off-peak, with a high tariff during peak periods and a low tariff during off-peak time. In case of hourly or more quickly fluctuating prices, this is referred to as Real-time pricing (RTP). RTP customers are then informed about the prices on a day-ahead or hour-ahead basis.

In the era of market liberalization, price-based mechanisms such as RTP (Real-Time Pricing) are regarded as a good tool to stimulate energy efficiency, because prices are supposed to carry all the necessary information for the customers to choose between energy efficiency or more supply. Current research concerning DR is focused on large-scale DR of local devices, such as domestic appliances and electric cars.

Note that the use of DR requires the controlled devices to either be able to shift/reschedule their operation or have some form of storage to continue operation during interruptions. Such storage could be typically a battery, but also the hot water tank of a boiler. It also means that DR does not necessarily

reduce the total amount of energy used by the devices. Losses in the storage process can even increase the total energy usage.

Stakeholders and objectives

From the above description, it is apparent that a successful implementation of DR involves the interaction of multiple actors in the electricity system, with particular objectives:

- Consumers: A difference has to be made between small and large consumers. Large consumers can apply DR on industrial processes, sometimes with direct interaction from the TSO. Examples include cold storage in warehouses or electric arc furnaces. Very large consumers tend to pay for their connection capacity and peak load rather than the energy volumes. Some companies already offer DR services on smaller scale, such as [5] to CHP owners.

  DR for small, residential consumers is based upon the control of smart appliances, including refrigerators, heat pumps, boilers and battery storage, that are equipped with a control module. The consumer's motives for participating in a DR system are typically the potential cost savings through reduced energy usage or shift to off-peak hours, at the expense of little or no reduction in comfort. Eventually, consumers are interested in the service provided by the energy (such as cooling, light or heating), and not energy itself.

- Appliances: The economic feasibility of residential DR will largely hinge on the availability of affordable devices with built-in DR functionality. The benefits brought by automation and DR savings has to offset the cost of the necessary embedded control hardware. Furthermore, standardization plays an important role in the decisions of manufacturers to enter the smart appliance market. Devices that have large power requirements or energy storage capability, such as heat pumps and charging EVs, are the most interesting to equip with this functionality.

- DSO: The distribution grid operator is concerned with maintaining a stable operation and adequate power quality for its customers throughout the distribution grid. It has to make decisions whether certain locations need infrastructure upgrades (such as wiring and transformers) to cope with the evolution of load profiles or if the use of DR can postpone these investments. As the DSO is also responsible for metering, it plays an important role of middleman in the application of DR.

- Aggregator (also referred to as Energy Service Company or Energy Service Provider): This is a new role created by DR, following the concept of a Virtual Power Plant (VPP). As the energy shifting potential per individual customer is small and the markets require minimum bid sizes, it cannot be offered directly on the energy markets. Mediation through aggregation of all individual DR potential is needed, a role filled in by an aggregator. Depending on the contract between the aggregator and the clustered customers, the aggregated flexibility can be used to further its own objectives, e.g. minimizing the cluster's total energy costs, reducing uncertainty of a production portfolio or simply providing convenience services to the customers.

- TSO: The transmission system operator is responsible for grid stability on the transmission system level, by managing power flows and taking preventive actions through interaction with the energy markets. During the day, in order to prevent outages, reserve generating units are dispatched by the TSO such that, if a contingency were to occur, no drastic corrective action needs to be taken. The IEA has noted that this reserve capacity is gradually shrinking [6] unless new investments are made. With DR, a reduction of demand from such expensive electricity generating units can be achieved as loads can be shifted from peak to off-peak periods [7], leading to a more efficient utilization of the available infrastructure. This is referred to as ancillary services (AS). Sections 1.3 and 3.6 provide additional insight on the use of DR clusters as AS.

Besides these actors, the energy markets play an important role in the interaction between the different actors.

1.3 Ancillary services

In a well-functioning power grid, generation and load is balanced at all times by means of energy scheduling. Since deviations from the schedule can occur, additional mechanisms operating at short time-scales are in place. In the ENTSO-E (European Network of Transmission System Operators for Electricity), these are referred to as primary (0–30 sec.), secondary (30 sec.–15 min.) and tertiary reserves (> 15 min.), depending on their activation requirements. These are able to respond to contingencies like the sudden loss of a generator or transmission line (contingency reserves), the area control error (regulation reserves), the unexpected ramping of solar or wind generation sources (flexibility reserves) or voltage drops (reactive power and voltage control), and commonly referred to as ancillary services (AS) [8]. AS only involve small

amounts of energy, but are able to respond quickly and reliably to maintain balance in the power grid [9].

A demand response cluster is technically capable of providing ancillary services. In fact, curtailment of load through DR is usually a lot faster than ramping of e.g. thermal generators or hydropower plants. But the challenge lies in terms of the required response speed and accuracy, and the fact that contracted AS needs to be operational year-round, and not just during peak-hours.

1.4 Challenges & requirements

Demand response is not a new concept, all the technologies required for implementation have already been developed and applied before. Nonetheless, adoption has been very slow. This can be attributed to several remaining challenges [10]:

- **Information and Communication Technology (ICT) infrastructure** is not in place; especially for large-scale applications, communication and (embedded) hardware plays an important role. Participating devices send messages with their requirements or needs to an aggregator, while aggregators need a way to distribute the coordination instructions back to the devices in order the steer the cluster's power. Depending on the amount of intelligence, computing power and independence assigned or available in the devices, the weight of this aspect is either on the side of the aggregator or the devices.
- **Competitiveness** compared to traditional solutions: to economically justify DR, a costs versus performance trade-off has to be established. As mentioned in section 1.2, the expected benefits over the lifetime of a device should offset the cost of adding computing hardware. Thus, residential DR capabilities will likely be reserved to a few particular devices.
- **Complexity** is higher compared to traditional solutions. Of course, DR will always be more complicated than a *fit-and-forget* approach to counter increasing uncertainty of renewables. Hence a modeling and simulation environment is needed to test various approaches and their benefits before committing to a large-scale roll-out.

It follows that wide-scale application of DR requires low-cost, low-complexity, but scalable architectures and algorithms that take technical constraints into account.

1.4.1 Communication

In this work, we are mainly concerned with demand response of charging electric vehicles and the relation to the ICT infrastructure challenge. This entails challenges on two separate, but coupled, levels:

1. The **market operation** level entails actions with the objective of following beforehand traded volumes on the wholesale electricity markets, where trading takes place on relatively long-term scale (months, seasons) and amounts are expressed as energy quantities –usually MWh– in time slots of typically 1 hour or 15 minutes.
2. The **real-time operation** level entails the actions to comply with instantaneous consumer preferences and respect local grid constraints. Because changes and control are relatively more instantaneous and dynamic at this level, real-time operation (or technical operation) is usually expressed in terms of electrical power, e.g. kW. Granularity is in the range of minutes to seconds. At this level, fast responses are important and the number of exchanged messages will be limited.

In most of the literature, algorithms and their simulations are based upon the use of time slots, wherein time is divided into discrete intervals with a typical fixed length of one hour or sometimes 15 minutes. This division closely matches with aforementioned market operation, but imposes a limitation on response speed of the cluster. Plainly reducing the length of time slots is not optimal from a computational or communication perspective.

In order to realize large-scale field implementations it is desirable to be able to coordinate devices (charging vehicles but also other appliances) on a continuous timescale, as such systems operate asynchronously, driven by the occurrence of events rather than a central clock.

A central research question of this thesis then is how existing algorithms can fit into an event-based architecture, while limiting the messaging between members of the DR cluster. And, does this influence the aggregators' business case?

1.4.2 Market objectives versus grid congestion

In literature, the division between technical side and market side during the coordination of charging of EVs is often overlooked. A large part of research on integration of EVs is aimed at optimal coordinated charging from a market-level perspective, facilitating larger shares of renewable energy sources or providing

system-wide ancillary services. At the same time, a lot of work in literature has been carried out towards the use of EVs to avoid distribution grid overloads or reducing losses [11, 12], objectives that are situated in the technical operation level.

The market and technical level can come into conflict, which typically occurs when the distribution grid is constrained or overloaded, at which point the technical objectives will intervene in the market objective. As market operation is overruled, consumption will deviate from what is intended by the aggregator. This aspect is also discussed in [13, sec. 3B], where an "emergency brake" signal from the DSO would suspend all charging operations in a grid, and in [14, sec. 5.2.4], where a (physical) separation between market information (e.g. tariffs and incentives) and technical information (such as state variables of the distribution grid) is proposed.

One question to be answered is on what scale this conflict situation occurs. Or, how big is the impact of being overruled by technical objectives on the business case of aggregators?

1.4.3 Multi-aggregator situations

It is possible to conciliate the technical and market objectives by introducing additional grid congestion management mechanisms [15, ch. 6]. But do we have an indication that an additional, complicating layer is justified from a market level point of view, in particular when multiple competing aggregators are active within the same distribution grid?

The work of this thesis is specifically focused on the case of EV coordination, but the presented coordination mechanisms and results can to a large extent be translated to a more generic demand response perspective.

1.5 Outline & context

Chapter 2 gives a brief technical background on the charging of electric vehicles, together with a description of the current or upcoming options to establish communication between EV chargers and aggregators in a smart grid. The latter expands on previous work about smart metering communication standards [16, 17] and the SPARC project [18].

Chapter 3 presents an overview of algorithms or techniques that are relevant for demand response. In a second part, a more elaborate description of the Market Based Control (MBC) technique is given, and why it is used as the basis of the DR algorithm in this work.

Chapter 4 introduces the smart grid simulator framework that was developed in the context of this thesis. Also the models and the data sources used in the simulations are explained.

Chapter 5 describes how the Multi-Agent MBC is applied to the problem of electric vehicle charging, and how information on the future is incorporated to overcome the limitations of the original MBC algorithm regarding scheduling.

Chapter 6 discusses the modifications to the Multi-Agent MBC of chapter 5 so that it can function as an event-driven system. A large part of the work in this chapter is based on [19].

Chapter 7 goes on to validate the event-driven Multi-Agent MBC in a few straightforward market-operation scenarios. The part on the trade-off between the amount of communication and optimality of control is based on [20].

Chapter 8 introduces more realistic scenarios during which both technical and market level are taken into account. First, scenarios containing only a single active aggregator are looked at. In a second part, a second and competing aggregator is introduced.

Chapter 2

Electric Vehicles & Communication

In section 1.1, the electrification of transport was mentioned. Due to ever tightening emissions regulations for internal combustion engines (ICEs), car manufacturers have began offering vehicles with alternative drivetrain technologies, such as found inside electric vehicles (EVs), because these reduce or eliminate local greenhouse gas emissions.

A distinction is made between Hybrid Electric Vehicles (HEVs) and Battery Electric Vehicles (BEVs). Both contain a battery to power an electric motor, but a Hybrid Electric Vehicle also contains an internal combustion engine that can recharge the battery or operate as a range extender. BEVs and Plugin HEVs (PHEVs) are charged through the electric power system, which can lead to increased congestion of the grid. Especially the impact on the low-voltage grid can be significant, if the peak of arriving EVs that plug in to charge at home corresponds to the residential load peak [11, 21].

At the same time, while the charging of EVs requires a large amount of energy, vehicles tend to be stationary during long periods, for example during the night or working hours. This creates the opportunity to spread the charging of the batteries in time and thereby limit their impact on the distribution grid.
Coordinated charging of electric cars in a smart grid is an excellent application of large-scale DR of (domestic) appliances, and is the focus of a lot of current research. In this chapter, the technical context of EV charging is outlined, while in chapter 3, methods for DR using coordinated charging are discussed.

Table 2.1: Battery capacity of some contemporary EVs

	Type	Total battery capacity (kWh)	Note
Chevrolet Volt	PHEV	16.0	10.3 kWh usable (65%)
Toyota Prius Plugin	PHEV	4.4	3.4 kWh usable (77%)
Fisker Karma	PHEV	20.0	
Ford C-Max Energi	PHEV	7.6	
Volvo S60 Plugin	PHEV	12.0	
Honda Accord Plugin	PHEV	6.7	
Mitsubishi Outlander	PHEV	12.0	
Mitsubishi iMIEV	BEV	16.0	
Nissan Leaf	BEV	24.0	20∼22 kWh usable (80∼90%)
Smart electric drive	BEV	16.5	
Volvo C30 DrivE Electric	BEV	24.0	22.7 kWh usable (94%)
Ford Focus Electric	BEV	23.0	19∼20 kWh usable (85%)
BMW i3	BEV	22.0	18.8 kWh usable (85%)
BMW ActivE	BEV	32.0	
Renault Fluence ZE	BEV	22.0	
Renault Zoe	BEV	22.0	
Volkswagen e-UP!	BEV	18.0	

2.1 Charging of EVs and limitations

The charging process of an EV is primarily determined by the properties of its battery pack. Currently commonly used battery types for (PH)EV applications are NiMH (such as the Toyota Prius) and variants of Li-ion (Tesla Model S: $LiNiCoAlO_2$, Chevrolet Volt and Nissan Leaf: $LiMn_2O_4$). The battery size of some contemporary EVs is shown in Table 2.1.

Because of concerns for accelerated degradation, battery cells are not used between 0 and 100% of their potential energy storage capacity, as state-of-charge (SOC) levels close to empty and full put the highest strain on the cells. The Chevrolet Volt, for example, limits the usable capacity to within 65% of the total battery pack's content.

During charging, and at high SOC states, the amount of current that can be "sinked" into the pack is limited by the maximum voltage that can safely be applied over the cells [22]. If a cell is overvolted, chemical reactions start to occur that can permanently damage the cell. As a consequence, a high SOC also hinders brake energy recuperation. Similarly, a cell voltage that is too low leads to a progressive breakdown of its electrodes.

Because of the aforementioned risks, the charging process is controlled and guarded by a Battery Management System (BMS). During charging, a BMS will vary power depending on the SOC [23, 24]. Typically, there is a constant-

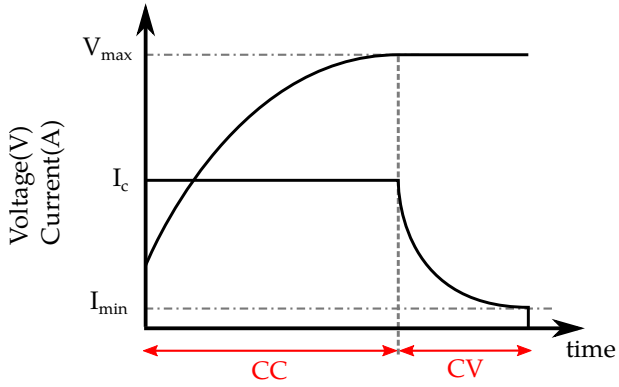

Figure 2.1: Lithium battery charging current and voltage profile versus time during CC-CV charging

current (CC) and a constant voltage (CV) phase, pictured conceptually in fig. 2.1. During CV mode, charging power decreases quickly and the amount of energy that is added to the cell during this phase is relatively small.

Vehicle-to-Grid

In case of vehicle-to-grid (V2G), vehicles are not only able to vary charging power, but also to inject power back into the grid. This can be beneficial for both the utilities and the grid [25, 26, 27, 28], but considering the reluctant stance of both manufacturers (battery wear concerns [29]) and DSOs (disruption of passive role of distribution grid)[30], V2G is not expected to be widespread in the near future.

2.2 Standardization efforts

To further the acceptance of electric vehicles, there is a need for common charging plugs and modes so that a vehicle can be charged anywhere without worry about incompatibilities between manufacturers. This is highlighted by the European standardization mandate M468 to CENELEC [31].

The main focus of EV charging in Europe centers around IEC standard 62196 [32], *Plugs, socket-outlets, vehicle connectors and vehicle inlets -*

Conductive charging of electric vehicles, and IEC 61851 [33], *Electric vehicle conductive charging system*, whereas in the US, SAE J1772 takes this role.

2.2.1 IEC charging modes

IEC 62196 defines plugs, socket outlets, vehicle connectors and vehicle inlets. It references the charging modes in IEC 61851-1. Table 2.2 gives an overview of these different modes of charging.

- Mode 1 provides basic charging capabilities for domestic use, such that standard electrical plugs and outlets can be used. Current in this mode is at most 16A, meaning that for a single phase connection, charge power is limited to ∼3.3 kW.
- Mode 2 allows for higher charge currents, but imposes additional safety measures on the vehicle port and charging cable. A *control pilot* (CP) pin in the charging cable or in-line control box and the vehicle's charge connector is used to indicate the maximum charge current supported by the cable. The operation of the CP pin is described in IEC 61851-1, which is briefly reviewed in the following section. Detection for proper earthing is also required.
- Mode 3 defines (fast) charging using an AC connection up to 55 kW and requires the use of dedicated EVSE (Electric Vehicle Supply Equipment), such as a wallbox. The requirement of a *proximity pin* (PP) with a shorter length ensures that a sudden disconnection or interruption is detected and the cable becomes unpowered.
- Mode 4 describes fast charging using DC, with an external charger. Work on standardization of DC charging is underway in IEC 62196-3.

Due to the limitations of typical residential electrical installations, charging at home using a single phase connection is limited to 16 A or 3.3 kW. With dedicated wiring, this could be extended up to 32 A or 6.6 kW, although such current is close to a household's fuse rating of 40 A. Thus, Mode 1 and Mode 2 charging will remain the dominant charging mode in residential environments.

2.2.2 Charging connections

Beside the different charging modes, standardized connectors for EVs are needed. Currently, the following plugs are in use:

Table 2.2: IEC 62196 charging modes

	Slow charging		**Fast charging**	**Fast charging DC** (offboard charger)
IEC Mode	Mode 1	Mode 2	Mode 3	Mode 4
Power	≤16A; 250V 1ph or 480V 3ph	≤32A; 250V 1ph or 480V 3ph	≤250A; 250V 1ph or 480V 3ph	≤400A DC
Signaling	None	Control pin on vehicle	Control & signal pins with EVSE	Control & signal pins with EVSE
Suitable plugs	Type 1, Type 2, IEC 60309 16A, Standard socket	Type 1, Type 2, IEC 60309 32A	Type 2, Type 3, IEC 60309 32A (limited)	Several proposals: Chademo , Type 2 Mode 3, SAE J1772 Combo, ...

- *IEC 62196-2 Type 2 "single and three phase vehicle coupler and mains plug and socket-outlet without shutters"*: This connector is manufactured by the German company Mennekes. When plugged in, a mechanical interlocking mechanism prevents disconnection during charging. It has become the most common connector on EVs in Europe, besides the well-known CEE 7/4 "Schuko" and derived CEE 7/7 plugs. Obviously the latter do not foresee vehicle-EVSE communication and are limited to 16A. A future extension to the 62196-2 standard allows for DC fast charging over this plug, and since the beginning of 2013, a version with shutters is also available to meet certain countries' regulations [34].

- *Chademo*: This is a DC fast charging system developed by TEPCo, Nissan-Renault and Mitsubishi, and later brought into the Chademo Association. Currently, it is the most dominant fast-charging connection, but it offers no features to control the charge rate from the grid-side nor can it be used for 'slow' charging. Besides Nissan and Mitsubishi, no major car manufacturer is backing Chademo and with the European Parliament [35] actively supporting the Combined Charging System (CCS) standardization, it can be expected that Chademo will be phased out in the coming years.

- *Tesla "Supercharger"*: A proprietary DC fast charging up to 120 kW, for the Tesla Model S sedan. An adapter to plug into Chademo charging stations is available.

- *Combined Charging System* or Combo2: The standardization of a fast charging connector in Europe is still ongoing. In the US, a unifying AC-DC charging connector [36] was proposed in 2010, in cooperation with the SAE and IEEE-SA. The combo connector on the vehicle side offers enough room for a IEC Type 1 or Type 2 connector, together with space

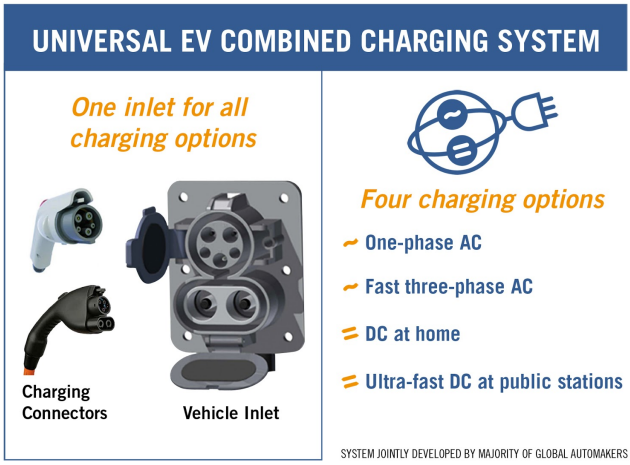

Figure 2.2: "Combo" Combined charging system (*electric-vehiclenews.com*)

for a two pin DC connector allowing up to 200A. It is shown in fig. 2.2. Many automakers have agreed to use this combo connector.

All of the above plugs and sockets, with the exception of the CEE "Schuko" plug, are designed to allow communication between the EV and the grid equipment, which is discussed in the next section.

2.3 Vehicle-grid communication

From section 1.4, it is apparent that communication between the vehicle and other actors (such as the aggregator) is needed to transfer charge power settings and schedules, illustrated in fig. 2.3. An overview using early standards can be found in [37]. The relevance of IEC 62196 with regard to a vehicle-grid communication interface is limited to the physical interoperability in terms of signaling pins and connector compatibility.

2.3.1 EV and EVSE signaling

IEC 61851-1 defines a low level signaling protocol over the control pin (CP), that was initially defined in the 2001 version of the SAE J1772 standard.

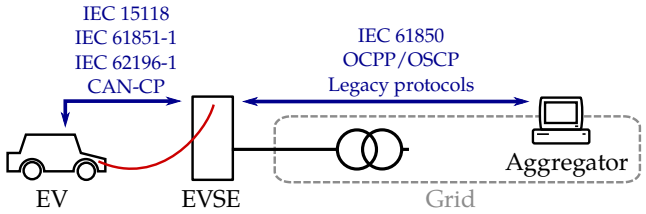

Figure 2.3: Vehicle-grid communication

Table 2.3: IEC 62196-1 EVSE-to-EV current capabilities

PWM Duty cycle	Max current
5%	Determined by higher level protocol
10% to 85%	6 A to 50 A
85% to 95%	51 A to 80 A

EVSE to EV

Signaling from the EVSE to the vehicle is performed using a 1 kHz PWM signal, from which the duty cycle is varied to indicate the current capabilities of the charging station. In the original 61851-1:2008 version of the standard, the signal's duty cycle can be linearly varied between 10% (6 A) to 85% (50 A) [38]. To support faster charging, the 2010 version extends this range to 95% to allow up to 80 A.

Additionally, a duty cycle of 5% indicates that a higher level protocol, such as IEC 15118, is to be used. Table 2.3 summarizes the EVSE-to-EV signaling. The standard requires that after a change in current capability, the EV complies within 5 seconds and that both PWM signaling and a higher level protocol can be used concurrently.

EV to EVSE

The EV can also send state information to the EVSE by switching load impedances between CP-PE (Control pin, Protected Earth) [39]. The EV's charger can indicate whether it is ready for charging or that ventilation is required during the charging process. Table 2.4 shows the possible states.

Table 2.4: IEC 62196-1 EV-to-EVSE state signaling

CP-PE Voltage	State
12V±1V / open	Standby & cable unpowered or Mode 1 16A charging
9V±1V / 2.7kΩ	Mode 3 EV connected, no charging
6V±1V / 880Ω	Mode 3 EV ready for charging
3V±1V / 240Ω	Mode 3 EV ready for charging, ventilation required

Cable power indication

In case of Mode 2 charging, it is possible to use 'separate' (meaning not permanently fixed to the EVSE) cables and adapters. To avoid the use of inadequate cables, a resistance value between the PP-PE pins (Proximity Pin, Protected Earth) indicates the maximum rating and cross section of the cable.

2.3.2 Advanced protocols

IEC 15118

In order to support more sophisticated EV charging applications, ISO and IEC started the Joint Working Group 15118 in 2009. The goal is to enable features like identification, payment, load leveling and value-added services (*EN15118-1, section 5.2, General considerations*). IEC 15118 uses a set of Open Systems Interconnection (OSI) Layer protocols for the communication between the EV and EVSE, completed with a set of application layer messages between the EV and EVSE. The latter are based on XML, and authentication is performed through the use of certificates. Communication between EV and EVSE is also encrypted with Transport Layer Security (TLS).

For the physical layer, IEC 15118 is based upon the use of Power Line Communication (HomePlug GreenPHY or G3 PLC) over the Control Pilot wire. The use of these options is described in IEC 15118-3.

The final specification has not yet been published, but the relevant parts regarding DR are described in *Use case 7.6.2: Optimized charging with scheduling from the secondary actor* and *Use case 7.6.3: Optimized charging with scheduling at EV*. Relevant to this work are the parts that describe a way to apply an externally determined charge schedule or a locally determined one, by the EV itself (e.g. based on a tariff table). Pausing and resuming of charging schedules is also mentioned.

CAN-CP

In the third edition of IEC 61851-1, expected in March 2014 [33], an annex D will be added that extends the functionality of the control pilot (CP) wire for point-to-point communication between EV and EVSE. Beside the signaling protocol, it describes the (optional) use of a bidirectional half-duplex CAN bus (Controller Area Network) on the CP line [40]. A few different modes are listed, such as basic CAN, advanced (using the CANopen protocol) and encapsulated IP (eIP). Data rates are modest, up to 500 kbps for the advanced and eIP mode. During CAN communication, the PWM signaling has to be interrupted.

As opposed to IEC 15118, the CAN-CP addition does not specify the application layer messages, but the use of eIP could allow the vehicle to e.g. directly access the internet and connect to external services.

2.3.3 EVSE to external actors

The upcoming IEC 15118 standard explicitly does not specify how the communication between the EVSE or charge pole and a backoffice (e.g. an aggregator that coordinates the charging of a whole fleet) should take place. A few efforts have started in this area, with the most noteworthy the Open Charge Point Protocol (OCPP) and IEEE P2030.1.

OCPP

OCPP is used by the E-laad.nl foundation to facilitate roaming between operators of public charge poles and is published as a free and open standard. The promotion of OCPP is now brought under the wings of the Open Charge Alliance [41]. The Open Smart Charging Protocol (OSCP) is an extension for OCPP developed by Enexis and GreenFlux that facilitates interaction between the DSO and a charge pole operator [42]. It is intended to allow the DSO to allocate capacity for the charging of EVs, that can then be distributed among the active charging operators.

IEEE P2030.1

IEEE P2030.1 currently has the title *Draft Guide for Electric-Sourced Transportation Infrastructure* [43]. It is not a standard defining a communications protocol itself, but rather "provides guidelines that can be used by utilities, manufacturers, transportation providers, infrastructure developers and end users

of electric-sourced vehicles and related support infrastructure in addressing applications for road-based personal and mass transportation."

2.3.4 Suitability for DR of EVs

In case of using vehicles for DR, varying the duty cycle of the PWM signal of section 2.3.1 can be used to change the charging power, as illustrated by a project of REstore and EDF where 150 EVs were used for load balancing [44]. However, this was not the intended application of the signaling protocol, and it can lead to undefined behavior, as some chargers do not tolerate switching power-levels often or being forced to charge at very low power. Furthermore, it can take up to 5 seconds before the EV applies a new charge setting, and there is no guarantee that the charger will not refuse the power level and stop charging altogether.

IEC 15118 is currently the only open standard that specifically addresses the use of EVs for coordinated charging in its use cases, but since this standard is not yet finalized, it is difficult to estimate the extent of its potential.

2.4 Conclusion

This chapter discussed the situation surrounding, and the standardization of, electric vehicle charging in Europe. The IEC 62196-2 Type 2 connector is quickly becoming the default solution for AC charging up to 32 A, while for fast charging, the Chademo is regularly used. However, it is not an official IEC or SAE standard and car manufacturers are looking at a unifying AC-DC (fast) charging connector, called CCS.

Due to the limitations of typical residential electrical installations, charging EVs at home using a single phase connection is limited to 16 A or 3.3 kW, unless dedicated wiring is added.

Since compatibility issues regarding the charging connections are now gradually resolved, attention is shifting towards enabling high-level communication between EVs and external services, which is needed for efficient implementation of DR. At the moment, IEC 62196-1 allows for simple signaling from and to the vehicle to determine and change the charging power, but more advanced solutions are essential to allow EVs to participate in large-scale DR systems. The upcoming IEC 15118 will address this kind of applications.

In the next chapter, a number of algorithms from literature for the optimization and coordination of demand response clusters will be discussed and classified.

Chapter 3

Algorithms for Demand Response of Electric Vehicles

The goal of a demand response algorithm is to find an as-optimal-as-possible schedule for a group of devices, referred to as a cluster, satisfying their individual but also global constraints, and then effectively control them. The use of global constraints implies an objective with coupled constraints. More specifically, the objective of an aggregator of a cluster of customers could be to minimize a certain objective function $f(\mathbf{x})$, e.g. expressed as energy cost and in function of each customer's power P_i, but with the global constraint that power for the cluster as a whole $\sum_i P_i$ at any time is limited to a fixed value P_{lim}. This is exemplified by (3.1).

$$\begin{aligned} &\min \quad f(\mathbf{x}) \\ &\text{with} \quad g(\mathbf{x}) \leq 0 \end{aligned} \tag{3.1}$$

for example with:

$$\mathbf{x} = \{P_1, P_2, ...P_n\}$$

$$g(\mathbf{x}) = \sum_{i=1}^{n} P_i - P_{\text{lim}}$$

At that point, the customers can no longer choose their individual power setting P_i independently from each other. In contrast, a mechanism where for example a price signal is distributed one-way to all consumers, which then decide for

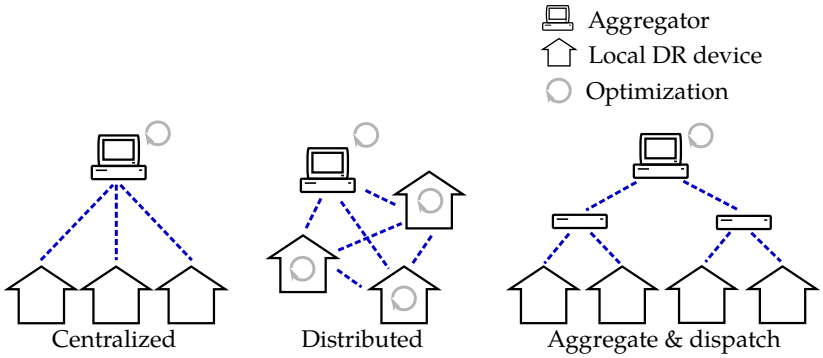

Figure 3.1: Illustration of the three classes of algorithms and coordination for DR

themselves how much or when to consume, does not have coupled constraints and is relatively easy to solve.

In this chapter, a selection of algorithms from literature for the optimal control of demand response clusters is presented, after which the decision to proceed with one system in particular is explained. In a second part, algorithms related to distribution grid constraints and services are briefly discussed.

Classification

Current research regarding the optimization and coordination of clusters of DR participants can roughly be divided according to the way the optimization is performed; distributed, centralized and aggregate & dispatch algorithms, as illustrated on fig. 3.1.

Distributed algorithms perform a significant part of the optimization process of allocating energy over the cluster at the participating devices themselves. This way, the computational complexity of finding a suitable solution is spread out over the demand response cluster, typically using an iterative process where information is communicated between the participants. However, the distributed aspect does not exclude the existence of an entity responsible for initiating or coordinating the convergence over the iterations. Additionally, while possible, the implementation of a distributed algorithm is not necessarily in a peer-to-peer-style fashion, as would be suggested by fig. 3.1.

Centralized algorithms are entirely the opposite. A central actor collects information that is sent to it from the DR devices. This information can consist of individual constraints and deadlines or comfort settings. Using the

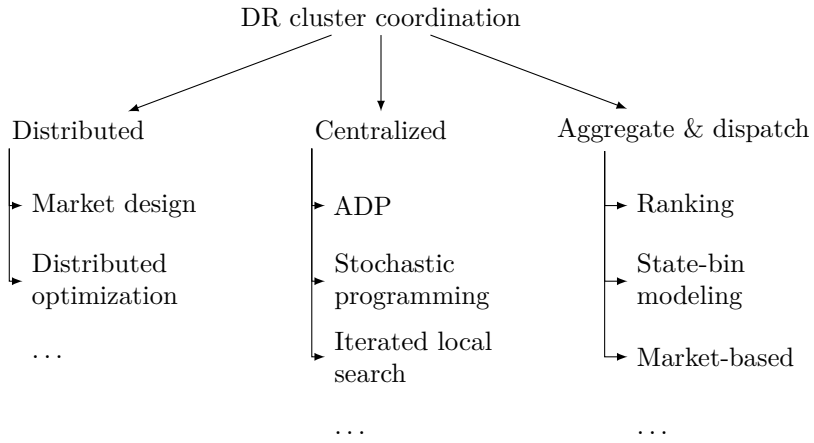

Figure 3.2: The three classes and some of the discussed algorithms

collected knowledge, and possibly including its own additional information such as predictions or stochastic functions, the central coordinator can perform a single optimization that returns an optimal schedule satisfying all the constraints at once. Inherently, this makes centralized algorithms the least scalable, as the optimization process quickly becomes intractable with an increasing number of participating devices. Furthermore, the communication towards and from a single point poses a potential bottleneck. Several solutions are proposed that help to overcome the tractability issue.

Inbetween distributed and centralized mechanism are the **aggregate & dispatch**. They decouple the optimization of the objective and the dispatch of its outcome, thus alternatively the term **dispatching mechanism** is equally fitting. An aggregate & dispatch mechanism allows information (such as constraints) from and to the central entity to be aggregated, reducing the complexity of the optimization and improving scalability, but carrying certain compromises or constraints regarding the optimality of the results.

Multi-agent systems

A returning concept in the design and implementation of DR algorithms is that of multi-agent systems (MAS). According to [45, p. 5], agents and multi-agent systems can be described as follows:

> An agent is a computer system that is capable of independent action on behalf of its user or owner. In other words, an agent can figure out

> for itself what it needs to do in order to satisfy its design objectives, rather than having to be told explicitly what to do at any given moment.
> A multi-agent system is one that consists of a number of agents, which interact with one another, typically by exchanging messages through some computer network infrastructure. In the most general case, the agents in a multi-agent system will be representing or acting on behalf of users or owners with very different goals and motivations. In order to successfully interact, these agents will thus require the ability to cooperate, coordinate and negotiate with each other, in much the same way that we cooperate, coordinate and negotiate with other people in our everyday lives.

In a DR system, we have a collection of users with their own objectives (minimizing energy cost or losses, maximizing comfort ...) that cooperate with each other and/or an aggregator. Since the actors involved are capable of taking autonomous decisions (up to varying degrees) in the DR cluster, they can be represented by agents inside a multi-agent system.

3.1 Distributed DR algorithms

Algorithms under the distributed category share the common trait that the computation of the DR scheduling problem is spread out over the participating devices. In the first section, 3.1.1, two methods are discussed that are often used and rooted in distributed optimization, while in section 3.1.2, game theory is used as a starting point, to prove the system's fairness.

3.1.1 Distributed optimization

One share of distributed algorithms in literature is based around distributed optimization techniques, in which a large optimization problem is divided in smaller parts that can be iteratively and independently solved. In particular the use of gradient ascent methods and its derivatives are common.

Dual decomposition

The work of [46, 47] deals with optimal energy scheduling for load control of residential loads. A utility company, taking the role of aggregator, sends pricing signals to the participating residences e.g. via an Advanced Metering Infrastructure (AMI). In order to minimize the electricity bill and maximize the end-user satisfaction, the smart meters adjust the power consumption profile of the various residential electric devices based on the pricing signals.

Each residential end-user has two classes of adjustable loads, in addition to a storage device. Devices belonging to the first class have to consume a specified amount of energy within a certain scheduling horizon, but the consumption can be spread over different slots in time. Charging PHEVs are mentioned as an example. The second class of devices have adjustable power consumption without a total energy requirement, but reducing power below the nominal point results in user dissatisfaction. An example of such a device is an airconditioner or space heater.

The objective of the scheduling is to maximize social welfare, represented by a combination of the cost of electricity, which is known in advance, and user satisfaction functions. Total power consumption of the cluster of devices is constrained in order to safeguard reliability of the distribution grid. The resulting multi-residence load control problem can be solved using Lagrange multipliers and is separable, meaning that the objective and the constraints comprise sums of functions that depend only on some optimization variables. Furthermore, it is shown that the Lagrange multipliers can be interpreted as

the price charged from the utility company at each time slot. From a high-level view, simple optimization tasks are assigned to the residences and the utility company, which are coordinated through AMI signaling to obtain the jointly optimal schedule. Essentially, the utility company broadcasts a price schedule to the residences' smart meters, which in turn optimize their consumption and storage schedules based on this information. The planned consumption schedules are then sent back and a new price schedule is determined until all constraints are met and convergence is reached.

Additionally, [46] shows that convergence is still reached when messages to or from the residences are lost and outdated information has to be used. However, while the use of *primal averaging* relaxes the requirements on the objective, the proposed method can only be used with convex cost or utility functions. Should the cluster contain devices whose utility is, for example, represented by a discrete on/off function, convergence is not guaranteed, as the individual residences' schedules can start to oscillate [47, 48].

Each time the consumption schedule is optimized, a number of iterations is performed, typically in the order of 50-500, during which messages travel from the aggregator to each smart meter and back. Depending on the network capacity, message cost, and delay and time slot interval, communication could become a bottleneck.

A variation of this approach can be found in [49].

In [50], dual decomposition is applied in a distribution grid setting with two energy providers and a DSO. During a first iteration, the energy providers make an estimate of the energy cost at each time step. Subscribers proceed by optimizing their planned consumption for the given price and send this information back to both the energy providers and DSO. Next, energy providers again update their price and the DSO assigns a price for using the network during critical situations. It can do this by approximating the influence of active power of each customer at each connection point in the distribution grid.

The iterative process will converge to the optimal solution, typically in about 50 steps, at which point the end-users adapt their consumption. In the preliminary iterations the planned consumption is communicated for the given price, but the consumption is not actually adopted. One iteration consists of a price update from the energy providers and DSO, the latter corresponding to a form of Locational Marginal Pricing (LMP) for the use of the network or individual phases, followed by a response of all the customers.

Alternating Direction Method of Multipliers

It is possible to improve the dual decomposition method so that it has a more robust convergence and no strict convexity of the objective is required, using the method of multipliers [51, ch. 3] (ADMM). This is beneficial in order to avoid oscillations when the cluster contains devices whose utility functions are discontinuous or stepped, for example in case devices can only turn on or off, but even with ADMM there is still no guarantee of convergence.

A separable, special formulation of the method of multipliers is the *exchange problem* [51, p. 58]. Essentially, the optimization is split into two steps. By adding a *proximal regularization term* to the optimization performed by the residences, the latter are incentivized to comply with the coupled constraints and congestion in one time period is avoided. The proximal term contains the deviation from the average of the last iteration's schedule and is broadcasted to all residences at the start of an iteration. After all the optimized schedules from the residences have been collected, the average is updated again and a new iteration commences.

While the ADMM method has improved convergence over DD, it increases the amount of data that has to be sent to the residences in every iteration, and is slightly more computationally intensive (due to a quadratic norm in the objective).

3.1.2 Game theory

In [52], a distributed DR algorithm is proposed, but this time starting from game theory to guarantee that the system is fair. Thus, besides convergence and optimality, the author tries to prove the following question:

> Is it beneficial for a user or a group of users to cheat and announce an incorrect energy consumption schedule to the other users?

The scheduling problem is formulated as an energy consumption scheduling game, where the players are the users and their strategies are the daily schedules of their household appliances and loads. Every household has a smart meter with Energy Consumption Scheduler functionality (ECS) that can perform optimizations and control the local appliances or a charging EV. All households in the distribution grid and the utility company are interconnected in a Local Area Network.

The utility company (referred to as the energy source) starts providing energy cost signals to the households, for example once a day. Then it selects random

households in a round robin fashion. Once selected, the ECS performs an optimization, broadcasts his planned consumption schedule to all other ECS's in the LAN. Upon receiving a schedule from another ECS, it is incorporated in a vector containing the daily scheduled energy consumption of all other users. Eventually the energy source is notified of when the selected ECS has finished its iteration and the procedure continues until convergence is reached, meaning no more schedule updates are announced. The authors prove that the system converges to a Nash equilibrium. Or, any behavior by a user which results in a deviation from the optimum will also harm the cheating user from a cost perspective, thereby deterring users from any malicious behavior.

The objective of the optimizations are minimizing the Peak-to-Average (PAR) inside distribution grid segment and energy cost for all consumers, by determining the optimal allocation of each appliance. Energy cost is represented by a strictly convex and increasing function, indicating the cost of generation at each hour of the day. A quadratic cost function for thermal generators is used.

It is not clear why the authors claim that user privacy is of no concern in this approach, as the daily schedule is still broadcasted to all others in the LAN, including the utility company.

3.2 Centralized DR algorithms

In centralized algorithms, a single entity is responsible for the optimization of the DR cluster's schedule. The major advantage of this approach is the ability to model each appliance individually, and the efficient application of techniques such as stochastic optimization, machine learning or prediction (which does not work as well when applied at each device separately, as opposed to an aggregated group). Since this becomes computationally very demanding when hundreds or thousands of appliances are involved, work on centralized algorithms aims mainly at managing complexity and scalability.

3.2.1 Approximate Dynamic Programming

In [53], distributed generation, storage and demand response are modeled as a stochastic system, which is composed of 5 parts:

- State variables s, for example battery energy content, generator outputs, demand and renewable generation quantities and their probability distributions.

- Decision variables x, for example charge and discharge settings, generator setpoints, etc.
- Exogenous information, describing the system's uncertainty.
- Transition functions that determine the evolution of the system. Given the current state and decision variables, it gives the state at the next point in time.
- An objective function by which the performance of decisions can be evaluated. This could be based on generation costs, conversion losses, risk factors, etc.

A policy $\pi(s) \rightarrow x$ maps state information to decisions, and optimally one has a policy that maximizes the objective for all possible states. The difficulty lies in the explosion of states and actions when evaluating a non-trivial policy, referred to as the *curse of dimensionality*. There are types of and different ways to construct a policy, one way is using the Approximate Dynamic Programming (ADP) and the Bellmann equation.

In [53], complexity is reduced by keeping the system linear and using computationally tractable approximations. Then the problem of finding the optimal policy is reduced to solving a deterministic maximization problem.

Approximate Dynamic Programming is used in [54] for coordinated charging of a fleet of PHEVs that are capable of bidirectional power flows (V2G, section 2.1). Both the minimization of the cost of charging and real power losses in the transmission network are taken into account. The aggregator operates all those present PHEVs simultaneously.

The objective function combines a linear cost model, with prices from the day-ahead market, and real power losses based on the created power flows through certain lines. Additionally, a quadratic penalty function assigns a cost to each PHEV departing with an SOC that is less than its target value.

The optimization objective is to obtain a feasible policy that minimizes the sum of costs starting from the initial state up to a horizon. Again, the state and control space's size will increase exponentially as the number of vehicles scales up, so that it is practically impossible to evaluate all the possible actions at every time step. Therefore, the state space (being the SOC of the batteries) is aggregated and substates are introduced to reduce the state space and control space (charging or discharging power) size, by essentially grouping multiple vehicles together. Avoiding iterations over all possible policies, the *approximate policy iteration* algorithm samples from the policies using a Monte Carlo process.

Simulations showed that coordinated charging reduced up to 77% of accumulated power losses and up to 70% of charging cost compared to an uncoordinated scenario. The scenario with bidirectional power flows (V2G) incurred lower power losses for the same total charging cost with that of the unidirectional counterpart.

3.2.2 Mechanism design

In [55], a model-free method for charging EVs rooted in online mechanism design and multi-agent systems (MAS) is presented. The focus of the work is on ensuring that vehicle owners truthfully report their value for receiving electricity, willingness to wait and maximum charging rate. Owners could misreport their availability, for example by unplugging early or plugging in the vehicle some time after arrival to try and get a better price.

Because of the market design background, a setting is devised in which multiple units of electricity are periodically sold at fixed time steps. A unit of electricity is the amount of kWh when charging at the lowest rate during that interval.

At arrival, vehicle agents report departure time, maximum charge rate and valuation for the required units of electricity. Then, at the start of each time step, all the available units are *pre-allocated*, to the highest bids. The authors mention that this greedy allocation is not always optimal [56, sec. 4], as agents can be assigned units that they, given the prices, would rather not have received. *(For example, an agent wants to receive one unit over two time slots, but with high value. It could end up getting two units, and thus pay in total more than it really wants.)* A solution is provided by "burning" units of electricity from the pre-allocation, by leaving any unit unallocated whenever the price for this unit is greater than the marginal value.

The advantage of this mechanism is that it providing an incentive for agents to truthfully report their departure times, but not all available resources are always used (sometimes units are de-allocated or burned). Also, it requires good valuation functions at the vehicle agent side. It seems a bit unrealistic to expect that drivers to enter elaborate data of their charging requirements while having no certainty on the expected fees until departure time.

3.2.3 Iterated local search with heuristics

In [57], an aggregator provides a load modulation option service to the TSO. The option relates to a maximum load modulation quantity which can be called once a day. More specifically, when the TSO calls its option, the aggregator decreases

or increases the total demand of its portfolio of loads over the relevant time interval, according to the TSO's instruction. The service can be deployed by the TSO once per market day, upon notification one period prior to the respective delivery. The unknown in the problem however, is the time interval in which the TSO will call for this modulation service, and whether this will constitute upward or downward regulation. Thus, from an aggregator's perspective, the objective is to maximize the sum of upward and downward regulation quantities it can sell to the TSO.

It is assumed that the loads involved can be accurately represented by a generic tank model, with the inflow a linear function of the load's consumed power. The tank model can be applied to several electrical loads such as heaters, heat pumps, fridges, electric cars and pump-tank systems. The choice for a linear model aids in reducing the complexity of the optimization problem, since linear constraints can be handled efficiently.

The whole problem can be formulated as a classic Mixed-Integer Linear Programming (MILP) problem, as found in unit commitment problems. However, the use of traditional solvers, e.g. such as based on branch and bound methods, becomes computationally too demanding when hundreds or thousands of loads get involved. In [57], an alternative algorithm is presented, which also finds a good solution in a much smaller amount of time. Three steps are involved; first a feasibility check is performed using a set of conditions, then an initial solution is determined, utilizing a heuristic (ranking function for the loads), after which the initial solution is improved upon iteratively (iterated local search).

In a test setting, 32 market periods and 100 loads are considered. The MILP problem solved by a commercial solver CPLEX and the heuristic based algorithm performed similarly, but the latter was an order of 10 times faster.

3.3 Aggregate & dispatch DR algorithms

This category of methods tries to reduce the complexity of the DR scheduling problem by building an aggregated model of the cluster of devices at a central entity. The resulting decisions then have to be dispatched back or 'disaggregated' to the devices, for example by using heuristics. The advantage of aggregate & dispatch algorithms lies in their significantly reduced complexity, but, due to lost accuracy during aggregation, at the cost of results that are theoretically suboptimal when compared to the centralized or distributed approaches.

3.3.1 Ranking

Galus [58] investigates the use of (PH)EVs to balance power flows in a hub network, using a mechanism based on a simple heuristic and a more sophisticated one using Model Predictive Control (MPC). The simulated network contains a wind farm and a CHP, together with residential and industrial loads. Production schedules for the hub are built based on wind forecasts, and the EVs are used during the day to offer secondary control reserve.

The production planning is presumed to be performed by a central entity, with the goal of minimizing energy costs for the system. Here, the Distribution System Operator is assumed to assess network security while performing the planning. The latter considers both electricity and heat loads of the system, and the planned wind generation based on forecasts. In case the wind power exceeds system demand or not enough PHEVs are present, the deficit power is fed into or drawn from the "external grid" connection. Time steps in the simulations have a length of 15 minutes. Cars can arrive during one time interval and hence would not be connected for the whole time.

In the simple heuristic-based approach, balancing takes places instantaneously, ignoring future events. EVs are ranked based upon their the product of their SOC and departure time. In case of positive wind power deviation the car with the lowest product value will be recharged first. In the opposite case, when the deviation is negative and cars need to discharge, simply the one with the highest SOC is scheduled first. Because this method minimizes the balancing costs only for the current time step, the outcome is most likely a suboptimal solution. The advantage of using a heuristic however is it can be computed very fast and gives acceptable performance.

A different approach could incorporate known departure times as well as more accurate short term wind predictions in order to schedule the PHEVs. With MPC, this information is combined with a system model and the resulting optimization problem is solved at each time step in a receding horizon fashion. In the results, it is shown that the heuristic method is able to find the optimal solution as long as the SOC of the vehicles is not too close to empty or full. The MPC method always finds the optimal solution, but was computationally a lot more expensive, which limited scalibility. Intelligent aggregation of the storage is mentioned as a way to make the application of the MPC method in large scale clusters feasible.

In the work from Biegel [59], an aggregator manages a portfolio of on/off DR devices, which are able to shift consumption within certain energy, runtime and downtime limitations, to collectively provide upward and downward regulation.

Two control strategies are presented to track a regulating power reference. The first strategy is a predictive controller requiring complete device information; this controller is able to utilize the full flexibility of the portfolio but can only handle a small number of devices. The second strategy, referred to as an agile controller, requires less device information and can handle a large number of devices but is suboptimal as it is unable to utilize the full flexibility of the portfolio.

The on/off devices are furthermore characterized by *minimum runtime constraints* and *minimum downtime constraints* describing that once a device is turned on, it must remain on for at least a certain amount of time; similarly, once a devices is turned off, it must remain off for a certain amount of time. Such constraints are common in on/off devices such as thermal systems and heat pumps where rapid switching of the compressor can reduce performance, significantly reduce lifetime or even cause damage.

The predictive controller relies on perfect information of the future, power rating, and capacity of all devices for a given horizon to solve a MILP. While having this detailed information on the future is unrealistic in reality and the problem is only tractable for small amounts of devices, it can serve as an *upper performance bound*.

The agile controller is implemented as a control system and integrates the power error between the power reference and the measured power consumption to determine a control signal to the dispatcher. Eventually the dispatcher translates the control signal into on/off signals. The principle behind the dispatcher is to maximize the agility of the portfolio, meaning that the least agile devices should be activated first. Additionally, to satisfy the above constraints and for a device to provide e.g. upward regulation, it must currently be in the on-state and be able to switch to the off-state which requires that it has been on for at least a minimum number of samples samples.

Two numerical examples are considered: a small-scale example with 20 devices where the predictive strategy and the agile strategy are compared and a large-scale example of 10 000 devices that only the agile controller is able to handle. A sampling time of 5 minutes is used. The predictive strategy is able to fully utilize the flexibility of the devices since it provides the largest possible amount of regulating reserves. The agile controller is able to track an energy reference even for a large number of devices and with very limited knowledge of the portfolio parameters; however, it is not able to utilize the flexibility to the same extent as the predictive controller.

3.3.2 State bin modeling

The work of Koch [60] uses Thermostatically Controlled Loads (TCLs, e.g. refrigerators or water heaters) to provide short-term balancing or frequency control services (see ancillary services in section 1.3).

Instead of aggregating large numbers of individual TCL models, [60] builds a discrete system model where the state vector represents how many TCLs are currently situated in a certain state bin. Each bin spans a certain temperature interval, and all TCLs in a certain bin can be either on or off. Since TCLs heat up or cool down, they move from between state bins with a certain probability, a process that can be modeled using Markov chains. Once its transition matrix is determined from historical data, the state bin model captures the aggregated dynamic behavior of the population of TCLs.

The TCLs send their internal temperature to a central controller. In turn the central controller can switch certain bins on or off by sending probabilities (a vector with probabilities for the bins) to the TCL population. The TCLs then switch with this probability, using an internal random number generator.

The controller uses Model Predictive Control (MPC) to steer the power consumption of the DR cluster towards a certain target trajectory. Using the state bin model, the behavior of the cluster is predicted, and a switching action for the next time period is derived. During the simulations, the state bin modeling approach was validated for a cluster of 1000 TCLs, by evaluating its tracking performance. The Root Mean Square Error (RMSE) on the tracking was about 0.8-2.27%. The biggest drawback of this method seems to be the need for historical data to build a good Markov transition matrix, since the temperatures will also depend on seasonal and weekly variations.

3.3.3 Market based control

The concept of market based control (MBC) is rooted in the theory of microeconomics, wherein economic activity is modeled as an interaction of individual parties pursuing their private interests [61, ch. 4]. The market mechanisms that apply provide a way to incentive the parties, referred to as economic agents, to behave in a certain way.

In an ideal market setting, it is assumed that each economic agent is a price taker, meaning that it decides on a quantity of resources that is small compared to the total volume traded in the market. Thus individual transactions have no influence on the unit price of the resource. Additionally, all agents respond to the same price, which corresponds to the point where the amount of resources

sought by buying agents equals the amount produced by the selling agents. In economics, this is known as a general equilibrium market. A requirement for an equilibrium market is that agents bid rationally. If this is not met (e.g. an agent buys more when the price is higher), situations can arise where no equilibrium price exists.

Under some assumptions (essentially requiring a perfect functioning market mechanism), the *first theorem of welfare economics* states that the equilibrium outcome is a Pareto-efficient allocation of the resources; no agent could be better off without making another worse off.

To determine equilibrium price, the market has to be cleared, a process that can be performed using an auction mechanism. In energy markets, the use of pay-as-cleared, sealed bid auctions is common [62, p. 12], e.g. on the Belpex Day-Ahead Market [63].

PowerMatcher: Multi-agent MBC

In [64], appliances in a DR cluster are represented by software agents. They have control over one or more local processes (e.g. heating of water or charging of an EV's battery), but compete for resources (electric power) on an equilibrium market with other agents. The system has been used in a number of field tests and is commercially known as PowerMatcher [65].

The system is based on the principle of Walrasian auctions. This is a type of simultaneous auction (since multiple units of the same resource are sold at a time [66, ch. 12]), where each agent wishing to trade determines its demand or supply over a relevant range of prices (price-quantity curve). A Walrasian auctioneer then aggregates these demand and supply functions and announces the market clearing price, corresponding to the equilibrium. Walrasian auctions therefore perfectly match supply and demand. An example of this process is illustrated in figs. 3.3a and 3.3b, for a case with 2 consuming and 2 producing agents.

The clearing of the market in [64, 67] is operated periodically, e.g. every 15 minutes, or using events, and is implemented in a hierarchical, tree-like manner [61], depicted in fig. 3.4. At the root of the tree is an auctioneer agent, directly connected to a number of *concentrator agents*. The auctioneer agent is a special type of concentrator agent and is responsible for the price setting process, just as in the Walrasian auctions. The concentrator agents lower in the tree aggregate the demand functions of their child agents. Because a uniform interface is used between the levels, an unlimited number of such aggregation

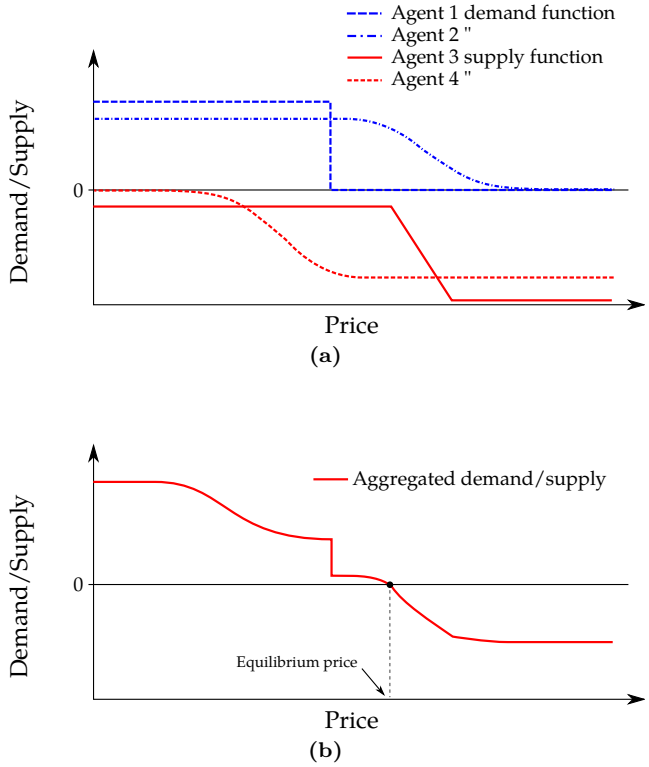

Figure 3.3: Market based control example with 4 agents. (a) Demand functions of 2 agents that can want to consume, and 2 agents that can generate. (b) Aggregated demand and supply curves, with equilibrium price at which supply and demand is balanced.

levels can be used. Eventually, at the bottom of the tree, we find the device agents themselves.

The device agents assemble demand functions representing their willingness to pay and consume, taking into account the specific constraints of the controlled device. Demand functions are sent upwards and an auctioneer agent performs a matching process with producing agents. An equilibrium price is communicated back to the agents, that start consuming or producing at the equilibrium level.

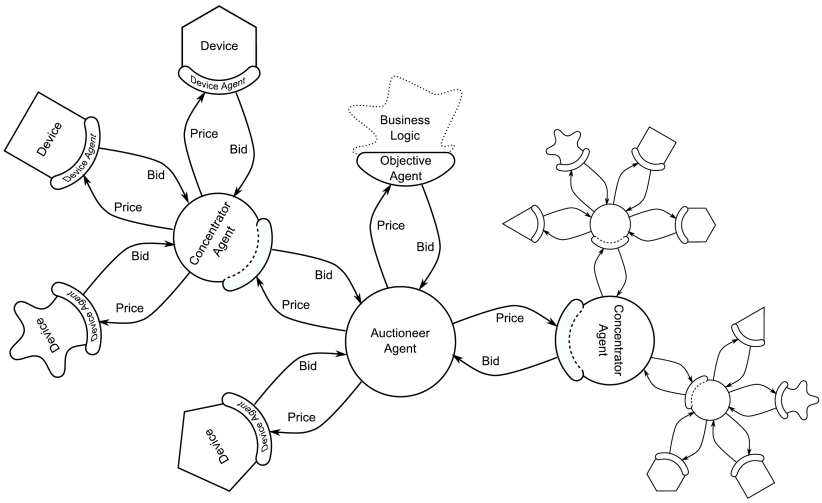

Figure 3.4: Example PowerMatcher agent cluster, from [67]

Benefits and drawbacks

Using a multi-agent market based control system (MAS MBC) for demand response, as exemplified by the PowerMatcher, offers several benefits:

- Scalability: In a centralized system, the central entity has to deal with all incoming and outgoing messages, $\mathcal{O}(n)$, quickly creating a communication bottleneck. Because of the aggregation on multiple levels in the PowerMatcher, the amount of messages that have to be dealt with per agent is reduced to $\mathcal{O}(\log n)$.
- Low complexity: The construction of demand function data and the matching process itself is straightforward, and is not based on any model. Determining a demand function for a device can be done during its development.
- Openness: Any kind of device can be integrated in the cluster, since operation only depends on the exchange of demand functions and price. Devices without flexibility are represented by an inelastic demand function.
- Privacy: Since demand functions are aggregated there is no central entity that collects all information. Furthermore, the physical processes of devices, bidding strategy and motives of users are all abstracted through the demand function.

However, a significant shortcoming compared to other methods presented in this chapter, is the lack of look-ahead functionality; the PowerMatcher is only able to perform instantaneous matching of demand and supply (even if it is external, e.g. live wind turbine output, or in chapter 7, where EVs are controlled to obtain a flat power profile over the day). No planning or information on the future from the EVs themselves is used when determining equilibrium prices. Of course, forecasting at the level of the objective and business agent (see fig. 3.4) is still possible and the adherence of the DR-cluster to a predefined power profile then is expressed in the bids of this agent [68].

If equilibrium prices are regarded as a pure control signal, so that there is no direct link to the cost of energy, the MAS MBC mechanism can be viewed as a dispatching method for the aggregator's business case. In such a scenario, the demand function data is regarded as input for a scheduling algorithm, and the equilibrium price as a level to steer the cluster towards its outcome.

3.4 Conclusion on the DR algorithms

From the discussion of the above algorithms, we can draw some high-level conclusions regarding their application in a DR cluster

Centralized algorithms provide a way to incorporate a large amount of diverse information and constraints in the DR scheduling problem, which can then be solved by well-established mathematical techniques. This guarantees that the outcome is as-optimal as possible given the problem's constraints. However, due the complexity involved, the time needed for solving quickly spirals out of control when scaling to large clusters of devices and more advanced scenarios are taken into account. This is referred to as the curse of dimensionality, and can be partly addressed by the use of approximation and search techniques.

As an alternative, the DR scheduling problem can be broken down so that it can be distributed over multiple participants in the DR cluster. A method such as dual decomposition works by iteratively exchanging demand information and coordination signals between a central entity and the cluster's autonomous devices until convergence is reached. Alternatively, the use of game theory can provide proofs regarding the fairness of the scheduling process.
The downside of the distributed algorithms is related to the need to exchange additional messages between the devices, since either multiple iterations are required or they communicate directly with each other, and the additional complexity involved due to the need for a more advanced communication system.

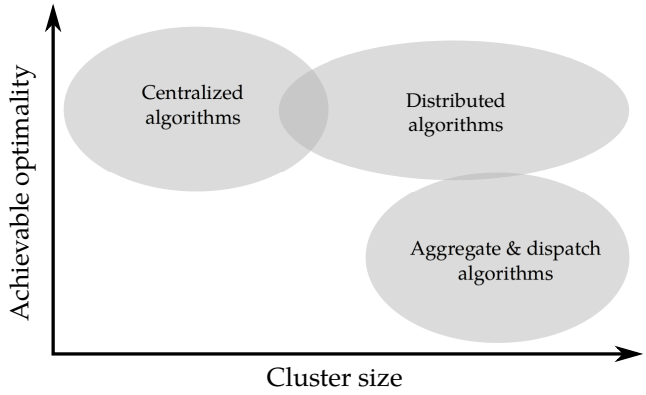

Figure 3.5: Suitability of algorithms in DR cluster implementations

The division of the algorithms into centralized and distributed is also loosely tied to the control architecture in which they would be implemented; a centralized algorithm will have a single entity where all data for the optimization is collected and coordination signals to the individual DR devices is sent out from. In the distributed case, devices are more autonomous and may even communicate in peer-to-peer fashion.

An alternative to the centralized and distributed algorithms is provided by aggregate & dispatch algorithms. These methods use an aggregated model to represent or approximate the collective state of the DR cluster. The model is updated with state information from the individual devices. Scheduling then takes place using the aggregated model and the result is dispatched to the DR devices through e.g. a heuristic methods. Because the aggregated model fails to capture some of the details of the individual devices' state and heuristics are not perfect, aggregate & dispatch methods do not achieve the most optimal schedule. However, they obtain results which are close to the centralized or distributed algorithms, but at much lower complexity, and scale well to DR clusters containing large amounts of devices. Referring back to the statements of section 1.4, aggregate & dispatch methods constitute a good trade-off as they can achieve most of the benefits of DR at a large scale, but at low complexity and consequently cost.

In the light of the above description, fig. 3.5 shows the placement of the three classes of DR algorithms against each other.

Because the MAS MBC method from PowerMatcher, in section 3.3.3,

- can be easily applied to all kinds of DR devices, as long as they can be represented by a bid function,
- has favorable computational properties, lending it to be implemented on resource constrained, e.g. low-cost, embedded hardware,
- is already proven in a few field-tests,

the remainder of this work, starting from chapter 5, is based around the use of a MAS MBC based algorithm for the coordination of charging EVs.

3.5 Distribution grid congestion

As the electricity grid can not get physically congested, the term *grid congestion* refers to a situation where the demand for active power exceeds the nominal power transfer capabilities of the grid [13]. Grid congestion can be mapped to the violation of one or more constraints at its connection points.

3.5.1 Grid constraints

We make a distinction between physical constraints and power quality problems:

1. Physical constraints, directly linked to the limits of cables and grid equipment.
    - Maximum allowed transformer power.
    - Transformer aging due to increased heating in the windings [69, 21] and the mechanical stresses due to expansion/contraction.
    - Aging of cable insulators and switches [21].
2. Power quality problems due to the resistive and unbalanced nature of distribution grids. The European EN 50160 standard, "Voltage characteristics of electricity supplied by public distribution systems" [70], describes the following important specifications:
    - *Over- and undervoltage*: "The European EN 50160 standard specifies that the 10 minute mean RMS voltage deviation should not exceed $\pm 10\%$, measured on a weekly base. For undervoltages, a wider range is allowed in the measurement procedure: -15% to -10% for maximum 5% of the week."
    - *Voltage dip*: EN 50160 allows 1000 voltage dips per year, during which the voltage drops at most to 85% of its nominal value, for a duration of less than 1 minute. Interruptions, defined as lasting less than 180s, should occur less than 500 times/year.
    - *Voltage unbalance factor (VUF)*: When magnitudes of phases or line voltages and the phase angles are different from balanced conditions. "The European EN 50160 standard specifies that the 10 min mean RMS value of the voltage unbalance factor should be below 2 % for 95% of time, measured on a weekly base." Different ways to compute the VUF exist, and here we will use *True VUF* as shown in (3.2).

More information on the definitions and calculation of VUF can be found in [71].

$$\%\text{VUF} = \frac{\text{negative sequence voltage component } V_n}{\text{positive sequence voltage component } V_p} \cdot 100 \quad (3.2)$$

with

$$V_p = \frac{V_{ab}+a\cdot V_{bc}+a^2\cdot V_{ca}}{3}$$

$$V_n = \frac{V_{ab}+a^2\cdot V_{bc}+a\cdot V_{ca}}{3}$$

and V_{ab}, V_{bc}, V_{ca} the three-phase unbalanced line voltages, and $a = 1\angle 120°$, $a^2 = 1\angle 240°$.

- *Harmonics*: Caused by the power electronics inside converters such as found inside vehicle chargers or PV inverters. While not looked into here, it is worth mentioning that the use of power electronics such as found inside EV chargers can create problematic harmonics [23].

The aspects of transformer and cable aging will not be looked into in this work, and we will solely focus on the voltage magnitude part of the EN 50160 standard when discussing grid congestion.

Because of the largely resistive nature of distribution grids, power consumption and injection will cause a deviation from the nominal voltage. This means that in so called weak grids, having limited cable diameters or long sections, power quality problems will arise more quickly and often.

3.5.2 Congestion mitigation

The DSO, when faced with grid congestion problems, can opt for a number mitigating strategies.

1. **Reactive power and voltage control** to increase the (local) transfer capacity. This is already used in wind generators connected to the MV network. In distribution grids, reactive power and voltage control can be achieved through the use of tap changers and capacitor banks, and their switching is planned using load forecasts. For example, [72] optimizes the switching of such devices to minimize daily energy losses, while limiting the number of switching operations.

2. **Coordinating the power flow** throughput via shifting or curtailment of demand, possible through the implementation of demand response,

or through the mandated implementation of voltage droop control (see section 3.6.1).

3. **Increasing the transfer capacity** of the local grid by replacing or upgrading equipment (adding or replacing cables, installing a bigger transformer, etc.). While this option is attractive because it limits the involvement of the DSO (retain 'passive' role, no forecasts, etc), the cost of this option can be substantial and thus it is only considered when other solutions are exhausted or deemed infeasible.

The first option is already used today. However, in practical operation, LV-grid tap changers are usually off-load types and barely used [73]. Tap positions are calibrated and changed only in case of network extension or modification [74]. Automated and remotely controllable on-load tap changers (OLTC) exist, but their use in distribution grids is still reserved to a few test cases [75], due to high costs.

The third option is technically attractive for DSOs, since it fits within their predominantly off-line role of installation, maintenance and asset management at the distribution network level. Adding parallel cables to or upgrading existing lines by using new cables with higher cross sections is considered a straightforward solution [74]. No additional tasks such as day-to-day load forecasting, extensive state estimation and monitoring are required. The high investment costs will likely reserve this to some corner-cases.

In the remainder of the thesis, congestion management will refer to the use of the second option; the coordination of active power demand at congested grid locations.

3.5.3 Design of grid congestion management mechanisms

The task of a grid congestion management mechanism is to limit the managed loads to the capacity of the distribution grid assets. This can be achieved by adding a network cost or penalty for the use of the network during certain times of the day. In [13], algorithms for congestion management are classified according to strategy.

Distribution grid capacity market: In this mechanism, the DR aggregators involved (responsible for managing a group of DR devices) will start by optimizing the schedule for their EVs in absence of a network tariff. The schedule is sent to the DSO, which evaluates whether the network constraints are met. If not, the aggregators will receive a price that reflects

congestion at each node in the network and are requested to update their schedule.
The procedure is then repeated until convergence, at which point the network tariff and charging schedules are fixed. As the mechanism is essentially the same as dual decomposition, from section 3.1, the use of non-strict convex objective functions can cause problems. In [76, 77], this method is used.
A capacity market would be complex to implement and the iterations add a lot of computational burden. The DSO could be offloaded by externalizing the process into a separate capacity market, in which it still has to provide measured and estimated power.

Advance capacity allocation system: The idea behind this mechanism is that the DSO pre-allocates grid capacity at each transformer or line to the aggregators, based on the free capacity remaining at each line or transformer, after inelastic load (mainly household consumption) has been accounted for. The allocation between aggregators would be based on auctioning of this free capacity.
While relatively straightforward, there are some drawbacks to this method. First of all, the DSO needs to map all its customers' connection points to their respective aggregator. Secondly, there is no way to incorporate the time-dependency of demand; if an aggregator bids for the capacity during a certain period, that bid depends on what was allocated before and after that time-period. An iterative approach would solve this, but also increases complexity again.

Dynamic grid tariff: In this case, a time varying location dependent grid tariff is determined by the DSO beforehand, based on expected consumption levels at each node in the grid. Predicting loads and estimating price sensitivity is entirely the responsibility of the DSO. Once the tariffs are published to the aggregators, the latter integrate them into their scheduling. In case of severe deviations from the expected value, the DSO may resort to controlled interruptions in real-time, which in turn also holds a risk for the aggregators.
The work of [78] uses this approach. The biggest drawback consists of the high complexity of the problem that needs to be solved by the DSO (predictions, load flow calculations), let alone when the stochastics of inevitable uncertainties are taken into account.

The work of [15, p. 97] provides an overview and comparison of the 3 types of mechanisms. While all of the mechanisms should lead to the same optimal EV charging profile, the complexity involved limits their practical implementation. It is also not clear how deviations during the course of the day should be

handled, which will inevitably occur as the algorithms are based on the use of allocations in time slots (e.g. 15 minutes in [77]), besides the last resort of DSO controlled interruptions.

In [15, p. 100] the use of a proxy tariff is proposed, such as a historical Time-of-Use or real-time tariff, as a compromise. Unfortunately, following simulations, the conclusion suggests that the use of proxy tariffs does not necessarily reduce system peak load, leads to higher costs (approx. +20%) and distorts the economic signal of the electricity price.

3.6 Ancillary services and grid support

The use of DR for ancillary services was introduced in section 1.3. A fleet of EVs can perform ancillary services through varying of their charging rates around a predetermined operating point. This is shown in [79], where a central scheduler simultaneously tries to minimize EV charging costs for its customers and provide upward and downward regulation reserves to a North-American utility. The degradation of the battery due to the use of V2G is taken into account using 3 different replacement cost scenarios. Simulations with a cluster of 1 000 EVs show that, even though the costs associated with battery degradation are considerable, the aggregator receives significant profits while keeping consumer costs for energy very low. In addition to the extra flexibility provided, peak load is generally reduced due to the energy discharged from the batteries.

In [80], the business case of offering secondary downward reserve on the German market using a pool of EVs is analyzed. Secondary reserve is activated automatically to restore nominal frequency [81]. Special attention is paid to the implications of the current regulatory framework on the use of EVs as reserve, and the cost of the support infrastructure. In contrast to [79, 26], simulations show limited capabilities of the EVs to offer the required flexibility, and subsequently a low revenue per vehicle. This is attributed to the need for constant availability during the whole contract period, which is the main burden for an offer of reserve. In the conclusions, it is stated that, based on the results, future research should focus on developing simple models with less need for complex and expensive control structures on markets without availability requirements.

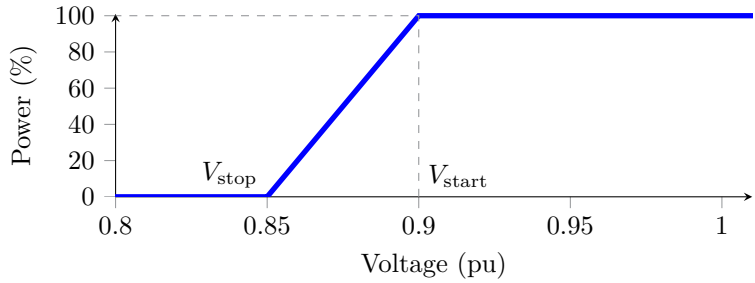

Figure 3.6: Example voltage droop control characteristic

3.6.1 Droop control

Droop control is a control strategy commonly used with generators for primary frequency control. In general, the objective of droop control is to compensate for voltage or frequency deviations, by varying the amount of generated power. Providing commercial primary frequency control using a DR cluster is not economically appealing because of strict regulatory requirements regarding response speed and obligations on availability [81, 82]. However, in a microgrid or island scenario, lacking sufficient generator inertia, it could make sense [14, sec. 7.3.1].

In case of smaller scale problems, such as those encountered in constrained/-congested distribution grids, voltage droop control can be used. In these grids, lines behave resistively rather than inductively, causing voltage deviations along the line when large loads are drawn from or large currents injected into the grid.

In some countries, large PV installations are now required to be able to provide grid services to the distribution system operator. Similarly, small PV installations are required to respond to overfrequency and overvoltage by limiting injected power or temporarily disconnecting [83, 84].

But PV output is determined by the uncontrollable radiation of the sun, whereas charging rates of (PH)EVs can be varied and shifted arbitrarily in time. Thus, in addition to the coordination at the market level, a fast-acting grid-supportive behavior similar as used in PV installations can be implemented inside a charger [85, 25]. It is not unthinkable that the use of automatic droop for EVSE becomes mandatory as well once their impact reaches a significant quantity.

Nonetheless, a droop control scheme is robust and easy to implement because it only requires the measurement of voltages and a way to adjust local active

or reactive power settings. No communication with a central entity is needed. Figure 3.6 shows one way an EV's charging power could be scaled down in function of the measured voltage, the latter which is expressed in units of the nominal voltage. Between V_{start} and V_{stop}, power is scaled linearly. The voltage droop controller can be implemented as a P-control loop. We will come back to droop control for EV chargers in section 4.3.3.

On the downside, activation of the droop will almost certainly conflict with market level coordination [14, sec. 5.2.4]. For example, at some point the fleet manager would send its optimal power set-points or an equilibrium priority to the vehicle agents. But due to local grid problems the EVSE is forced to reduce power. The result is that, even if the real resulting power setting is communicated back to the fleet manager, the deviation holds a disparity from the original optimal market level energy plan. The resulting energy shortfall (negative imbalance) may result in a penalty for the fleet manager.

Investigation of this relationship is one of the research questions of this thesis, as outlined in section 1.4.

3.7 Conclusion

In the first part of this chapter, a selected number of algorithms from literature for the optimization and coordination of demand response clusters were discussed and classified. A distinction is made between distributed, centralized and aggregate & dispatch algorithms.

Eventually, in section 3.4, the preference for aggregate & dispatch methods was justified from a complexity/optimality trade-off perspective. The second part of the chapter focused on grid congestion problems and mitigating solutions.

In order to answer the research question from section 1.4.2, related to the perceived conflict between market objectives of the DR aggregator and grid congestion at the local level, a simulation framework is needed that can simulate market-based DR coordination strategies applied to a fleet of EVs, while performing load flow analysis in realistic grid situations. This will be addressed in the next chapter.

Chapter 4

Simulator for Demand-Response Interaction

To answer the research questions outlined in chapter 1, a simulator framework has been developed that allows to simulate the behavior and interaction between entities involved in smart grid demand response scenarios. The focus of this simulator lies, but is not limited to, the interaction between electric vehicle charging coordination algorithms and the various actors in the electricity grid, such as EVs, aggregators and distribution system operators (DSOs). Starting from the work of [86], the framework was heavily extended and reworked.

First, in section 4.1, an overview is given on how software agents in the framework interact with the simulated smart grid environment. Then, in section 4.2, the framework's features to log, export and analyze interesting data generated during simulation are introduced. Next, in section 4.3, the integration between the agent framework and a MATLAB-based load-flow simulator is discussed, together with the provisions to simulate a voltage droop controller inside DR devices. Eventually, in section 4.4, more information is given on the data models used during simulations, such as for vehicle driving behavior and wind power output.

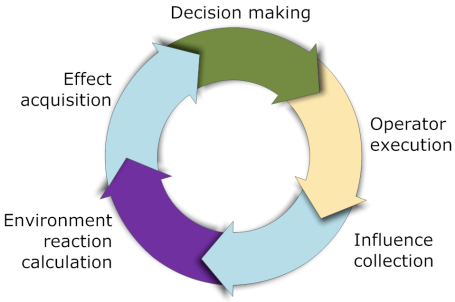

Figure 4.1: Execution-reaction cycle in agent-based simulation [87]

4.1 Structure overview

In the simulator, multi-agent functionality is implemented in a Java framework, according to the execution-reaction cycle [87]; agents perceive the simulated environment and take actions accordingly, then the environment state is updated to reflect the agents' influences. A synchronous evolution of a multi-agent system is obtained as each agent inspects the environment, takes an action and the environment is updated.

4.1.1 Environment

Two types of objects make up the simulated environment of the framework, shown on the left of fig. 4.2.

- Entities are the objects that represent physical parts of the electricity network, such as transformers, feeders, nodes and various consumers in the grid. The relations between these objects reflects the static (and typically hierarchical) grid structure, while their properties reflect the dynamic state of the grid. Examples of such dynamic state variables are:
  - Voltage and phase angle at a node.
  - Power consumption or injection at a certain point (e.g. charge rate of an EV or injected power for PV installation).
  - Connection state of consumer (e.g. availability state of an EV).
  - State-of-charge of an EV battery.

- Hardware that hosts the agent software and enables the exchange of messages between agents. The behavior of these objects has not been modeled in depth, and is limited to the introduction of communication delays according to a statistical distribution or simple hardware failures.

4.1.2 Agents and controllers

A distinction between 3 types of agents is made in the simulator. They are shown on the top of fig. 4.2.

Node agents: node agents are directly associated with a physical connection point to the grid and are responsible for the coordination of devices attached at this point. In a typical demand response scenario, this could consist of an EV, a PV installation, household appliances, etc.

Manager agents: manager agents are responsible for a subset of node agents. They are used in situations where information from node agents is aggregated in a hierarchical manner. Manager agents can be associated with a Transformer entity in the environment.

VPP Manager agents: VPP manager agents are responsible for a set of manager agents or node agents. Typically, only one instance of this agent will exist, unless scenarios containing multiple concurrent aggregators are simulated. Control algorithms for DR are usually implemented at VPP Manager agents. Most of the time, VPP Managers are associated with a TopLevelTransformer entity.

In reality, agents are implemented as software running on an (embedded) computer. They can influence the environment by calling functions to e.g. change the power setting of the EV battery charger, request the actual state-of-charge, or send out messages through the network interface of their host. In the simulated environment, the same functions are made available to the agents, by abstracting them into controllers that act as interfaces for the physical entities in the environment. The controllers are shown on the bottom-right of fig. 4.2. Depending on the type of agent, different functions are be available. For example:

- Node agents have functions to read out or influence the power consumption of an associated physical device, using e.g. `getNodeInterface().getPower()` or `getPHEVInterface().charge()` to set the charging power of an EV.

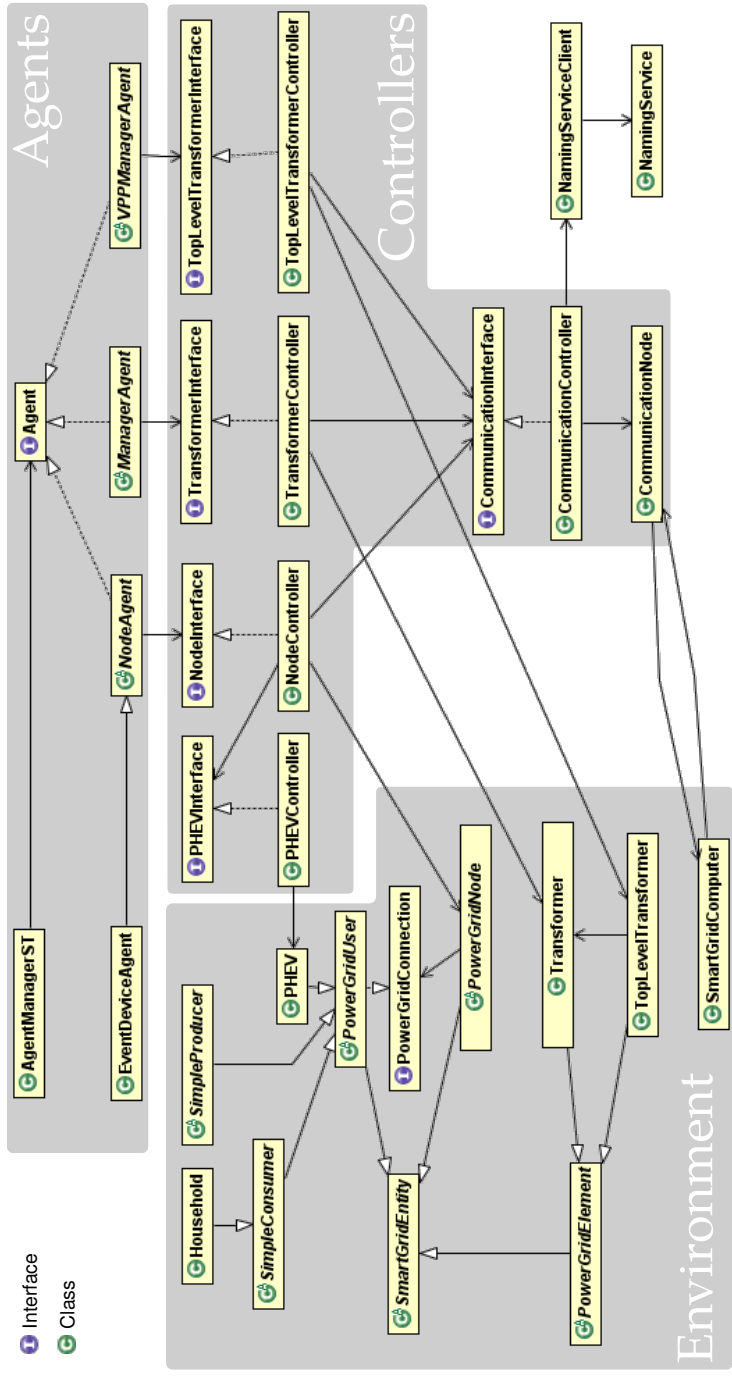

Figure 4.2: Main environment entities, agents and controllers of the simulation framework

- Manager agents can determine the actual power through a transformer and directly send messages to the VPP Manager agent with `getTransformerInterface() .getCommunicationInterface().sendMessage()`.
- VPP Manager agents can also determine the actual power through top-level transformers and broadcast messages to the Manager agents.

Additionally, to allow the operation of multiple independent DR clusters within a single simulation, nodes in the network can be assigned to specific aggregators, each implementing their own business case. Consequently, Manager and VPP Manager agents assigned to an aggregator can only see the properties of member node agents.

The decision making part of the cycle is performed through an AgentManager, which will sequentially call the `step()` function of the available agents in case of the single-threaded AgentManagerST implementation. Multithreaded versions were developed at one point, but discarded due to the increased overhead when assigning step-functions to the individual threads.

4.1.3 Actors

After the agents have finished their decision making process and taken actions by calling controller functions, an environment reaction calculation step is performed to update the state of the environment. This is handled by several Actors:

- PowerGridUserActor: This Actor has the task to update entities in the environment that are related to the electricity grid. It consists of several subcomponents:
  - PHEVActor: Contains the model of a PHEVs and updates battery state, represents a driving profile, responds on departure and arrival times, ...
  - SimpleProducerActor: Responsible for loading and updating the production profile of simulated PV panels and wind turbines. These profiles are stored in separate database files.
  - SimpleConsumerActor: Responsible for loading and updating consumption profiles of consumers such as Household entities.
- CommunicationActor: simulates the communication network that routes the agents' messages from one communication node to another. One possibility is to include channel specific delays (DelayCommunicationActor).

- LoadflowActor: if DC loadflow analysis of the grid is not sufficient, this actor can simulate the state of a distribution grid and update the voltages at all or select groups of nodes inside it. An more detailed explanation on this actor can be found in section 4.3.2.

Both the AgentManager and ActorManager call their members sequentially, making the order in which the different actors are called important; for example, if the PowerGridUserActor updates the environment after the LoadFlowActor does, the agents will perceive the environment state differently than when it is the other way around.

Therefore an execution priority is assigned to each Actor so that the effect on the environment is predictable and independent of the way the scenario is constructed.

4.2 Data logging and Matlab interface

The amount of data generated during a simulation increases very fast, making analyzing and plotting it a tedious task if one has to rely on exporting/importing data files from the Java simulator. A uniform data logging framework automates this process.

In the framework, logging is implemented using a singleton Data Directory class, where variables to be tracked are collected into groups and items. During initialization, agents register their variables according to a certain item type or look up already existing items to store their reference. Various plots and statistical items are predefined. A short example of adding a plot-type and a datapoint to it is shown in listing 4.1.

Listing 4.1: Data logging example

```
//Plot with power versus time, infinite length
private TimePlotUnlimited powerPlot;
...
//Set up plot and insert into Data Directory
powerPlot = new TimePlotUnlimited("phevpower", 2);
powerPlot.setLegend(0, "measured");
powerPlot.setLegend(1, "expected");
DataDir.getInst().put(getName(), powerPlot);
...
//Add data to plot at current time
powerPlot.addPoint(0, power);
```

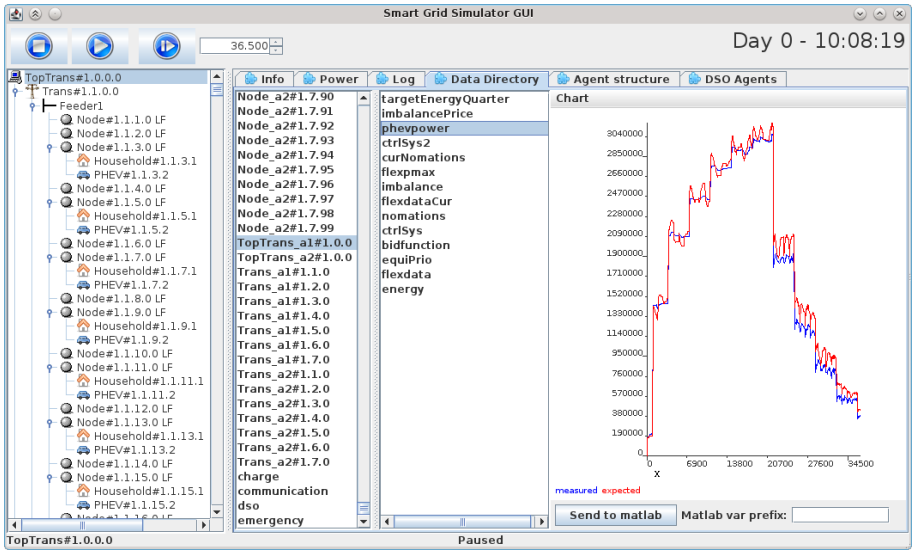

Figure 4.3: Optional GUI interface for the simulator, showing the grid structure on the left and the contents of the Data Directory on the right.

At the end of the simulation, items marked as such are automatically transferred into the active MATLAB workspace, according to a hierarchical naming scheme `<group>_<item>_<axis>`.

The Java simulator can also access the current MATLAB workspace and call functions in it. This allows to efficiently handle and debug optimization problems. In all scenarios, IBM's CPLEX [88] was used through the Yalmip [89] interface to solve LP or QP problems written as .m files and called from the VPPManager agents.

Message logging is organized in a similar but simplified manner, as no data types are required. Each agent registers itself during initialization and can then write log messages to a statically accessible class. At the end of the simulation, the result is optionally written out to a single chronological file.

To aid in debugging, a modular GUI shows a representation of the environment and the loadflow data. Separate modules can show the content of the Data Directory and the most recent logged messages, as depicted in fig. 4.3. Most simulations are run in a headless mode (only console output) however.

4.3 Loadflow simulation

To be able to evaluate the impact of coordination strategies at the local grid level, it is necessary to include a model of the distribution grid where the coordinated and uncoordinated loads are situated and a loadflow solver that is able to calculate the voltage magnitudes and phase angles at every node in this distribution grid.

Because the scenarios in the agent simulator are typically run for many consecutive simulated days and with a resolution of one second, the overall convergence performance of the loadflow solver is particularly important in avoiding very long simulation times. Therefore an additional requirement is the need to be able to simulate a large cluster of coordinated vehicles, but for which only a subset would produce relevant loadflow results. In such cases it is beneficial to ignore the other part of the cluster during loadflow calculations. Furthermore, there is a need to be able to implement a form of node-level feedback on a sub-second basis (e.g. when implementing voltage droop control).

In order to fulfill these requirements, it was chosen to use an existing MATLAB-based loadflow solver developed at ELECTA. This solver is implemented in a fully object-oriented manner and has already been validated and used in other projects [90] such as Linear. Loads are modeled as constant power, meaning that a lower voltage leads to a higher current consumption and vice versa. This is a good way to represent switching power converters such as commonly found inside EV chargers.

4.3.1 Principle

The MATLAB-based loadflow method for three-phase unbalanced radial grids as used here is based on the backward–forward sweep technique [91]. With this method, all three-phase impedances between the nodes are represented in an impedance matrix where the complex impedance between every two nodes x and y is held. To find the voltages at the nodes, an iteration i over 3 steps is started:

1. Nodal current calculation: for each node, the current is calculated from the power consumption or injection and the voltage at that point.
2. Backward sweep: Line currents are summed.
3. Forward sweep: Node voltages are updated using the impedance matrix and line currents.

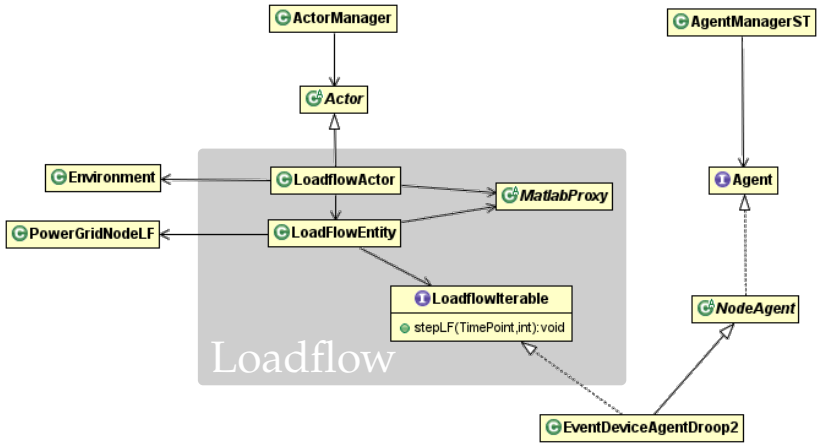

Figure 4.4: Parts of the loadflow simulation in the simulator

After each iteration, the voltage difference with the previous iteration $i-1$ at each node is used as convergence criterion. As long as $|V_i - V_{i-1}| \geq \epsilon$, the 3 steps are repeated. In this work, ϵ is set at 0.1V.

4.3.2 Integration in the Java framework

To centralize the configuration files, the build-up of the grid structure is entirely done from within the Java simulator. The grid structure in the simulator is built from an XML description, that can optionally specify directives to enable and configure the loadflow in certain segments of the grid. Afterwards, the Loadflow Actor scans the completed Environment and constructs an equivalent grid object structure inside the active MATLAB workspace. Internally, a bidirectional HashMap keeps track of equivalent PowerGridNode objects and MATLAB nodes and cables in the loadflow solver. This allows the Loadflow Actor to quickly set power values in the solver, run the loadflow and get voltage results back from it.

To increase the speed of simulation and avoid wasting calculations, each PowerGridNode object is extended into a PowerGridNodeLF object, having a `powerChanged` flag. Every time an agent or Actor modifies the power setting of a PowerGridNode, this flag is set. The loadflow Actor can query and reset this flag to decide whether an update of the voltages in this part of the grid is required.

Additionally, during initialization, the LoadFlow Actor will create separate LoadFlowEntity objects that group together the parts of the grid that must be

Listing 4.2: Example XML grid definition for the Java simulator

```
<?xml version="1.0" encoding="UTF-8"?>
<powergrid xmlns:xsi="powergrid.xsd" xsi:noNamespaceSchemaLocation="powergrid.xsd"
     id="flexgrid">
  <topleveltransformer id="vpp1" quantity="1">
    <transformer quantity="1" loadflow="true" nominalVoltage="230.0"
         type="GridParameters.TransformerTypeLibrary.Tr_400kVA_10kV_400V">
      <feeder quantity="1">

        <!-- 250m cable to first node -->
        <node aggregator="a1" distance="250" level="0"
             cable="LINEARonly.GridParameters.EandisCableTypes.EIAJB_1kV_3x70_50">
        </node>

        <!-- Cable to first house -->
        <node aggregator="a1" distance="8" level="0"
             cable="LINEARonly.GridParameters.EandisCableTypes.EIAJB_1kV_3x70_50">
        </node>
        <!-- Cable from street to inside household connected on phase 1 -->
        <node aggregator="a1" distance="10" level="1"
             cable="GridParameters.CableTypeLibrary.EXVB_1kV_4x16" phases="1">
          <household/>
          <phev/>
        </node>

      </feeder>
    </transformer>

    <!-- Some agents outside distribution grid -->
    <transformer quantity="1">
      <feeder quantity="1">
        <node aggregator="a1" quantity="200">
          <phev/>
        </node>
      </feeder>
    </transformer>

  </topleveltransformer>
</powergrid>
```

updated as a whole. This is to avoid the need to update the loadflow for all distribution grids in the simulation after a single PowerGridNode has changed.

It is important to point out that loadflow calculations have only meaning under steady-state conditions, from a power systems perspective. In reality, fast changing power setpoints for example will elicit more dynamic behavior, such as damped oscillations. As long as these effects are contained well within a single second, calculating the voltage every second will still correspond to steady-state behavior [92].

However, to include voltage droop control in the agents, as discussed in section 3.6.1 and in more detail in the next section, a fast response that corresponds to a real-time control loop needs to be simulated. In the loadflow

Actor, such behavior is achieved by iterating within the normal 1-second time steps of the agents until a steady-state voltage at all the relevant nodes is reached.

To that end, agents can optionally implement the LoadFlowIterable interface. The loadflow Actor will iterate over the implemented `stepLF()` methods it finds until voltage convergence is reached. At that point, normal iterations using the agent's `step()` method are resumed. See fig. 4.4 for a conceptual overview of the implementation.

4.3.3 Voltage droop control implementation

In section 3.6.1, the possibility to use a voltage droop controller inside devices connected to the distribution grid was briefly discussed. To evaluate the behavior of droop control enabled chargers coordinated by a market based fleet agent, an optional voltage droop control loop is added to the vehicle agents. More details on the vehicle and charging model can be found in section 4.4.1.

Because loads are modeled as constant power, the droop control system works by scaling the maximum active power draw of the device in function of the measured voltage deviation from the nominal voltage. The latter is measured at the device's corresponding household terminal in the grid model of Figure 8.2, and is expressed in fractions (pu) of the nominal bus voltage (being 230V).

As visible on figure 3.6, the response can be characterized with two thresholds V_{start} and V_{stop}. When the voltage at the node sags to 0.9 pu, power is scaled down linearly until 0.85 pu, at which no more charging takes place. In essence, the droop control system is a simple P-controller, with a slope and deadband parameter determined by the thresholds.

However, the droop control logic in a realistic power-electronic device is supposed to operate on a real-time basis, measuring voltages and responding within tens or hundreds of milliseconds. The device agent software on the other hand, operates on a larger time base and is basically a "slave" to the outcome of the droop controller.

Furthermore, if the bandwidth of the droop control loop is too limited, load synchronization effects will start to appear as, for example, multiple EVs receive control data at almost the same instant. These will then adjust their charging power and influence the voltage on the grid, after which the droop intervenes. Node voltages change again and, without damping, the droop controllers can exhibit oscillations. This can be avoided by decoupling the droop control loop from the rest of the agent software functions.

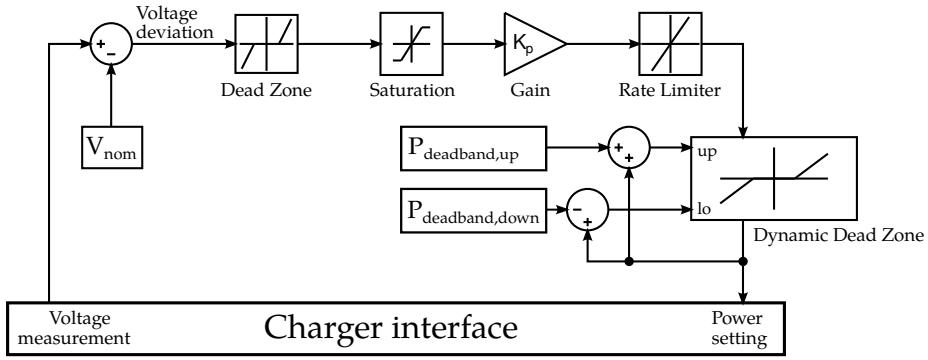

Figure 4.5: Droop control loop as implemented in the EV agents

From the previous section 4.3.2, each device agent can implement an optional "Loadflow-iterable" code-segment, which is independent from the main agent software. This code-segment can be seen as the real-time, low-level operating control loop and is iterated over by a Loadflow Actor until a convergence threshold is reached regarding the voltages at the nodes or a time limit is reached. Afterwards, the "normal" agent software resumes from this steady-state condition.

Figure 4.5 shows the block diagram of the implemented droop control within the "Loadflow-iterable" of the device agents. A *rate limiter* dampens the response, while the *dynamic dead zone* helps to avoid long iteration loops due to minuscule changes in power setting.

4.4 Data models

4.4.1 EV model

The model of the electric vehicles (hybrid plug-in or full electric) in the simulation consist of two main parts: a battery model and a usage profile. A PHEV Actor is responsible for updating the real world status of this battery and the EV's connection status, depending on the selected driving profile and vehicle parameters (fig. 4.6).

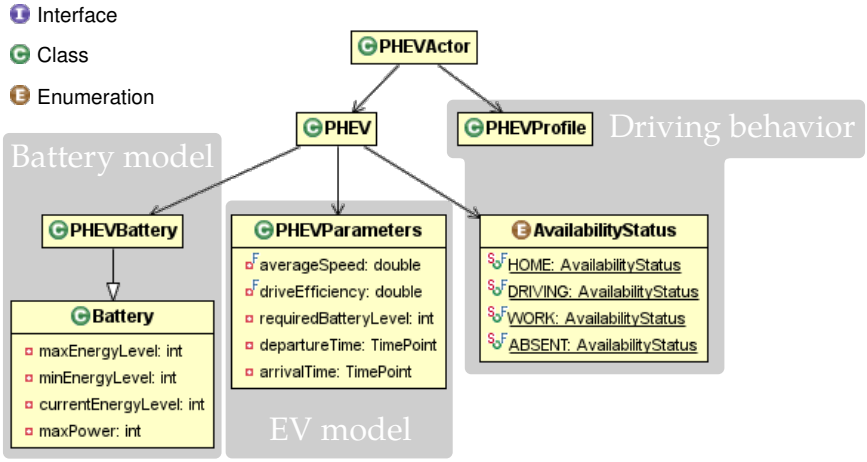

Figure 4.6: EV model components and Actor

Battery and charging model

In literature, a great deal of research has been done on the characterization and the use of batteries for electric drive train applications. The purpose of the envisaged model in the simulator does not include aspects such as aging and depreciation costs, and are subsequently left out in favor of a simple first order approximation of the storage capacity of the battery.

In section 2.1, the charging behavior of lithium battery cells was outlined, and the fact that maximum charging current has to decrease before the battery reaches a SOC of 100%. Here, the charging and discharging process in the EV is simplified to a constant power behavior, and the capacity is chosen such that it corresponds to a DOD of 80 to 90%. This is a valid consumption, as the SOC of existing EVs is also kept within a certain DOD to extend battery life.
Furthermore, the decision was made to equip all vehicle instances with the same usable battery content of 20 kWh. For comparison, Table 2.1 shows the battery capacity of some contemporary EVs. Technically speaking, 20 kWh would represent a BEV with a total battery capacity of around 24 kWh.

In section 2.2.1, it was briefly mentioned that technical constraints in residential installations will limit charging power to around 3.3kW (16A) or 6.6kW (32A). In fact, to avoid problems due to inadequate wiring or installations, manufacturers even decide to only enable the 3.3 kW power level when the vehicle is plugged into so-called dedicated wall-box. Charging though standard outlets is then typically limited to 2 to 2.5 kW.In the model used here, charging takes place at

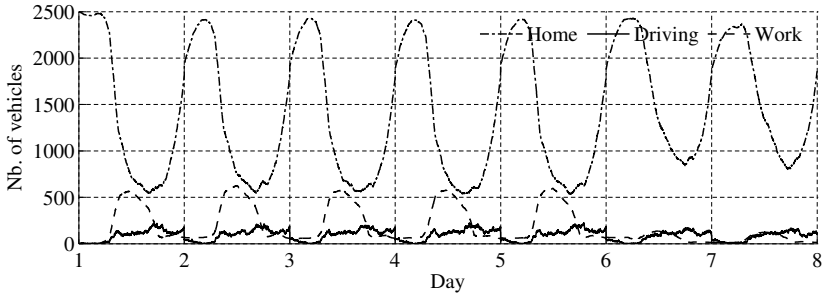

Figure 4.7: Example of the vehicle availability profiles, cumulative for 2 500 vehicles over 7 days

a variable power level between 0 and 3.3 kW.

Driving behavior

To complete the EV model, data about the state of the vehicle during the day (idle at home, driving, unavailable, ...) and the energy consumption while driving is required.

In the work of [93], the results of the 3rd Flemish Mobility Study (OVG3) were analyzed. The latter was commissioned by the Flemish government and looks at the transportation behavior of 8 800 drivers during September 2007 and 2008. Recorded data includes the number of trips each day, distances, motives, departure times, etc. From this, synthetic availability profiles were prepared that can be used in simulations. An example for 2 500 vehicles is shown in fig. 4.7, where the number of vehicles that is at home, driving or at work over the course of 7 days is plotted. It can be seen that behavior of an aggregated fleet is very periodic and therefore predictable.

For the energy consumption model, required power during acceleration and braking (related to vehicle size, aerodynamics and driver habits) has to be added on top of auxiliaries such as lighting, heating, wipers, etc. More information can be found in [14, ch. 2], and [93, 94]. From [93], an average driving speed of 42 km/h is combined with an energy efficiency of 250 Wh/km.

These numbers result in a theoretical range of 80 km for each simulated vehicle. Figure 4.8 shows the cumulative distribution of the SOC of the battery at arrival time, after a simulation with 1 000 vehicles and over 7 days. From the figure, half of the arrivals happened with a battery of almost 80% SOC or more.

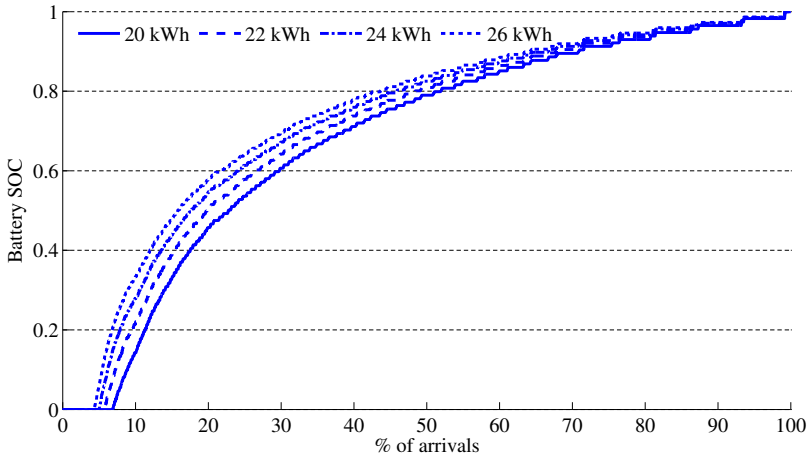

Figure 4.8: Effect of simulated battery size on SOC at vehicle arrival, for different battery sizes, obtained for a set of 1000 vehicles over 7 days

However, for 6.8% of the trips, 20 kWh was insufficient. Simply increasing the usable battery size to 24 or 26 kWh does not eliminate these occurrences, so these trips are too far for the average BEV. It will therefore be assumed that these drivers are using a plug-in hybrid electric vehicle (PHEV) to complete their journey.

On a sidenote, to make simulations repeatable and consistent, a list containing all vehicles is built during initialization of the simulation. After sorting, the order for assigning the driving profiles is determined in such a way that a vehicle is assigned its own profile every time, and independent of the amount of aggregators that is added.

In the simulator, the state of each vehicle at any time is described by its AvailabilityStatus. It has 4 possible values: `HOME`, `DRIVING`, `WORK` and `ABSENT`. The `HOME` state means the vehicle is connected and able to charge. `DRIVING` means the battery is being discharged. `WORK` means connected and able to charge, atlhough in our simulations we have disabled work-charging, since we have no information on the grid connection at the work location, and the amount of vehicles that connects at work is a lot smaller than the amount that charges at home. Lastly, `ABSENT` means a vehicle is not driving and not connected either. Figure 4.7 shows an example set of availability profiles for the home, driving and work states.

4.4.2 Wind energy

In some scenarios, renewable energy production from wind turbines is taken into account. For several locations in the Netherlands, both wind speed measurements and predictions are available. The predictions were calculated by the *Aanbodvoorspeller Duurzame Energie* (AVDE) at ECN [95, 96].

The wind speed values still have to be translated to the correct height of the turbine, as winds aloft generally have a higher velocity than winds at ground level. This effect of altitude on wind speed is logarithmic and can be expressed as in (4.1).

$$\frac{u_z}{u_g} = \left(\frac{h_z}{h_g}\right)^n \tag{4.1}$$

where u_z = wind velocity at height z

u_z = wind velocity at ground station height

u_g = wind velocity at height z

h_z = height z

h_g = ground height z

n = function of the Pasquill stability class and the terrain type

This equation is used to convert the wind speed values to their relevant altitude, depending on the chosen turbine.

Output power profile

The resulting wind speed has to be put alongside the turbine's specified output power. For the turbine specifications, two models from manufacturer Nordex are used, the N80/2500 and the N100/2500 [97, 98]. Both are 2.5 MW turbines, but the N80 is intended for use in strong wind locations, such as offshore, and has a rotor diameter of 80 meters, while the N100 is to be used inland.

Turbines have a cut-in speed which is the minimum wind speed before anything happens, and a cut-out speed, to protect the turbines from too strong winds. Output power is zero during a cut-out. In the model for the simulator, the turbine's power curve is taken from the manufacturer's datasheet and interpolated, as pictured in fig. 4.9.

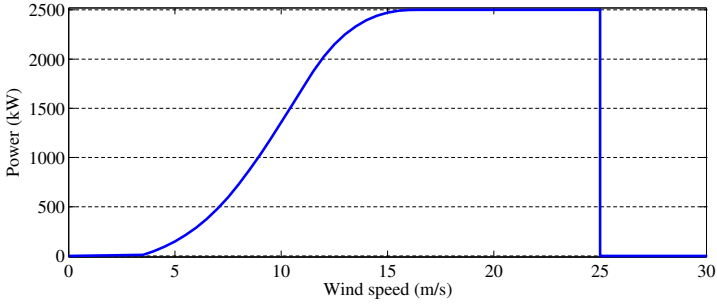

Figure 4.9: Nordex N80/2500 power curve

Predictions

Some scenarios require the use of day-ahead nominations, since the Belgian TSO requires that nominations relating to offtake or injection points are submitted by no later than 14h30 the day before [99]. The available wind generation data consists of predictions that have a horizon of 48 hours, and are updated every 6 hours, meaning that the most accurate predictions that can be submitted are those generated at 12h00 the day before.

4.4.3 Household consumption

To be able to simulate the effects on voltage quality in a distribution grid, realistic household consumption profiles are required. Synthetic aggregated profiles, as available from the VREG and used by energy retailers to estimate their customers' consumption, are too generic. In the Linear project [100], measurements at 100 households were performed over the course of a year, with a resolution of 15 minutes. These profiles were integrated in the simulator, after removal of the 3 profiles with the highest peak load (>20 kW). When more profiles are needed the available set is rotated.

In fig. 4.10, the consumption profile over 7 days of 20 individual households has been plotted on top of each other, starting at day 115 of the year.

4.5 Conclusion

In this chapter, the Java-based framework, which is used as foundation for the implementation and simulation of the DR algorithms and all subsequent

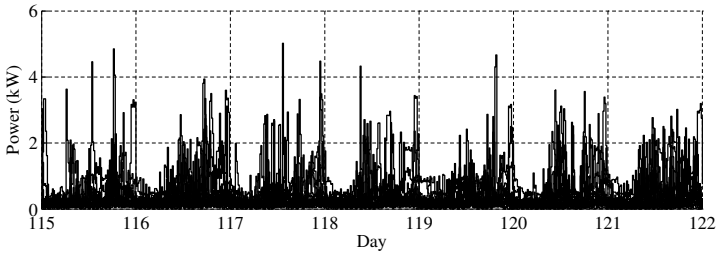

Figure 4.10: Example of the household profile data, for 20 individual households, starting at day 115

scenarios, was introduced. Also the integration with a MATLAB-based loadflow simulator, the logging functions and the implementation of voltage droop control at the DR devices were discussed. In its current state, the simulator encompasses more than 25 000 lines of code, spread over 400 classes.

The next two chapters will elaborate on the agent-based implementation of the MBC algorithm, as first discussed in section 3.3.3.

Chapter 5

Multi-Agent Market-Based Control for Electric Vehicle Charging

5.1 MAS MBC

In section 3.3.3, the fundamentals of Multi-Agent Market Based Control (MAS MBC) and the PowerMatcher were introduced, and the decision to continue with this DR algorithm was explained in section 3.4. The work of [61] extensively describes the theory, advantages and applications of the PowerMatcher, as it was applied in several field tests [101].

In this section, we detail the application of the MAS MBC concept to the case of coordinated charging of EVs. No generating agents will be present in the architecture, shown in fig. 5.1.

First, the demand function strategy for the EV device agents will be discussed, after which the aggregation by the concentrator agents and the objectives by auctioneer or business agent is detailed. Secondly, a way to improve the MAS MBC system by adding planning capabilities is described, based on the work of [102].

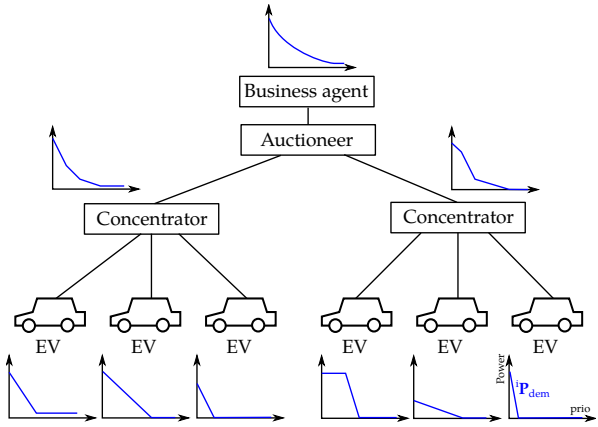

Figure 5.1: MAS MBC architecture for EVs

5.1.1 EV demand function strategy

One of the most crucial facets is the logic behind device agent bidding, as a bid represents the power flexibility or the utility function of an EV. For each device i, a demand function vector is defined as:

$$^i\mathbf{P}_{\text{dem}}(p) = \left\{ ^i f_d(p) \quad \forall p \in \{0,\ 0.1,\ 0.2, \ldots\ 0.99\} \right\} \tag{5.1}$$

with $^i f_d(p)$ the demand function used by the device agent, as a function of the price p. Note that the price is considered merely a control signal and contained within [0,1[for practical reasons. To avoid confusion, we will refer to this price as *priority*. Eventually, the function f_d is sampled at e.g. 100 points to get the demand vector $^i\mathbf{P}_{\text{dem}}$. During charging the utility function will continuously change, and thus the demand function has to be periodically updated to reflect the new state.

Requirements

Different requirements determine the willingness-to-consume of an EV and thus its function $^i f_d(p)$, including:

1. Functionality of the charger. Many currently available electric vehicles do not expose the functionality to be able to vary charging power on a continuous scale. End-of-charge behavior however, requires the charger to be able to reduce current, so the functionality is technically already inside,

and exposing it is mostly a matter of standardization. Some chargers can thus only be switched between on/off, or between a limited number of discrete power values. We refer to chapter 2 for a technical overview of EV charging.

2. Maximum charge power $P_{\max}$, either limited by the vehicle's power electronics or the grid connection. Situations exist during which $P_{\max}$ varies during the charging cycle:
   - In case the battery is almost fully charged and the BMS has detected the maximum cell voltage has been reached. Also known as end-of-charge behavior.
   - Local grid problems, such as voltage deviations, indirectly force the charger to cut charging power. This is also known as voltage droop control and its potentially negative effects on coordinated charging have been discussed in sections 1.4 and 3.6.1.
3. Time till departure Δt_{dep}. To maximize flexibility, it is assumed that the time of the next trip is known upon arrival. In practice, a driver will likely need to enter this time manually (or it is downloaded from a calendar on a smartphone).
4. Required energy E_{req} needed by time t_{dep}. The required energy can be based on the next trip distance, but it is more likely that drivers will want their vehicle fully charged by the time of the next trip. It is assumed that E_{req} is physically feasible; e.g. the required energy does not exceed what can be charged at $P_{\max}$ by departure time t_{dep}.

There are virtually unlimited ways of building an agent's demand function. As it is required for equilibrium markets that agents bid rationally (section 3.3.3), demand functions should always be monotonously decreasing with increasing price.

One relatively straightforward way of building a demand function is by using a corner priority p_r. The corner priority signifies the tipping point where a device agent i would rather not obtain the resource than pay a price for or assign priority ${}^{i}p_r$ to it. In the implementation and simulations of the upcoming chapters, the following demand functions are used.

Asymptotical demand function

The corner priority ${}^{i}p_r$ can be used to create a sloped curve, as illustrated in Figure 5.2. A higher ${}^{i}p_r$ value will give rise to a flatter curve and expresses the

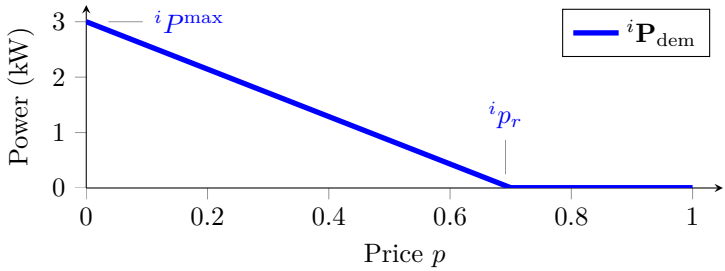

Figure 5.2: Example 'sloped' agent demand function

willingness of a vehicle agent i to consume at higher prices. For convenience, all p values in the system are kept within the range of $[0, 1[$.

$$^{i}f_d\,(p) = \begin{cases} ^{i}P_{\max} - \dfrac{p\ ^{i}P_{\max}}{^{i}p_r} & \text{if } 0 \leq p \leq {}^{i}p_r, \\ 0 & \text{if } p > {}^{i}p_r \end{cases} \tag{5.2}$$

By combining the stated requirements directly, the corner priority $^{i}p_r$ of agent i can be stated as shown in equation 5.3 (and as used in [58]).

$$^{i}p_r = \frac{^{i}E_{\text{req}}}{\Delta^{i}t_{\text{dep}}\ ^{i}P_{\max}} \tag{5.3}$$

As explained before, vehicle agents using a p_r greater than the equilibrium priority will not charge, others will charge at a rate proportional to their individual requirements. This means that less flexible cars (with a less steep demand curve) will be charged first. However, due to an ever decreasing Δt_{dep}, the corner priority p_r tends to increase asymptotically (illustrated by Figure 5.3a). This in turn leads to bids that keep edging towards higher charge power as departure time gets nearer.

Linear demand function

To avoid this effect, a 'linear' demand function can be considered and is shown in (5.4), where $\Delta^{i}t_{\text{dep}}$ and $^{i}E_{\text{req}}$ are combined in an exclusively linear way. The disadvantage of it is the need for a predetermined "offset" to scale these parameters and the fact that $P_{\max}$ is not taken into account. This means that the last point at which charging should commence cannot be taken into account. In (5.4), 12 hours is used as the maximum t_{dep} to consider, and the maximum

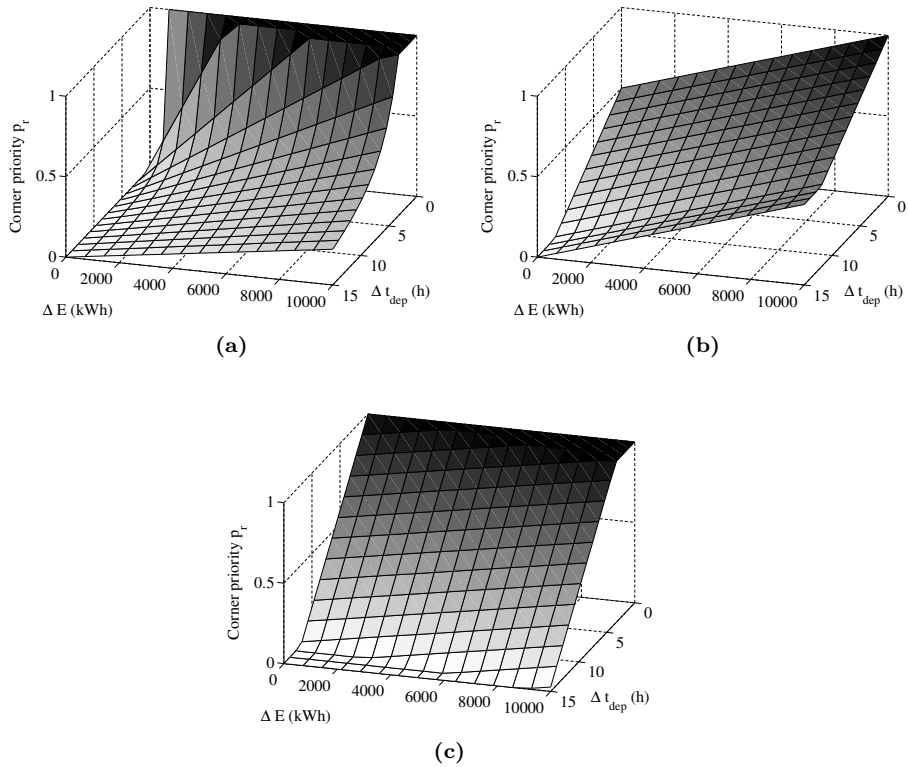

Figure 5.3: Behavior of corner priority p_r in case of the asymptotic function (a), the linear function (b) and the alternative linear function (c)

allowed battery charge $E_{\max}$ is used to normalize the required energy E_{req}.

$$ {}^{i}p_r = 1 - \left(\frac{1}{2} \Delta^{i} t_{\text{dep}}{}' + \frac{1}{2} {}^{i}E_{\text{req}}{}' \right) \tag{5.4} $$

$$ \text{with} \quad \Delta^{i} t_{\text{dep}}{}' = \begin{cases} \frac{\Delta^{i} t_{\text{dep}}}{12\text{h}} & \text{if } \Delta^{i} t_{\text{dep}} < 12\text{h} \\ 1 & \text{if } \Delta^{i} t_{\text{dep}} \geq 12\text{h} \end{cases} \quad \text{and} \quad {}^{i}E_{\text{req}}{}' = \frac{{}^{i}E_{\text{req}}}{E_{\max}} $$

The behavior of this function is illustrated in fig. 5.3b.

Alternative linear demand function

When the maximum charging power $P_{\max}$ is known, an alternative linear demand function can be used, incorporating the time left until the EV has to start charging to obtain its required charge. The function (5.5) is illustrated in fig. 5.3c.

$$ {}^{i}p_r = 1 - \left(\frac{\Delta {}^{i}t_{\text{dep}} - \frac{{}^{i}E_{\text{req}}}{{}^{i}P_{\max}}}{12\text{h}} \right) \tag{5.5} $$

Discrete demand functions

In case the device is limited to on/off charging or a limited set of power values, the demand function is reduced to a step or stair function. Essentially, if all agents bid using step functions, finding the equilibrium and dispatching to the EV agents becomes a ranking process where agents with a utility above p_r are selected to start charging and others have to wait.

$$ {}^{i}f_d(p) = \begin{cases} {}^{i}P_{\max} & \text{if } 0 \leq p \leq p_r, \\ 0 & \text{if } p > p_r \end{cases} \tag{5.6} $$

$$ {}^{i}f_d(p) = \begin{cases} {}^{i}P_{\max} & \text{if } 0 \leq p \leq p_1, \\ \frac{{}^{i}P_{\max}}{2} & \text{if } 0 \leq p \leq p_2, \\ \quad \vdots & \\ \frac{{}^{i}P_{\max}}{4} & \text{if } 0 \leq p \leq p_r, \\ 0 & \text{if } p > p_r \end{cases} \tag{5.7} $$

Figure 5.4 shows two examples of discrete demand functions.

Of course, different heuristics or a heterogeneous mix could be used as well. The choice of demand function has an influence on the behavior of the system, and agents could be allowed to independently select one that reflects their interests better.

Special case: emergency charging and $P_{\min}$

When a vehicle arrives with an energy requirement that cannot be met in time, or if it does not charge quickly enough despite altering its demand function, it is be able to switch to an inflexible charging mode referred to as *emergency charging*. During *emergency charging*, the battery will be charged using its

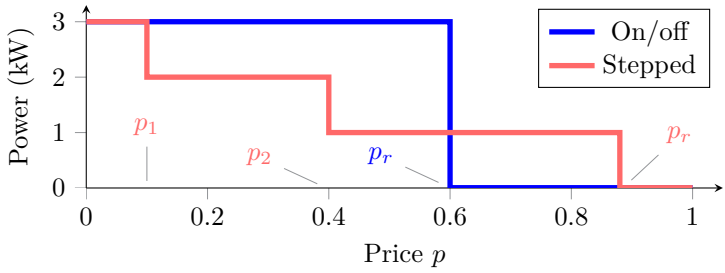

Figure 5.4: Examples of discrete demand functions, for on/off behavior.

maximum allowed power ${}^{i}P_{\max}$. In the MAS MBC system, the agent will represent itself using an inelastic demand function (a horizontal line). In [64], this is called a 'must-charge bid'.

When time is discretized in steps, the use of an inelastic demand function becomes slightly more complicated. Suppose a time interval t_{step} has a length of 15 minutes, and an agent departs in 30 minutes, but it cannot obtain the remainder of its required charge ${}^{i}E_{\text{req}}$ in 15 minutes at ${}^{i}P_{\max}$. Thus, a minimum charging power threshold ${}^{i}P_{\min}$ should be defined at the start of the remaining 30 minutes, such that when the last 15 minutes commence, it could still just get fully charged at ${}^{i}P_{\max}$.

$$\text{If } {}^{i}P_{\max}\left(\Delta^{i}t_{\text{dep}} - t_{\text{step}}\right) \leq {}^{i}E_{\text{req}}$$

$$\text{then } {}^{i}P_{\min} = \min\left(P_{\max}, \frac{1}{\Delta^{i}t_{\text{dep}} - t_{\text{step}}}\left({}^{i}E_{\text{req}} - \left({}^{i}P_{\max}\, t_{\text{step}}\right)\right)\right) \tag{5.8}$$

For very small time steps ($t_{\text{step}} \to 0$), (5.8) amounts to a 'switch' that enables charging at the maximum charging power as soon as the remaining time to departure reaches its critical value t_{critical}:

$${}^{i}t_{\text{critical}} = t \;\Big|\; {}^{i}E_{\text{req}} - {}^{i}P_{\max}\Delta^{i}t_{\text{dep}} = 0 \tag{5.9}$$

5.1.2 Aggregation

When the device agents communicate their demand functions to a higher level in the hierarchical structure, the intermediate agents receiving these will aggregate all incoming bids into a single new one representing the local "cluster". For an

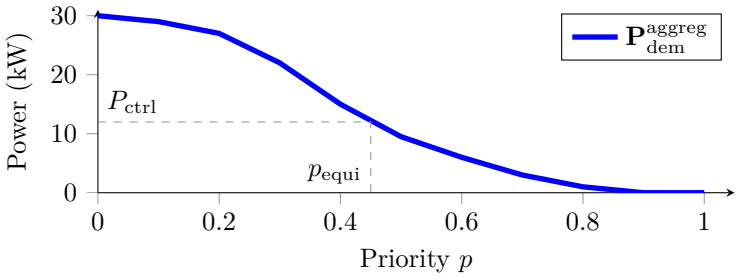

Figure 5.5: Aggregated demand curve example with equilibrium priority p_{equi} and corresponding cluster power P_{ctrl}.

intermediate agent having n connected child agents, the aggregated demand curve is simply the sum at all sampled points of all individual demand vectors:

$$\mathbf{P}^{\text{aggreg}}_{\text{dem}}(p) = \sum_{i=1}^{n} {}^{i}\mathbf{P}_{\text{dem}} \tag{5.10}$$

The differences in departure times of the aggregated demand curves gives rise to a smoothed curve as exemplified in fig. 5.5.

Optionally, the concentrator agents can be responsible for reshaping their aggregated demand curves $\mathbf{P}^{\text{aggreg}}_{\text{dem}}$ in order to enforce some local constraints, e.g. the maximum power limit of a transformer.

5.1.3 Auctioneer & objective agent

In the MAS MBC concept, the task of the auctioneer agent is to determine the equilibrium priority such that demand and supply is balanced. When used exclusively for the coordinated charging of EVs, there will be no device agents offering supply bids (with the exception of V2G enabled vehicles, but even in that case, supply and demand is likely to be uneven and fluctuating through time) and the cluster will not be able to balance itself.

Therefore the auctioneer agent is linked with a business agent, providing power setpoints for the cluster. The logic behind the setpoints can be based on a simple predetermined schedule, tracking the output of a wind turbine, etc.

Once a power setpoint P_{ctrl} has been decided, it is matched in the aggregated demand curve to obtain the corresponding equilibrium priority, as per (5.11). Then, p_{equi} is sent back to all the concentrators and device agents, who will

match p_{equi} with their submitted demand curve.

$$p_{\text{equi}} = \mathbf{P}_{\text{dem}}^{\text{aggreg}} \mid P_{\text{ctrl}} \tag{5.11}$$

5.2 Multi-agent MBC with planning

As explained in section 3.3.3, the MAS MBC algorithm ignores the interdependency in the demand of the participants over time. The reason is that a market with a single commodity, being power consumption during the next time slot, significantly reduces the complexity of the mechanism.

Some types of loads, such as a washing machine, have a fixed uninterruptable power profile once started, or depend on unpredictable user behavior, such as a water tank heater, complicating the modeling of their constraints over a horizon. For loads that can store electric energy, such as EVs, this is much more straightforward, using an energy constraints graph.

5.2.1 Energy constraints graph

To be able to capture the time-dependent part of a vehicle's energy constraints, additional information is added to the information sent by device agents [102].

Individual agent's energy constraints

The individual energy constraints of each EV i are expressed by two vectors ${}^{i}\mathbf{E}_{\max}$ and ${}^{i}\mathbf{E}_{\min}$.

The vector ${}^{i}\mathbf{E}_{\max}$ is the energy path of an EV agent i if it were to start charging immediately at maximum power and then (at ${}^{i}t_{\text{idle}}$) stay idle until its departure ${}^{i}t_{\text{dep}}$. On the other hand, ${}^{i}\mathbf{E}_{\min}$ represents the case when charging is postponed as long as possible (up to ${}^{i}t_{\text{critical}}$). This is expressed in equations 5.12 and 5.13 respectively and illustrated in fig. 5.6. All area in between ${}^{i}\mathbf{E}_{\max}$ and ${}^{i}\mathbf{E}_{\min}$ represents the flexibility of the charging process.

$${}^{i}\mathbf{E}_{\max} = \left\{ {}^{i}E_{\max}(t) \mid {}^{i}E_{\max}(t) = \min\left(t\ {}^{i}P_{\max}, {}^{i}E_{\text{req}}\right) \right.$$
$$\left. \forall t \in \left\{0, 1, ...\Delta {}^{i}t_{\text{dep}}\right\}\right\} \tag{5.12}$$

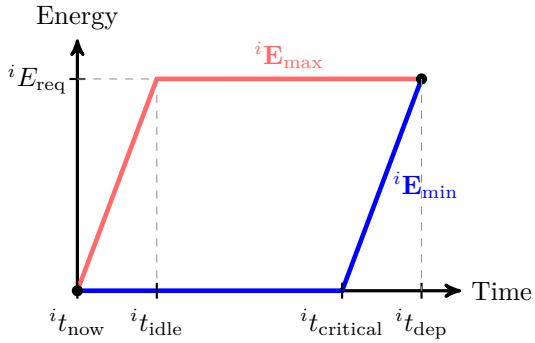

Figure 5.6: Energy constraints graph for an individual agent i

$$ {}^{i}\mathbf{E}_{\text{min}} = \left\{ {}^{i}E_{\text{min}}(t) \mid {}^{i}E_{\text{min}}(t) = \max\left({}^{i}E_{\text{req}} - \left(\Delta^{i}t_{\text{dep}} - t\right) {}^{i}P_{\text{max}}, 0\right) \right. $$
$$ \left. \forall t \in \left\{0, 1, ...\Delta^{i}t_{\text{dep}}\right\}\right\} \quad (5.13) $$

Thus t in above equations is used as a relative index of the vectors ${}^{i}\mathbf{E}_{\text{x}}$, with $t = 0$ corresponding to the current time t_{now} and $\Delta^{i}t_{\text{dep}}$ to the remaining time before departure.

$$ \Delta^{i}t_{\text{dep}} = {}^{i}t_{\text{dep}} - {}^{i}t_{\text{now}} \quad (5.14) $$

For practical reasons, time in the graphs is discretized in steps with length t_{step}, which does not have to equal the step size used in section 5.1.

In case of *emergency charging*, described in 5.1.1, the agents' ${}^{i}\mathbf{E}_{\text{max}}$ and ${}^{i}\mathbf{E}_{\text{min}}$ vectors will simply overlap, leaving no flexibility; no other path than charging at maximum power is possible.

Aggregated energy constraints

To represent the battery constraints of an entire PHEV fleet of n vehicles, the individual constraints are aggregated into collective battery constraints $\mathbf{E}_{\text{max}}$ and $\mathbf{E}_{\text{min}}$, at the intermediate agents and the auctioneer agent. This is illustrated in fig. 5.7.

$$ \mathbf{E}_{\text{max}}^{\text{aggreg}} = \sum_{i=1}^{n} {}^{i}\mathbf{E}_{\text{max}} \quad (5.15) $$

$$ \mathbf{E}_{\text{min}}^{\text{aggreg}} = \sum_{i=1}^{n} {}^{i}\mathbf{E}_{\text{min}} \quad (5.16) $$

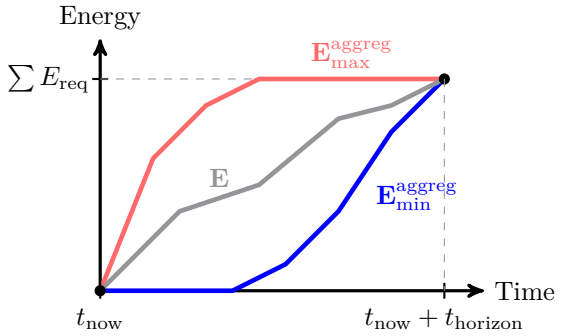

Figure 5.7: Aggregated energy constraints graph and an energy path $\mathbf{E}$

5.2.2 Optimization

With an aggregated energy constraints graph available to the auctioneer/objective agent, it is possible to determine a charging schedule that respects the charge constraints of the vehicles (represented in $\mathbf{E}_{\text{min}}^{\text{aggreg}}$ and $\mathbf{E}_{\text{max}}^{\text{aggreg}}$) and plans an optimal allocation of their energy consumption over the time period $[t_{\text{now}}, t_{\text{now}} + t_{\text{horizon}}]$. This optimal energy path $\mathbf{E}_{\text{opt}}$ can be determined by means of various objectives.

In a Time-of-Use (ToU) scenario, for example, energy for the fleet is bought by the aggregator with the goal of minimizing total cost. Examples of costs involved are distribution costs, generation costs and energy bought at energy markets (e.g. at the day-ahead or intra-day market). With ToU, the market energy price is volatile and can change every hour, so fleet charging can be optimized to take place as much as possible during low-price periods.

The cost model C, a function of the aggregated EV charging energy $\mathbf{E}$ over the time horizon, and the aggregated energy constraints constitute the complete optimization problem:

$$\mathbf{E}_{\text{opt}} = \underset{\mathbf{E}}{\text{argmin}}\, C(\mathbf{E}) \tag{5.17}$$

$$
\begin{aligned}
\text{with:} \quad & \mathbf{E} = \{E^{\text{aggreg}}(t) && \forall t \in \{0, 1, \ldots, t_{\text{horizon}}\}\}\,, \\
\text{subject to:} \quad & P_t \leq P_t^{\text{limit}} && \forall t \in \{0, 1 \ldots, t_{\text{horizon}}\} \\
& E_t^{\min} \leq E_t \leq E_t^{\max} && \forall t \in \{0, 1 \ldots, t_{\text{horizon}}\} \\
& E_{t+1} = E_t + P_t \Delta t && \forall t \in \{0, 1 \ldots, t_{\text{horizon}} - 1\}
\end{aligned}
$$

where t_{horizon} is the horizon of the aggregated graph, and P_t^{limit} the power limits of the cluster. Power limits can be built from the devices' energy constraints graph and aggregated into a cluster-wide P_t^{limit}.

Depending on the shape of the objective function C, different solution methods can be used to solve this problem (e.g. linear or quadratic programming). The result of solving this optimization problem is the energy vector $\mathbf{E}_{\text{opt}}$. In turn, the energy values in this vector can be translated into power setpoints for each time step, $\mathbf{P}_{\text{ctrl}}$ which defines control values from time 0 (t_{now}) until t_{horizon} for the entire fleet:

$$\mathbf{P}_{\text{ctrl}} = \{P_0,\ P_1,\ P_2,\ \ldots\ ,\ P_{t_{\text{horizon}}}\} \tag{5.18}$$

From $\mathbf{P}_{\text{ctrl}}$, the first step P_0 is selected and translated into an equilibrium price p_{equi} using the aggregated bid curve. The procedure of controlling the vehicles follows the same logic as for the MAS MBC without planning (section 5.1.3).

5.3 Shortcomings

While the addition of the energy constraints graph provides an elegant way to add scheduling capabilities to the MAS MBC algorithm, it also has a few shortcomings.

- Energy constraints graphs are well suited when dealing with electric storage devices, such as EVs and fixed battery storage. However they are less than ideal for other types of appliances, such as thermal storage units, micro CHPs or household devices that have variable consumption and cannot be interrupted once started.
- The use of heuristics to assign power among the device agents is not always optimal compared to a central optimization [102], resulting in a deviation from the optimal path determined by the aggregator's business

logic. This cause of path deviations will be explained further down this section.

- Lack of 'multi-commodity' optimization. Multi-commodity can mean different types of energy (heat, gas, electricity) in the same market, but also energy at different points in time.
  - It is not possible to include interdependencies between electricity used in different time periods in the device agent's 'bidding'.
  - Combining e.g. a micro CHP or heat pump with charging EVs in one virtual market also poses a problem, since one group of consumers could 'dominate' the behavior of the other group. It therefore makes sense to keep the demand functions of different types of agents separated. The optimization at the auctioneer or business agent can still take these into account.

As already touched upon before in section 3.4, the MAS MBC approach represents a compromise between a fully centralized and fully distributed approach. While other algorithms might result in a closer-to-optimal outcome, they add a lot of computational burden and/or would be difficult to implement in practice at reasonable cost. The hierarchical architecture using the concentrator agents gives the MAS MBC good scalibility properties.

Path deviations

In fig. 5.8, the mechanism leading to energy path deviations is shown for a fictitious case of two charging vehicles. EV1 wants to depart at time t_1 while EV2 wants to depart at a later time, t_2. The aggregator's objective is to charge both EVs in time at the lowest possible cost according to the price profile at the bottom of the figure. The optimal solution would be to first charge EV1 before the first price peak, and then EV2, which has still enough time left to be scheduled to charge during the lowest part of the price curve. This situation and optimal energy path E_{opt} is represented on the left of the figure.

In reality though, energy will be consumed according to the energy path on the right side version in the figure. In the optimal case, before time t_1, EV1 charges exclusively. But, due to the use of demand curves and equilibrium priorities to distribute charging power among the fleet, EV2 will take part of the charge power that would optimally go entirely towards charging EV1.

The latter is illustrated by fig. 5.8b, where the demand curves for both vehicles, before time t_A, are plotted. Because the demand curve of EV2 is not zero at the equilibrium priority p_{equi}, EV2 will charge at a low power. After time t_A, when

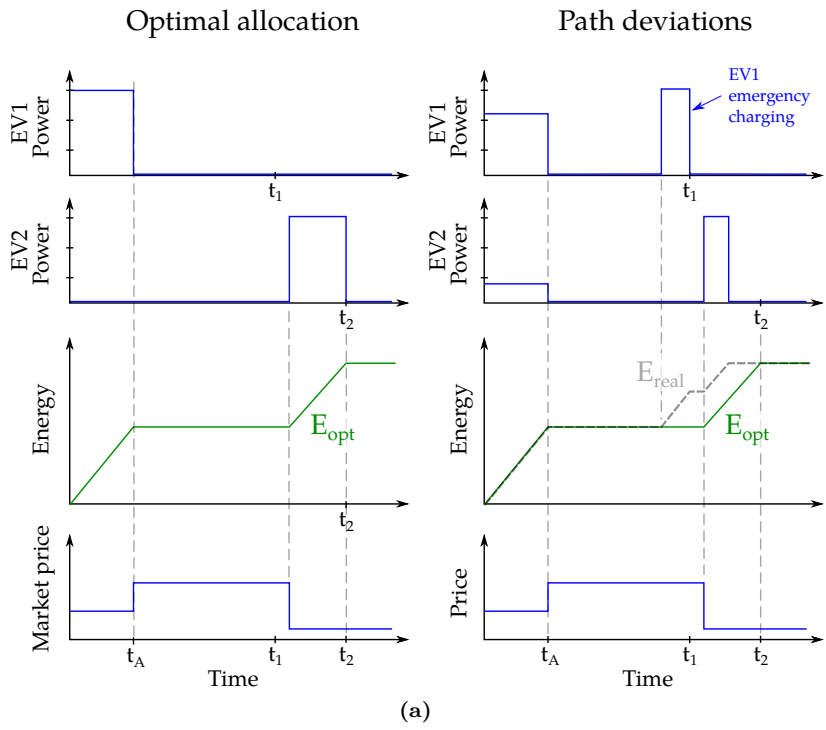

(a)

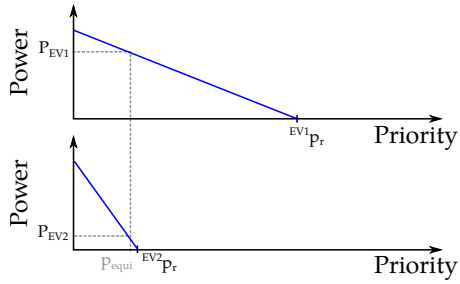

(b)

Figure 5.8: Underlying mechanisms of path deviations; (a) power profiles and aggregated energy path of EV1 and EV2, and aggregator price profile and (b) demand curves of EV1 and EV2 before time t_A

the price rises, the aggregator will choose a high equilibrium priority, to avoid charging taking place. But, because EV1 was not fully charged yet, its agent will be forced to enable emergency charging at a time when this is not optimal anymore from a cost perspective. Later on, EV2 will again start charging, but already has most of its charge and terminates earlier than during the optimal allocation. The result is that the followed path E_{real} deviates from the optimal one E_{opt}.

Use of time slots

In section 1.4.1, the need for coordination on a continuous time scale was stated. However, the MAS MBC method inherently relies on the use of time slots to periodically send updates of the demand function, and the energy constraints graphs are discretized in time for practical reasons. In reality, EVs (and other appliances) operate asynchronously, and it could be very useful to be able to quickly dispatch schedule changes to every DR device at any instance.

There are several ways to overcome this, mainly by either increasing the frequency of updates, or switching to an entirely event driven architecture to exchange the coordination information. Since smaller time steps only partially address the response-time problem and will increase the amount of communication between the DR agents and the concentrators, a native event driven solution is preferred.

5.4 Conclusion

In the first part of this chapter, the application of the MAS MBC DR algorithm from section 3.3.3 to charging EVs was expounded. Subsequently, the use of energy constraints graphs was explained in order to add planning functionality, originally the work of [102]. Eventually, a few shortcomings were discussed, being mainly the occurrence of path deviations due to the use of a heuristic to dispatch the planned power.

The goal of this chapter was not to introduce new contributions to the MBC approach, but to provide a solid foundation of its concepts when applied to EVs, such as the demand functions, and give a more detailed description of the shortcomings of this aggregate & dispatch algorithm. The following chapter will introduce our modifications to the Multi-Agent MBC so that it can function as an event-driven system. A large part of the work in that chapter is based on [19].

Chapter 6

Event-based Multi-Agent Market-Based Control: RT-MBC

In this chapter the challenges associated with integrating existing charge coordination algorithms in a real-world environment are discussed, after which a number of modifications to the MAS MBC algorithm are proposed to overcome these problems.

6.1 Introduction

As explained in chapters 1 and 2, communication takes on an important role in demand side management of EVs. Charging requirements and constraints need to be communicated to an aggregator, while aggregators need to send control signals back to EVs in order to steer their charging power towards cluster-wide goals. In terms of integrating charge coordination algorithms into a realistic "real-world" environment, two challenges are identified: continuous coordination, and messaging limitations.

6.1.1 Integration challenges

The first challenge is the need for continuous coordination of the charging process. In energy markets, charging only needs to be optimized in terms of energy volume per hour. However, vehicles arrive and depart continuously, and will want to start charging or depart at asynchronous times. This means that, ideally, control and coordination actions should also commence immediately, especially for fast-charging applications, and allow for quickly altering the fleet's behavior if the need arises.
Consequently, charging needs to be coordinated at two levels: a market level, where time is divided in time slots, and a real-time, event-driven level that is focused on responsiveness.

The second challenge is related to the exchange of messages between EVs and an aggregator. In reality, the underlying infrastructure places constraints on the communication, pertaining to packet delays, link reliability or maximum throughput. In the latter case, the exchange of messages should be limited by the coordination mechanism.

6.1.2 Coordination levels

In addressing these challenges, two levels of operation in coordination mechanisms for demand-side management are identified; a *market operation level* and a *real-time operation level*:

1. The market operation level entails actions with the goal of following beforehand traded volumes on the wholesale electricity markets, where trading takes place on relatively long-term scale (months, seasons) and amounts are expressed as energy quantities (usually MWh) in time slots of typically 1 hour or 15 minutes. This is shown on the right of fig. 6.1.

2. The real-time[1] operation level entails the actions to comply with consumer preferences and respect local grid constraints. Because changes and control are relatively more instantaneous and dynamic at this level, real-time operation is usually expressed in terms of electrical power (e.g. kW). Granularity is in the range of minutes to seconds. At this level, fast responses are important and the number of exchanged messages will be limited. This is shown on the left of fig. 6.1.

[1]With real-time, we denote occurrences of asynchronous and continuous nature, or happening in 'short notice'. No link with real-time constraints as in having strict deadlines is implied, although this might be of relevance for the control systems involved at this level.

Figure 6.1: The two levels involved in coordination of a cluster of devices

This notion has common ground with the conflict in control between Commercial Virtual Power Plants (CVPP) and Technical Virtual Power Plants (TVPP), by the FENIX project [103, 104].

From chapter 3, it was clear that many existing algorithms make use of time slots. While convenient during simulations, they inherently do not consider changes that occur within a time slot, such as arriving or departing vehicles or external events. This approach can be problematic in a direct field implementation. Decreasing the time slot interval length to the order of seconds or minutes addresses this problem only partially, as it directly affects scalability; agent communication and required computational power would rise quickly and prevent the use of large clusters of agents.

Therefore, to bring the approach from section 3.3.3 and 5 to the real-time domain but retain its favorable scalability properties, we introduce the following additions:

1. *Dual coordination* by splitting the auctioneer agent in an asynchronous[2] part, the fleet manager, and a synchronous part, controlled by a market operator agent.
2. *Event-based interaction* between the agents, for communicating constraints and equilibrium priorities.
3. *Caching* of constraints and equilibrium priorities.
4. Energy *constraints graphs alignment* and start point estimation.

In the next sections, these additions will be discussed in detail.

[2]Asynchronous as the opposite of periodic.

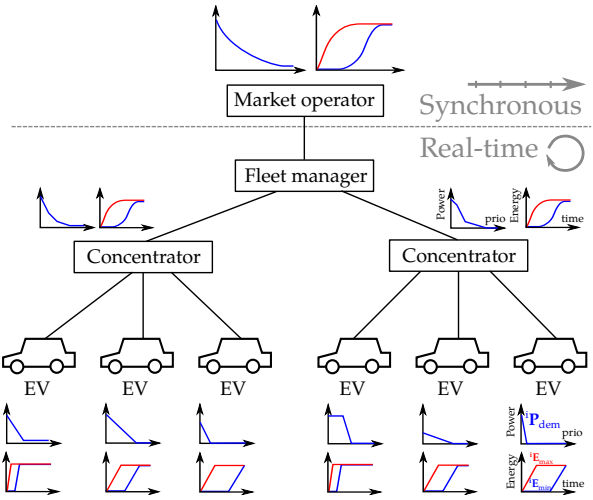

Figure 6.2: MAS MBC architecture with dual coordination

6.2 Dual coordination

The dual coordination approach separates the synchronously operating auctioneer agent of section 5.1.3 into a real-time part, the fleet manager, and a periodically moving part, the market operator. Additionally, to improve scalability, concentrator agents are inserted. The resulting agent hierarchy is illustrated in Fig. 6.2.

The *market operator* is responsible for global optimization of the cluster. Because of its connection to the energy markets, the market operator will typically act on a periodic basis, for example every hour or 15 minutes. When it has determined a new strategy or optimum, it will pass a power or energy setpoint to the fleet manager.

The *fleet manager* is in the real-time domain and receives the result of the optimization by the market operator as a schedule containing power setpoints. Using the demand vector, it will attempt to steer the global consumption of the fleet in real-time towards this schedule by varying the equilibrium priority p_{equi}.

Concentrator agents aggregate the charging constraints from an underlying cluster of agents and appear as a single entity to the agent above it. They also perform the necessary agent-housekeeping by keeping track of arriving and departing EVs. By aggregating constraints data, concentrators improves the scalability of the system. If necessary, multiple levels of concentrator agents

could be used.

6.3 Event-based interaction

As mentioned in the previous section, one of the major additions to the MAS MBC is the step towards an event-based approach, to bring the charging coordination system in line with real-world implementations. The first subsection provides a general overview of the term *event-based system* in literature, after which the application in the MAS MBC is discussed.

6.3.1 Event-based systems in literature

The design of distributed computer systems today is mainly influenced by the effects of networking. There are two main requirements: scalable communication mechanisms to support large numbers of possibly dynamic components, and automation of data processing to improve functionality [105, ch. 1].

Middleware

To facilitate communication between entities under these requirements, *middleware* was introduced. Middleware is an additional layer positioned between the operating systems of individual nodes and a distributed application. In client-server middleware, system components direct inquiries to remote objects (e.g. databases) using response-reply interaction. Well-known examples are RPC and SOAP.

However, some shortcomings of request/reply interactions appear when used in a dynamic environment. Because communication proceeds synchronously and clients have to poll remote data sources to check for changes, resources are wasted and scalability suffers. Additionally, the configuration of the system is mixed with the application logic (e.g. by hardcoding the remote procedure calls) which is problematic, especially when there are functional dependencies between the system's components.

Event-based computing

Event-based computing contrasts with the conventional request/reply interaction by loosely decoupling the system components. Components communicate by

generating or receiving event notifications. An event in this context is any transient occurrence of a happening of interest, e.g. a state change observed in or by a computer [106]. A notification is created by the observer of the event and can contain data about the event and additional information (e.g. time-value pairs). Notifications are then conveyed between endpoints of a communication system via messages.

Event-based systems are commonly implemented as publish-subscribe middleware, where the components either act as producers or consumers of notifications. Figure 6.3, from [105, ch. 2], shows its constituents.

- A *producer* publishes notifications, and the decision to publish a state change is part of its core functionality. Important is the fact that a producer is not directly aware of any receivers, as the published notifications are passed to a notification service which handles further distribution.
- A *consumer* reacts to the notifications delivered to it by the notification service. Similar to the producers, they are not aware of the specific senders of the notifications. Consumers need to subscribe with the notification service to receive the notifications they are interested in. A consumer can simultaneously be a producer as well.
- The *event notification service* is the mediator that decouples abovementioned producers and consumers. It implements a publish/subscribe interface. Advertisements describe the available set of notifications and filters are used to forward the notifications to the subscribed consumers.

The event-based interaction model separates computation from communication [105], which promotes evolvability of the system. But the orchestration between the components considerably increases complexity and depending on an application's particular requirements, parts of the above components can be simplified or even omitted.

6.3.2 Event-based multi-agent MBC algorithm

Multi-agent systems are inherently suitable for asynchronous operation as all agents are autonomous entities that execute concurrently. The MBC concept on the other hand is inherently synchronous, because it needs to clear a virtual market at predetermined intervals. In PowerMatcher, a typical trading period is 15 minutes [107], down to 5 minutes.

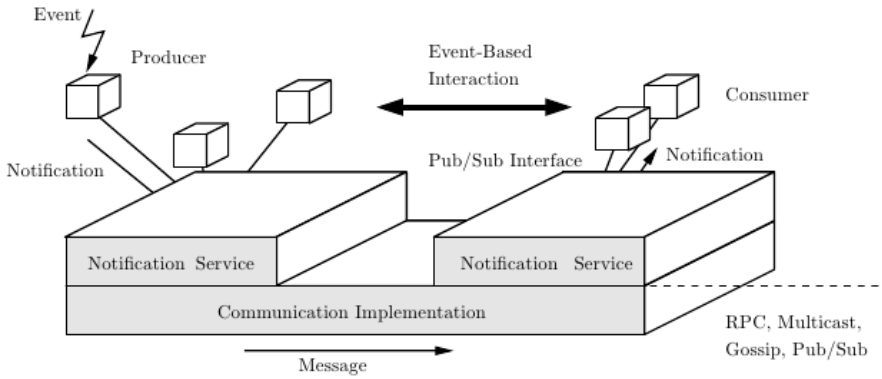

Figure 6.3: Components and interactions in an event-based system [105, ch. 2]

Event identification

Making the step from a synchronous algorithm to a an event-driven one, the possible events in the real-time part of the system are identified:

- Vehicle arrival or departure: a vehicle is plugged in for charging or disconnects. The latter can happen either if the driver departs or when the battery is fully charged, meaning no further charge coordination can be done.
- Availability of updated constraints data: the agent (or the driver himself) changes the charging schedule. The demand vector ${}^{i}\mathbf{P}_{\text{dem}}$ is updated to reflect these changes.
- Availability of updated equilibrium priority p_{equi}: the fleet manager or concentrator agents distribute new priority data.

Following the notion of an event-based system in literature, a separate event notification system, advertising functionality and event filtering would be needed. However, for the needs of the event-based MAS:

- Only a limited number of event types & notifications can occur.
- Only a limited number of different components are involved.
- Notifications between agents in the hierarchical structure always move between two adjacent levels. A central notification service would impact scalability and robustness, thus each level would benefit from its own event-based system.

This leads us to simplify the event-based system design, but such that the principles of event-based systems from section 6.3.1 still apply.

In case of the arrival event, the associated device agent registers itself with the local concentrator agent. A mutual subscription is established: the concentrator agent is notified when new demand functions are available from this agent and the agent is subscribed to notifications of new equilibrium priority information. When departing, a similar "unregister" action is performed.

Furthermore, agent addressing is handled by a separate lookup service (an agent directory), that has meta information on agent hierarchy.

This enabled e.g. device agents to query for their closest concentrator agent. In full-fledged event-based systems, everything is handled by notification services, while here we have some sort of *dependency injection* pattern.

Message ordering & time stamps

As opposed to a time slot based control system, interaction between agents happens asynchronously. For demand vector data that passes from one agent to a higher level in the tree, this could mean that replies carrying the latest p_{equi} are not necessarily related to the last submitted demand of that agent. This problem is visualized in Figure 6.4a.

Device agents would then apply this p_{equi} on a demand vector that has not yet been incorporated in the fleet manager's optimization. Caching will further aggravate this effect. To keep demand vectors and priorities partially ordered, inspiration was drawn from Lamport time stamps [108].

In this implementation, device agents add a time stamp from their local clock to the messages containing demand curves. It is supposed that this clock can be derived from an accurate source such as a GPS receiver. When a concentrator assembles an aggregated demand curve message, it adds the time stamp of the most recent included demand curve. The fleet manager preserves this time stamp when sending back an equilibrium priority. Upon receiving the priority, the time stamp can be used to look up the relevant demand curve, if a more recent one was submitted already. This requires that the device agents store the 2 or 3 last demand functions they sent. See Figure 6.4b.

6.3.3 Caching

When an event occurs at the EVs, a constraints update is sent upwards, a new equilibrium determined and then propagated downwards again. To avoid a

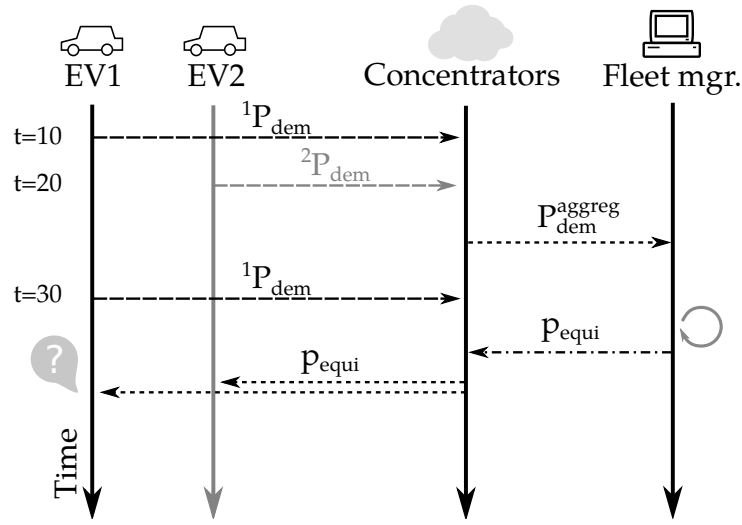

(a) Visualization of the ordering problem when demand function and equilibrium priority data is passed asynchronously. When EV1 receives the equilibrium priority, it cannot know to what submitted demand function it refers.

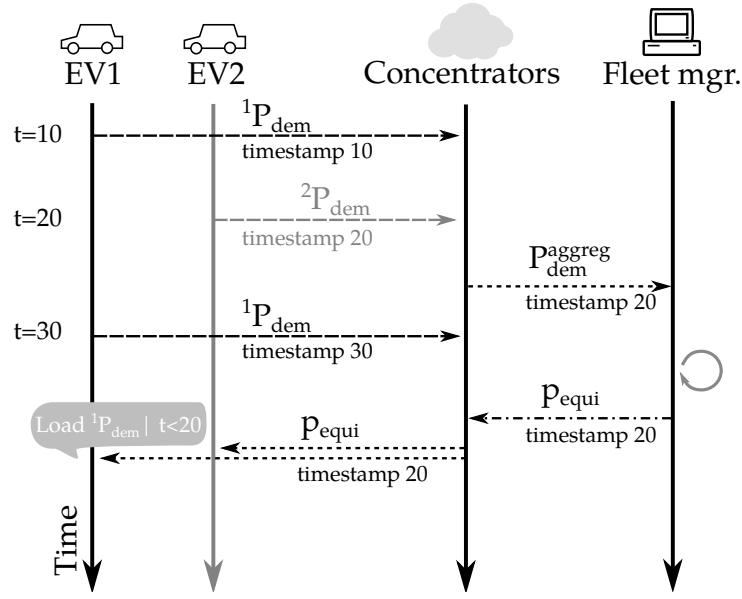

(b) Using time stamps to find the relation between submitted demand function and equilibrium priority

Figure 6.4: Demand function ordering problem (a) and its solution using time stamps (b)

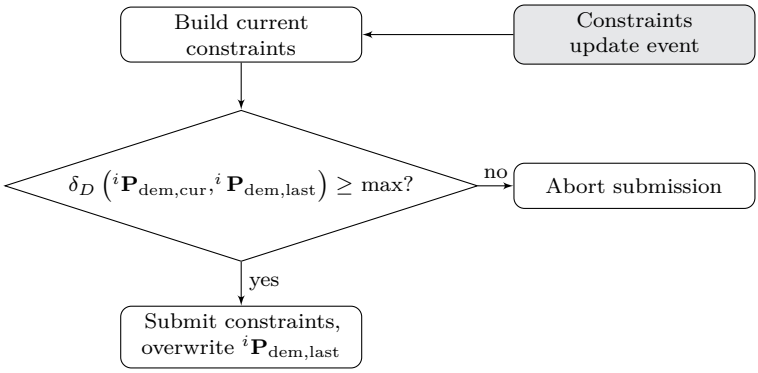

Figure 6.5: Demand vector caching strategy for a real-time EV agent i

continuous flood of these updates in case of large fleets, a caching scheme is implemented. Updates are sent when changes are deemed to have sufficient impact on either the demand vectors or the equilibrium priority.

Demand vectors

At the level of EV agents, the periodically rebuilt demand vector ${}^i\mathbf{P}_{\mathrm{dem,cur}}$ is compared with the last one sent to the local concentrator, ${}^i\mathbf{P}_{\mathrm{dem,last}}$. Their difference is quantified by determining the bounded discrete Fréchet distance between two demand vectors $\mathbf{P}_{\mathrm{dem},1}(p)$ and $\mathbf{P}_{\mathrm{dem},2}(p)$ as shown in 6.1.

$$\delta_D\big(\mathbf{P}_{\mathrm{dem},1}(p), \mathbf{P}_{\mathrm{dem},2}(p)\big) = \min_{\substack{\alpha[0,1[\\ \beta[0,1[}} \left\{ \max_{t\in[0,1[} d\left[\mathbf{P}_{\mathrm{dem},2}\left(\alpha(t)\right), \mathbf{P}_{\mathrm{dem},2}\left(\alpha(t)\right)\right] \right\} \tag{6.1}$$

with d the Euclidian distance function and $\alpha(t)$,$\beta(t)$ arbitrary discrete nondecreasing functions such that $\alpha(t), \beta(t) \in \{0.1,\ 0.2, ...0.99\}\, \forall t \in [0, 1[$. δ_D will then give the shortest coupling distance between the two demand vectors, which is a measure of how much $\mathbf{P}_{\mathrm{dem},1}$ and $\mathbf{P}_{\mathrm{dem},2}$ resemble each other. If $\alpha(t) = \beta(t)$, a simple maximum distance remains. The demand vector caching process is shown in fig. 6.5.

Demand vector caching is also applied at the concentrator agents to decide if an aggregated vector should be sent upwards. Logically, the maximum allowed deviation should be larger than for an individual agent.

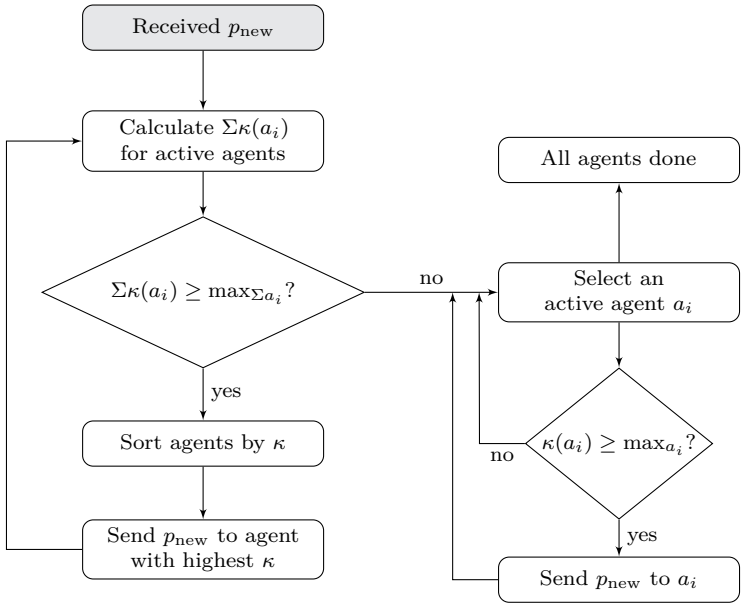

Figure 6.6: Real-time concentrator agent equilibrium priority caching strategy

Equilibrium priorities

Upon receiving a new equilibrium priority from the fleet manager or another concentrator agent, a decision needs to be made whether to send this information immediately to agents lower in the tree or hold on to it for longer. During this process, illustrated in Fig. 6.6, impact numbers κ are calculated according to (6.2). They are the difference between (estimated) power $P(\mathbf{P}_{\text{dem}}, p)$ when the old equilibrium priority p_{old} is kept and when the new one p_{new} would be applied on agent a_i's last submitted demand vector ${}^{i}\mathbf{P}^{\text{dem}}_{\text{last}}$ instead.

$$\kappa(a_i) = \left| P({}^{i}\mathbf{P}_{\text{dem,last}}, p_{\text{old}}) - P({}^{i}\mathbf{P}_{\text{dem,last}}, p_{\text{new}}) \right| \tag{6.2}$$

For every newly received p_{equi}, a distinction is made between impact of the concentrator as a whole, $\sum \kappa(a_i)$, and individually per PHEV agent managed by that concentrator, $\kappa(a_i)$.

The downside of using caching techniques on the equilibrium priority is that agents higher in the tree structure have no way to know whether each device agent will receive the new information. This will invariably lead to deviations between the real consumed power and the optimized value by the fleet manager. Of course, more aggressive caching parameters will give rise to larger discrepancies

but less messages to the device agents. The choice of caching parameters will be further looked into in section 7.2.

If the power values of the device agents are known on a short time-base, it may be possible to compensate these discrepancies at the fleet manager. This is discussed in section 6.4.

Energy constraints

Energy constraints graphs are not cached, because they do not change in the same way the demand function does. However another problem arises when using energy constraints graphs in a continuously changing system, and is discussed in the next subsection.

6.3.4 Energy constraints graphs

The energy constraints introduced by [102] are tailored to the use of time slots; the starting time t_{start} is always the same for every agent that submits constraints. In the asynchronous situation, this does not hold; at the time of aggregation t_{now}, the energy constraints from the PHEVs stored at the concentrator differ in the time they were built. Figure 6.7 illustrates this problem. To avoid contacting every device agent again when aggregating, some adjustments are made:

Sampling interval

If a 15 min. sampling interval would be used as in [102], the maximum error arising due the time discretization at a consumption of 3.3 kW amounts to 413 Wh (as time is rounded to the nearest sampling interval multiple, but charging power is not allowed to exceed the charger's maximum of 3.3 kW). By reducing it to 180 secs, the error is reduced to 83 Wh. The increase in amount of samples can be offset by parameterizing the graph and resampling it upon aggregation, or by using non-uniform sample intervals.

Alignment & energy estimation

During aggregation, the devices' individual energy constraints need to be re-aligned such that all of them start at the current time t_{now}. As a consequence, the aggregated energy constraints graph can become "open-ended" on both

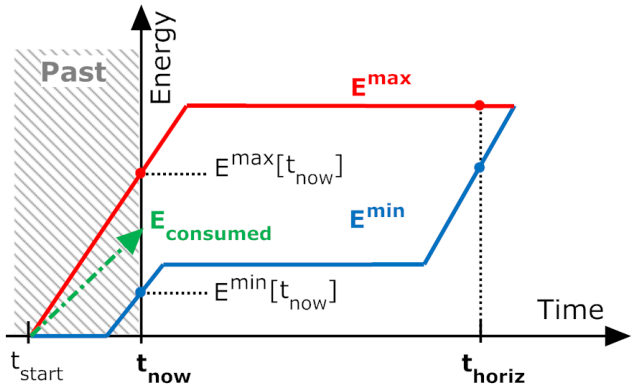

Figure 6.7: Concentrator energy constraints estimation. If the aggregated energy constraints graph is based on data received some time before t_{now}, the shifted start of the vectors $E_{\max}$ and $E_{\min}$ at t_{now} will not overlap. The concentrator has to make an estimate E_{consumed} on the followed energy path of the EVs under its control.

sides (meaning that $E_{\min}$ and $E_{\max}$ do not coincide at the graph limits t_{now} and t_{horiz}) as illustrated by Fig. 6.7.

If the starting point of one or more devices' constraints curve lies in the past (e.g. t_{start}), it means that by t_{now} the concentrator's devices will have accumulated some energy E_{consumed} (6.3). Neglecting E_{consumed} leads to an energy underestimation during optimizations by the market operator, in turn leading to overestimated power setpoints for the fleet operator.

As the concentrator holds the constraints and priorities associated with every agent i, it is possible to estimate $E_{\text{consumed},i}$ by integrating $P\left({}^{i}\mathbf{P}^{\text{dem}}_{\text{last,t}}, p_{\text{last,t}}\right)$, where ${}^{i}\mathbf{P}^{\text{dem}}_{\text{last,t}}$ is the last submitted demand vector at time t of agent i for which a corresponding priority $p_{\text{last,t}}$ was sent back. This is shown in equation (6.4). Deviations can occur when there is a delay between the concentrator sending priorities and the devices acting upon it.

$$\mathbf{E}_{\max}[t_{\text{now}}] \geq E_{\text{consumed}} \geq \mathbf{E}_{\min}[t_{\text{now}}] \tag{6.3}$$

$$\text{and} \quad E_{\text{consumed}} = \sum_{i} E_{\text{consumed},i}$$

$$E_{\text{consumed},i} = \sum_{t=t_{\text{start}}}^{t_{\text{now}}} P\left({}^{i}\mathbf{P}^{\text{dem}}_{\text{last,t}}, p_{\text{last,t}}\right) \Delta t \tag{6.4}$$

Eventually the aggregated constraints curve at t_{now} can be corrected by adding

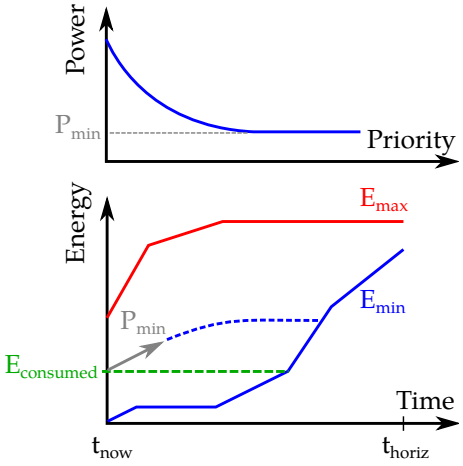

Figure 6.8: Inconsistency between aggregated demand function and energy constraints graph, after estimation of the current energy state E_{consumed}. The value of $P_{\min}$ from the demand curve can be used to construct an improved $\mathbf{E}_{\min}$, indicated by the dotted line.

$\sum_i \left(E_{\text{consumed},i} - {}^i\mathbf{E}_{\min}[t_{\text{now}}]\right)$ to ${}^i\mathbf{E}_{\min}[t_{\text{now}}]$ of the aggregated curve, and restoring monotonicity if necessary.

Inconsistency between aggregated demand function and energy constraints

A particular problem arises due to the use of shifted and re-aligned energy constraints graphs; at a concentrator agent, the aggregated demand function can indicate a $P_{\min} > 0$, as illustrated at the top of fig. 6.8. At the same time, the aggregated energy constraints graph indicates that a charge power of 0 is a valid path. This is due to the energy estimation process, which can only assume that $\mathbf{E}_{\min}$ does not decrease below E_{consumed} after t_{now}. The latter is shown in the bottom part of fig. 6.8.

The problem with using such energy constraints graphs is that they tend to amplify the occurrence of path deviations, which have been previously explained in section 5.3. In order to overcome this problem, the aggregated energy constraints needs to be modified after the energy estimation process has taken place. Unfortunately, the only valid assumption that can be made is that exactly at t_{now}, the slope of $\mathbf{E}_{\min}$ corresponds to $P_{\min}$.

Since choosing a path close to $\mathbf{E}_{\min}$ gives rise to more path deviations, the course of $\mathbf{E}_{\min}$ after E_{consumed} can be altered, starting from $P_{\min}$. Therefore,

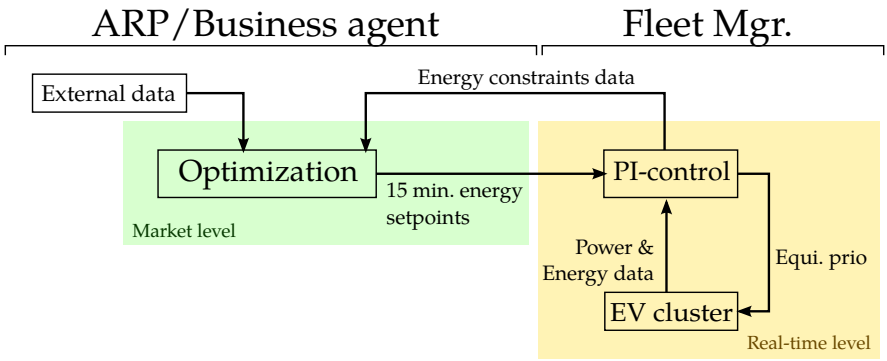

Figure 6.9: Integration of energy compensation loop in the event-based MAS MBC architecture

an exponential decay function is applied on $P_{\min}$, as illustrated in fig. 6.8. The factor of decay was determined experimentally to lead to the best results between $\frac{1}{6}$ and $\frac{1}{20}$. A similar technique can be applied to $\mathbf{E}_{\max}$ using the aggregated demand function's maximum power $P_{\max}$.

6.3.5 Preemptive application of equilibrium priority

To further reduce communication with the device agents, the latter can be allowed to change their charging power even if no new equilibrium priority was received by them. In such a case, after submitting a new demand vector to the local concentrator agent, a countdown timer is started. If no new message containing an equilibrium priority is received before the timer reaches zero, the last-known priority is applied on the last submitted demand vector.

At the concentrator agent, this feature is integrated into the caching mechanism by evaluating the power difference upon receiving a new demand curve from a device agent.

In the simulations from chapters 7 and 8, this aggressive kind of caching will not be used, except in section 7.2 on communication limitations, since it increases path deviations. It is only useful when reducing the number of messages is the main objective, regardless of path deviation problems.

6.4 Energy compensation

As mentioned near the end of section 6.3.3, a possible way to compensate for deviations induced by the caching method is through the use of a compensation loop. This is especially useful when adhering to energy volumes over certain periods is important, as deviations in energy tend to build up in one direction.

In such a case, a feedback is integrated at the fleet manager, collecting data on actual consumption from EV agents, estimating the expected energy at the end of the desired period, and adjusting the equilibrium priority when needed. Practically, a PI loop is used in the simulations later on, but other techniques could be used as well, such as Model Predictive Control or a self-learning algorithm. An abstract view of the implementation is shown in fig. 6.9.

This method assumes that it is possible to get near real-time power or energy measurements (10 to 60 sec. intervals) from the concentrators or EV agents, which poses its own challenges regarding the communication. Nonetheless, even if these measurements arrive only irregularly every hour, a correction factor could be derived and compensation still performed.

6.5 Conclusion

In this chapter, the MAS MBC algorithm for the coordination of charging EVs was adapted to work as an event driven system. Several additions have been introduced.
The dual coordination approach splits the auctioneer agent into an event driven entity focusing on the real-time level, the fleet manager, and a time slot based part responsible for the market-level operation, the business agent. Energy setpoints are passed from the business agent to the fleet manager to coordinate the EV cluster.
The event-driven part features a caching system to reduce the number of messages exchanged between EV agents and concentrators. An optional PI loop at the fleet manager can compensate for deviations due to the caching.
At the concentrator agents, a few modifications were necessary to allow the asynchronously arriving energy constraints graphs to be aggregated. However, most changes are performed from the assumption that the DR cluster only consists of EVs. The applicability or changes required to use other types of DR devices has not been investigated.

The next chapter 7 will evaluate the performance of the previously proposed demand functions for EVs and validate the event driven MAS MBC in a generic

setting. Additionally, the impact of the use of caching on the communication in the DR cluster is investigated. Then, in chapter 8, the algorithm is applied to realistic situations, using market objectives, simulated distribution grids, voltage droop control and multi-aggregator settings.

Chapter 7

Validation

In this chapter, the algorithms from chapters 5 and 6 are validated in the simulated environment that was introduced in chapter 4. The focus lies on abstract scenarios to evaluate some of the choices that were made within the context of coordinated charging of EVs.

First we want to evaluate the influence of using different EV demand functions. This is done both with an MAS MBC implementation based on the use of time slots and without planning horizon as in PowerMatcher, and then with the event-based implementation with planning. From the latter, the benefits of using an event-driven implementation over a time slot based one can be determined. In a second part, we want to learn more about the communication aspects of using caching techniques in the event-based implementation, more specifically the suspected trade-off between the amount of messages that are exchanged with the EV agents and the accuracy of the coordination.

7.1 Demand function evaluation

As mentioned in section 5.1.1, agents operating in a market-based control setting have an internal utility function to express their willingness to consume (or produce) at certain equilibrium prices. For charging electric vehicles, the corner priority p_r was used to build such demand function. Two different ways of obtaining a suitable p_r were introduced:

1. The first, referred to as "asymptotical", is based on a direct combination of the charge requirements into a corner priority price. See equation (5.2).

This direct method is also used in [58, 102] and seems to give acceptable charging behavior in a variety of settings, as will be shown further on. The downside is the fact that it behaves asymptotically as $\Delta^i t_{\text{dep}}$ approaches zero close to the departure time ${}^i t_{\text{dep}}$. It is to be expected that this will have an effect on the performance of the heuristic to distribute power among the agents.

$$\textbf{asymptotic} : {}^i p_r = \frac{{}^i E_{\text{req}}}{\Delta^i t_{\text{dep}} \, {}^i P_{\max}} \tag{7.1}$$

2. The other corner priority functions use a linear combination of the charge requirements. Two variants were shown in section 5.1.1; one with the use of an agent i's maximum power ${}^i P_{\max}$, and without. The equations have been repeated in respectively (7.3) and (7.2). Both variants require the normalization of the remaining time to departure t_{dep}.

$$\textbf{linear1} : {}^i p_r = 1 - \left(\frac{1}{2} \Delta^i t_{\text{dep}}{}' + \frac{1}{2} {}^i E_{\text{req}}{}' \right) \tag{7.2}$$

$$\text{with } \Delta^i t_{\text{dep}}{}' = \min \left(\frac{\Delta^i t_{\text{dep}}}{12\text{h}}, 1 \right)$$

$$\text{and } {}^i E_{\text{req}}{}' = \frac{{}^i E_{\text{req}}}{E_{\max}}$$

$$\textbf{linear2} : {}^i p_r = 1 - \left(\frac{{}^i t_{\text{critical}}}{12\text{h}} \right) \tag{7.3}$$

$$\text{with } {}^i t_{\text{critical}} = \min \left(\Delta^i t_{\text{dep}} - \frac{{}^i E_{\text{req}}}{{}^i P_{\max}}, 12\text{h} \right)$$

In the next subsections, the behavior of above demand function strategies regarding electric vehicle agents is compared, using a few scenarios. Eventually, a single demand function is selected for use in upcoming validation sections.

7.1.1 Peak-shaving with static power limit

In a PowerMatcher-style peak-shaving scenario, the objective is to keep the power consumption of a fleet below a fixed limit P_{limit}. The role of the auctioneer agent is then simply to periodically determine and distribute the equilibrium priority that corresponds to this fixed limit P_{limit}.

Table 7.1: Peak-shaving scenario common simulation parameters

Time slot length Δt_{step}	15 minutes
Duration	3 days
Number of (PH)EV agents	1 000
Number of concentrator agents	4
Usable battery content	20 kWh
Max. charging power	3.3 kW
Charging location	Home

The parameters used are shown in table 7.1. Time progresses in discrete time slots of 15 minutes. At the start of every time slot, demand vectors are aggregated, and an equilibrium priority corresponding to P_{limit} is sent to all active agents. Vehicle availability and charging is based on the models from section 4.4.1.

It is, of course, essential that a suitable P_{limit} for the fleet is chosen. If P_{limit} is set too low, an energy deficit will build up in the cluster. Because of the *emergency charging* feature of the agents (explained in section 5.1.1), sooner or later agents are forced to start charging at their maximum power and P_{limit} is exceeded. If P_{limit} is chosen too high, peak-shaving potential is wasted and agents more or less charge uncontrolled and below the limit.

Performance in function of P_{limit}

Figure 7.1a illustrates aforementioned effect for the three demand functions. During simulation, the maximum observed power $P_{\max}$ of the fleet is recorded, in function of the chosen peak shaving power limit P_{limit}. When P_{limit} is too low with respect to the charging demands, $P_{\max} > P_{\text{limit}}$ as more agents switch to emergency charging. On the other hand, when P_{limit} is high compared to the charging demands, P_{limit} is respected, but peak shaving potential is lost at other times, and the difference between the lowest and highest power values increases, as shown on fig. 7.1b. The former is also visible in the power profile of fig. 7.2a, which will be discussed below.

Fixed P_{limit} result

The minimum $P_{\max}$ for the 'linear2' demand function is situated around a P_{limit} of 440 kW. At this setting, the power profiles of the three demand functions during the 3-day simulation are shown in fig. 7.2a. The 'asymptotic' demand function performs considerably worse than its counterparts, because as

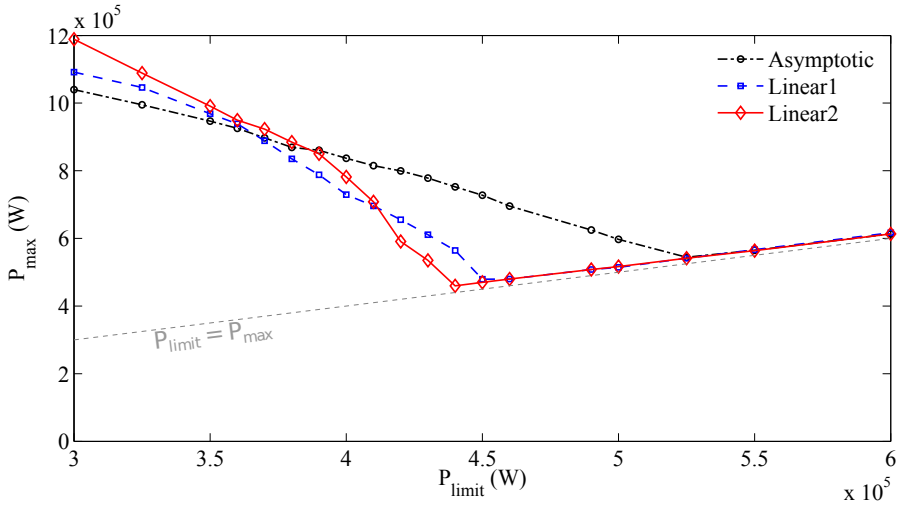

(a)

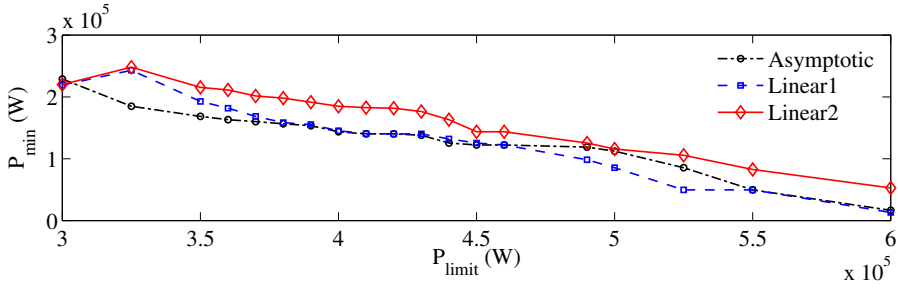

(b)

Figure 7.1: Effect of the choice of demand function and P_{limit} on (a) the fleet's peak power $P_{\max}$, and (b) $P_{\min}$, during a 3-day peak-shaving scenario.

mentioned above, first P_{limit} is exceeded and then a deficit occurs as not enough vehicles are available anymore for charging. The 'linear1' demand function performs better, but still leads to an unwanted peak, whereas the 'linear2' demand function is able to keep close to P_{limit} for the longest amount of time.

The three demand functions still lead to the same amount of energy consumption during the charging of the vehicles, but the way it is consumed differs during the course of the day. In 7.2b, the equilibrium priority p_{equi} is plotted. The asymptotic demand function results in a very sensitive response on the aggregated demand functions $\mathbf{P}_{\text{dem}}^{\text{aggreg}}$, as the price quickly varies from near-zero to its maximum value. Without interpolation within ${}^{i}\mathbf{P}_{\text{dem}}$ by the device agents, power consumption would behave erratically.

Figure 7.3a shows the percentage of active vehicles that are charging in emergency mode. 'Active' in this context means that they are able to respond on equilibrium price information. Inactive agents are either busy driving, fully charged or not connected to the grid (see section 4.4.1).

Finally, fig. 7.3b shows the cumulative number of vehicles that activate emergency charging. This figure needs to be interpreted alongside table 7.2. It is apparent that the "linear1" curve leads to the highest number of emgergency charging activations, but on average, these activations apply only for a small time Δt_{dep} and amount of energy ΔE_{req}. This explains why its "nbEmg" curve showing emergency charging states over time from fig. 7.3a still looks comparable to that of the "linear2" curve. Also important to note is the fact that the total amount of vehicles that entered emergency charging during the simulation but could not achieve the required charge before their t_{dep} is the same for the 3 demand curves. The reason for this energy deficit is inherent to the use of time slots and further explained in section 7.1.2, when comparing with event-based operation.

Summary

From the results, the asymptotic demand function tends to charge vehicles early on, but not necessarily those that would benefit the most (disproportionately favoring those low on time). This leads to a relatively low amount of active vehicles of which a high share has to commence emergency charging early on. These are signs of heuristic-induced path deviations, discussed before in section 5.3.

Contrastingly, the 'linear1' demand function keeps vehicles active during the longest time. But the emergency charging using 'linear1' behaves very differently than with the other demand curves, as more vehicles activate it, but for a

Table 7.2: Emergency charging statistics for the Powermatcher scenario, 3 consecutive days, 1000 vehicles

Metric	Asymptotic	Linear1	Linear2
Avg Δt_{dep} when emg chg activates	1.97 h	1.24 h	1.48 h
Avg ΔE_{req} when emg chg activates	6124 Wh	3615 Wh	4510 Wh
Σ occur. of emg chg activations	2387	2957	2172
Σ_i occur. of ${}^i\Delta E_{\text{req}} > 0$ at ${}^i t_{\text{dep}}$	1384	1384	1384
$E_{\text{deficit}}/E_{\text{total}}$	1.3%	1.3%	1.3%

generally lower amount of time and remaining energy. This is due to the absence of the state-of-charge information in the calculation of its ${}^i p_r$. The 'linear1' function is therefore not recommended. The 'linear2' function performs best in the peak shaving scenario, as the amount of vehicles that enters emergency charging is the lowest and its peak is shifted furthest down in time.

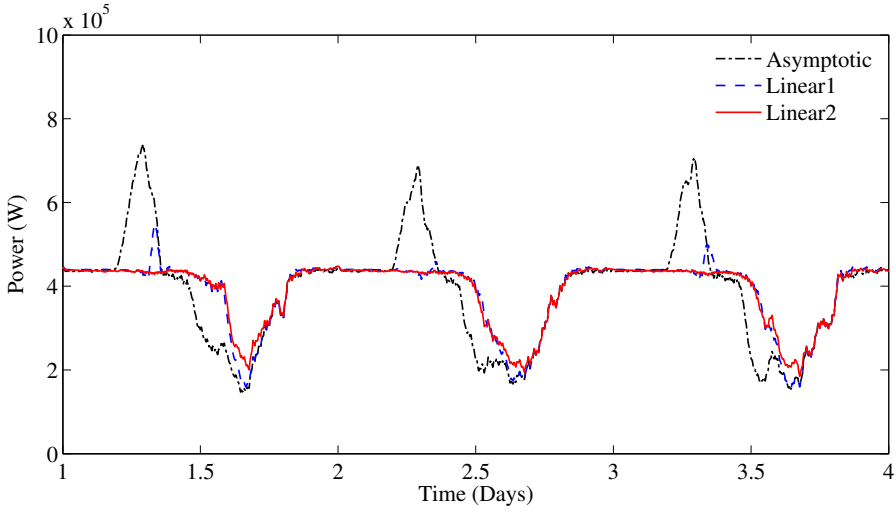

(a)

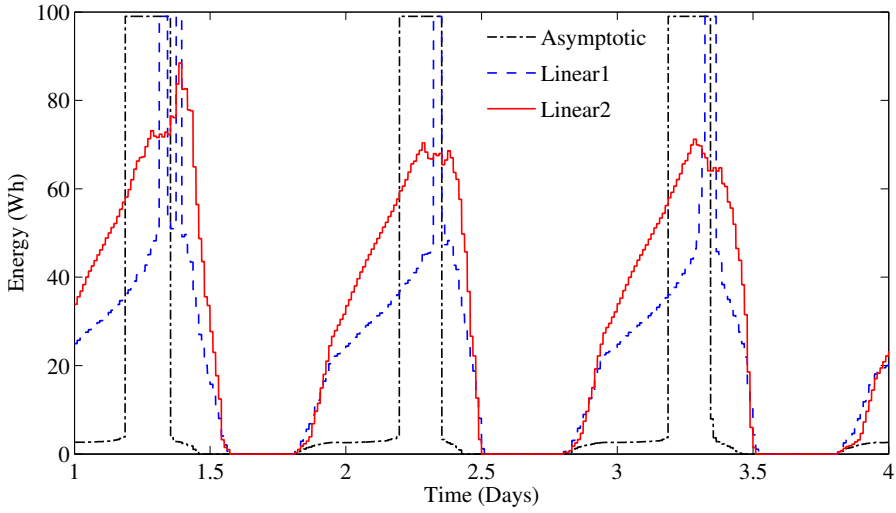

(b)

Figure 7.2: Effect of the choice of demand function on peak shaving behavior

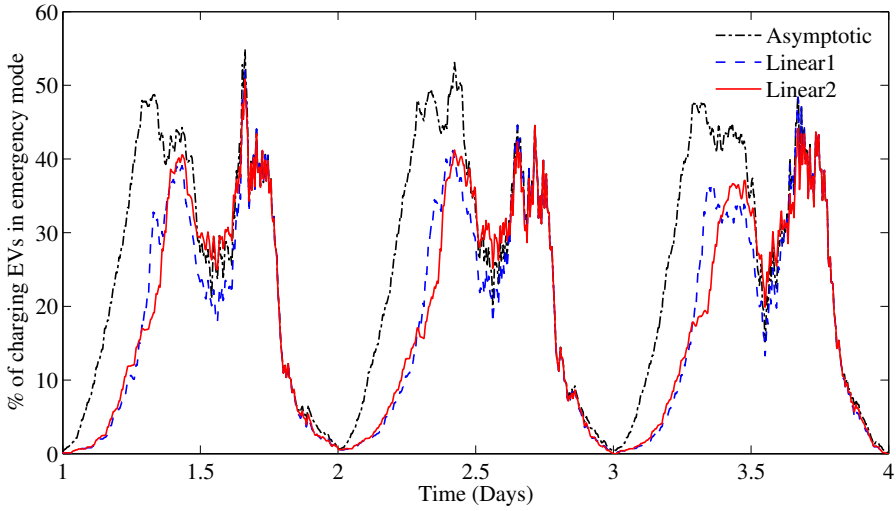

(a)

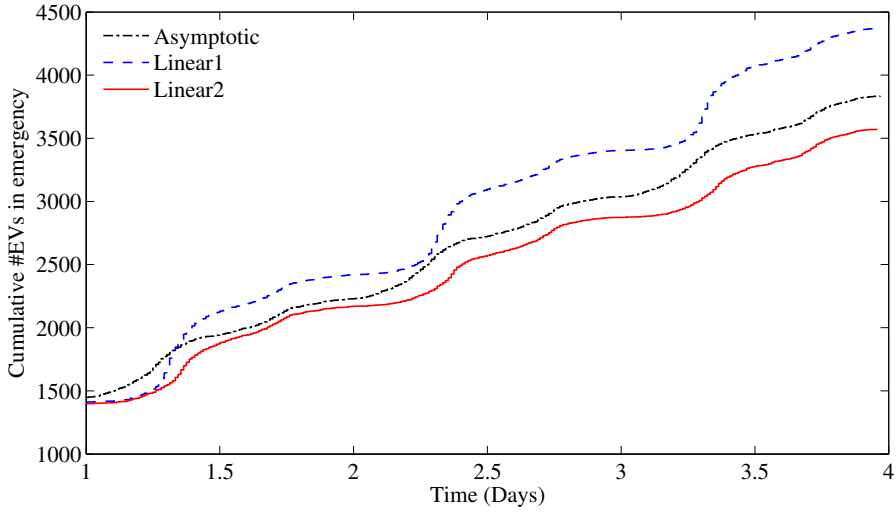

(b)

Figure 7.3: Effect of the choice of demand function on emergency charging during peak shaving scenario

7.1.2 Use in MAS MBC implementations with planning

The different demand functions were also evaluated with the MBC with planning approach. In this case, the auctioneer agent sets the equilibrium priority based on an external objective. A 'classic' scenario uses Time-of-Use, such as briefly mentioned in section 5.2.2. Herein, the objective is the minimization of the total fleet charging cost over a finite horizon, by using a linear or quadratic cost model. The constraints are the departure times of the currently known vehicles, meaning that no predictions for future arrivals of EVs are used.

The general description of the optimization problem using energy constraints graphs has already been outlined in section 5.2.2. In this scenario, we will be using a linear cost model C, that makes use of the energy price vector $\mathbf{p}$. This price vector contains the unit prices of energy over a 24-hour horizon at each interval t:

$$\min_{\mathbf{E}} \sum_{t=0}^{t_{\text{horizon}}} C(E_t) \tag{7.4}$$

$$\text{with} \quad C(E_t) = p_t E_t$$

Because of the LP (Linear Program) optimization, the control of the cluster will exhibit a strong *on/off* behavior, meaning that charging is postponed as much as possible until price is low, at which point the majority of EVs will start charging simultaneously. This kind of control behavior has the tendency to reinforce path deviations, since the intended energy path of the cluster is kept close to the borders of the energy constraints graph. Path deviations have been previously discussed in section 5.3.

Energy deficit

One particular problem arises when arriving vehicles have an E_{req} that is larger than what is feasible to charge in the time till departure Δt_{dep}. As mentioned in section 5.1.1, the device agents will proceed by requesting only the maximum amount of energy that can be charged in this time within the battery constraints ($E_{\max}$, $P_{\max}$). However, due to the synchronous operation of a time slot based system, agents remain idle until the next time slot before they can commence charging. The amount of energy that could be charged during this idle time is lost, which means vehicles in this situation will not be able to receive all of the requested charge. The total energy lost in this way is referred to as the *deficit*,

which is shown in (7.5).

$$E_{\text{deficit}} = \sum_{\text{period}} \left(\sum_{i} {}^{i}E_{\text{req},t} - {}^{i}E_{\text{batt},t} \mid t = {}^{i}t_{\text{dep}} \right) \tag{7.5}$$

For each vehicle i, the remaining energy ${}^{i}E_{\text{req}}$ at its departure time ${}^{i}t_{\text{dep}}$ is taken, and added together for the whole period of interest.

This is important for fleet charging cost comparisons. If the amount of energy consumed by the fleet in one scenario is less due to a non-zero deficit, charging cost will also be lower, but provided service quality is less. To compensate for this, a cost has to be assigned to the missing amount of battery energy, E_{deficit}. In our case, we will set this cost to €50/MWh, corresponding to a rounded average Belpex day-ahead price.

Time slot based MAS MBC

In the time slot based MAS MBC with planning, operation is technically close to the PowerMatcher scenario, in the sense that time progresses in discrete time slots of 15 minutes. At the start of every time slot, demand vectors and energy constraints graphs are aggregated, an optimization is performed, and the first step of the resulting planning is sent as an equilibrium priority to all active agents. The device agents then adjust power and charging proceeds during the course of the time slot.

The parameters for the time slot based simulations are the same as those used during the PowerMatcher scenario, in table 7.1.

Event based MAS MBC

In the event based MAS MBC with planning, operation is based on the occurrence of events. Agents send demand vectors and energy constraints graphs when triggered to do so, and the equilibrium priority is distributed depending on the amount of change compared to the previous state. Details can be found in chapter 6.

In the simulations from this section, the caching parameters from table 7.3 have been used.

Table 7.3: Event-based MAS MBC ToU scenario caching parameters, see also section 6.3.3.

Device agent ${}^{i}\mathbf{P}_{\text{dem}}$ max. difference	350W
Concentrator $\mathbf{P}_{\text{dem}}^{\text{aggreg}}$ max. difference/device	40W
Concentrator $\max_{a_i}$	350W
Concentrator $\max_{\Sigma a_i}$	110W

Results

Now we will look at the differences between using a time slot based versus an event-driven approach, and to the effect of using the three different demand functions. Figure 7.4a and fig. 7.4b show the power profile of the cluster of EVs during 3 consecutive days of simulation, both for the time slot and event based versions of the MAS MBC algorithm with planning.

It can be seen that the event based algorithm leads to higher power peaks compared to the time slot-based one. As expected, the peaks correspond to the times when the energy price is the lowest, see fig. 7.4c. But the amount of energy in both implementations is the same, save for the energy deficit that occurs due to the use of time slots.
This effect cannot be attributed to the slower response of the time slot based version, since energy prices change on hour boundaries. However, in the time slot version, on average, vehicles have to charge slightly earlier, because there needs to be some margin between the departure time t_{dep} and the borders of the time slots. Consequently, slightly less flexibility is available overall compared to the event based system, and the difference in energy in the peak is spread out over the day.

The difference between the 3 demand functions is also more apparent in case of the event based system. The asymptotic function gives the highest peaks, which could be perceived as beneficial because it means more energy is charged when price is low. However, the underlying reason is the relatively high path deviations that occur when using the asymptotic function, leading to the charging of vehicles that could have been postponed longer. Path deviations were discussed in section 5.3 on shortcomings of the MAS MBC algorithm.

Figure 7.5 shows the corresponding followed energy path during simulations with the event based algorithm for the 3 demand functions. It is visible that the path followed by using the asymptotic curve deviates where the other two stay flat.

Next, we look at the cost of charging the fleet over these 3 days. The simulation

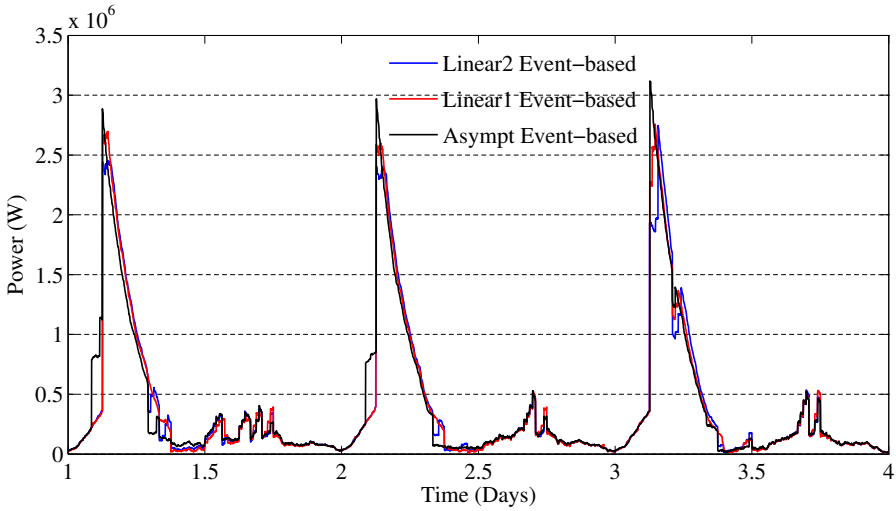

(a)

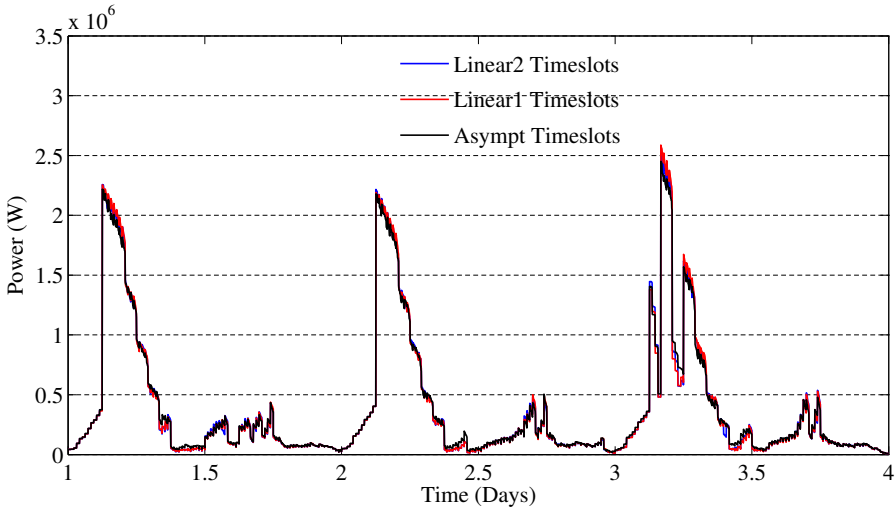

(b)

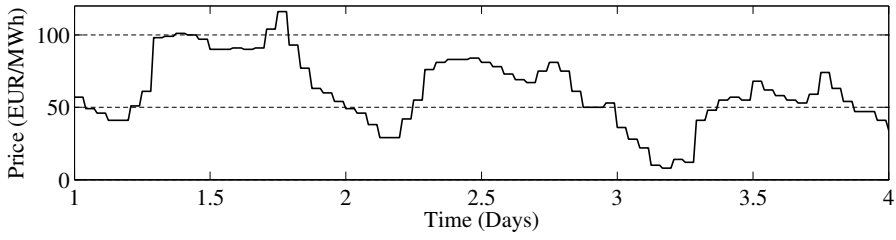

(c)

Figure 7.4: Effect of the choice of demand function on MAS MBC ToU scenario

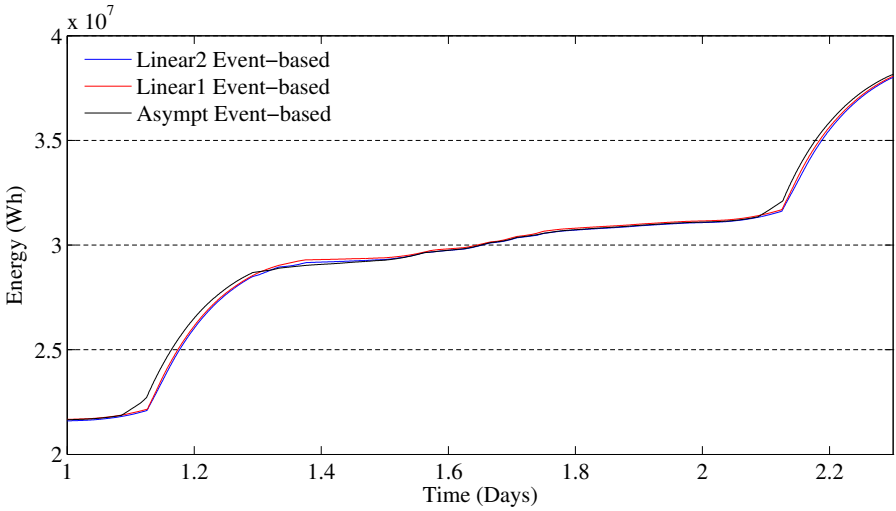

Figure 7.5: Followed energy path for the event-based system

is repeated 120 times for random days of the year and vehicle profiles. Deficit energy is also taken into account in the cost, according to equation (7.6).

$$\text{Total charging cost} = \text{charging cost} + €50/\text{MWh} * E_{\text{deficit}} \tag{7.6}$$

As in the previous section, the number of occurrences where the battery was not full at departure time t_{dep} and the missing energy at that point was recorded. The results are shown in tables 7.4a and 7.4b

When we compare the time slot and event-based implementation for the ToU case, the differences are relatively small.

Table 7.4: Charging cost of 120 randomized scenarios, 3 days, 1000 vehicles, (a) time slot based MAS MBC with planning, and (b) event-based MAS MBC with planning

(a)

	Charging cost	Deficit energy	#EVs defic.	Total chg. cost
Asympt.	€2422.0	479.3 kWh	999	€2446.0
Linear1	€2388.0	479.3 kWh	999	€2412.0
Linear2	€2386.6	479.3 kWh	999	€2410.0

(b)

	Charging cost	Deficit energy	#EVs defic.	Total chg. cost
Asympt.	€2394.1	0 kWh	0	€2394.1
Linear1	€2377.3	0 kWh	0	€2377.3
Linear2	€2385.9	0 kWh	0	€2385.9

Table 7.5: Summarized emergency charging statistics for the ToU scenario, 3 consecutive days, 1000 vehicles, (a) time slot based MAS MBC with planning and (b) event-based MAS MBC with planning

(a)

Metric	Asymptotic	Linear1	Linear2
Avg Δt_{dep} when emg chg activates	1.91 h	1.81 h	1.84 h
Avg ΔE_{req} when emg chg activates	5889.9 Wh	5618.9 Wh	5733.0 Wh
Σ occur. of emg chg activations	2426.3	2238.9	2194.3
Σ_i occur. of ${}^i\Delta E_{\text{req}} > 0$ at ${}^i t_{\text{dep}}$	999	999	999
$E_{\text{deficit}}/E_{\text{total}}$	1.68%	1.68%	1.69%

(b)

Metric	Asymptotic	Linear1	Linear2
Avg Δt_{dep} when emg chg activates	1.53 h	1.59 h	1.60 h
Avg ΔE_{req} when emg chg activates	4962.8 Wh	5155.7 Wh	5204.5 Wh
Σ occur. of emg chg activations	2120.5	2009.5	2084.8
Σ_i occur. of ${}^i\Delta E_{\text{req}} > 0$ at ${}^i t_{\text{dep}}$	0	0	0
$E_{\text{deficit}}/E_{\text{total}}$	0%	0%	0%

7.2 Communication limitations

In chapters 1 and 2, the importance of communication for large-scale DR was mentioned. With the use of the caching methods from section 6.3.3 in the event-based MAS MBC, it is possible to trade off the amount of messages between device agents and concentrator agents for accuracy of the coordination and responsiveness. More caching means less messages are exchanged between the agents, at the cost of increased deviations from the aggregator-determined optimum.
It needs to be mentioned that deviations will always appear in some form, independent of the algorithm or caching, as the amount of future consumed power needs to be quantified (e.g. if a device reports that it will consume 3300 W, but then only consumes 3260 W, this is related to physical limitations).

If the time slot based MAS MBC is considered as benchmark, we can compare it with different levels of caching in the event-based MAS MBC implementation and evaluate the trade-off between communication and coordination.

7.2.1 Fixed caching levels

A first series of scenarios consists of a fleet of 96 (PH)EVs simulated during 3 days. The task of the auctioneer agent comprises of balancing a linear static generator function with the demands of the charging agents, as shown in fig. 7.6. While such function is not truly representative for the generators' costs, we are here only interested in analyzing the communication aspects. Thus, a simple objective makes the scenarios easier to compare since the outcome of the behavior at the market level does not play a significant role.

As mentioned before, a time slot MBC system with 15 minute intervals is used for comparison with the event-based cases. In all cases, the hierarchical agent tree structure consists of 1 auctioneer agent x 6 x 4 intermediate agents (2 levels) x 4 (PH)EV agents, for a total of 96 (PH)EV agents. The maximum allowed power per vehicle is 3.3 kW and the driving behavior of the (PH)EVs is based on the availability model introduced in section 4.4.1.

As the goal here is to aggressively reduce agent messaging, the preemptive p_r addition from section 6.3.5 is used here. The aggregator agent follows a PowerMatcher-style objective, and matches the aggregated bid with a fixed supply-versus-price bid that is pictured in fig. 7.6.

The results of the simulated scenarios are evaluated by looking at two key values:

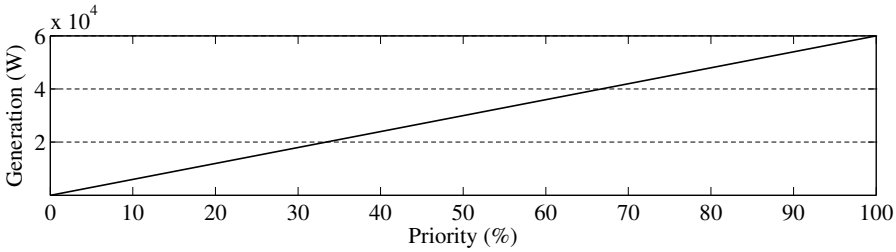

Figure 7.6: Static generator bid function at aggregator agent

1. RMS value of the power difference with the time slot MBC (Root Mean Square deviation). This gives an indication on how well or how bad a certain event-driven MBC scenario performs. However, the use of the time slot system as benchmark or reference case is not entirely justified because the use of time slots introduces delay in the actions taken by device agents which also degrades performance. Thus, another comparison scenario is added, scenario 4, and parameterized to be as uncompromising as possible; agents bid and receive equilibrium price updates almost instantaneously. Such a scenario should therefore be very close to a theoretical optimum behavior of the original MBC concept. The RMS values are normalized to ease comparison.

   If $\mathbf{p}_{\text{ts}}$ contains the power profile of the time slot simulation and $\mathbf{p}_{\text{s}}$ that from another scenario, then the normalized RMSD (nRMSD) between is given by (7.7):

$$\text{nRMSD}(\mathbf{p}_{\text{ts}}, \mathbf{p}_{\text{s}}) = \frac{\|\mathbf{p}_{\text{s}} - \mathbf{p}_{\text{ts}}\|_2}{\sqrt{n}\,(\max(\mathbf{p}_{\text{s}}) - \min(\mathbf{p}_{\text{s}}))} \tag{7.7}$$

2. The number of messages exchanged (sent and received) by device agents. These messages are likely to be the most expensive in terms of bandwidth and monetary cost. Alternatively, it could also make sense to focus on the number of messages exchanged by intermediate agents.

Scenarios

Table 7.6 summarizes the caching parameters for the event based scenarios. In the "uncontrolled" case, vehicles will simply start charging at full power as soon as they connect. Scenarios 1 to 4 are event-based MBC variants with different levels of caching, with the last one, 4, serving as the most uncompromising scenario. Scenario 3 uses an aggressive level of caching (meaning

that higher bid and equilibrium differences are allowed); scenario 2 aims for the opposite and is configured for accuracy, while scenario 1 fits in between at intermediate levels of caching.

Table 7.6: Continuous MBC system scenario parameters overview.

	Node agents			Intermediate agents						Top agent	
Simulation #	Bid interval	Bid timeout	Bid max diff	Bid interval	Bid timeout	Bid max diff	Total diff	Node diff	Low Treshold	Update interval	Total diff
Scenario 1	450s	120s	200W	45s	120s	200W	1000W	15%	200W	10s	15%
Scenario 2	240s	120s	10W	45s	120s	10W	50W	7.5%	50W	10s	5%
Scenario 3	900s	120s	400W	45s	120s	200W	1500W	22%	250W	10s	20%
Scenario 4	30s	15s	2W	30s	15s	2W	10W	2%	5W	5s	1%

Table 7.7: Summarized scenario results for a setting with 96 PHEVs, asymptotical bid function

Simulation	Node msgs	nRMSD Tslot	nRMSD Scen4
Timeslot	30000	0%	3.87%
Uncontrolled	0	33.88%	32.86%
Scenario 1	16825	6.01%	3.38%
Scenario 2	60415	4.27%	1.55%
Scenario 3	12182	13.17%	9.85%
Scenario 4	265595	3.68%	0%

Table 7.8: Summarized scenario results for a setting with 96 PHEVs, linear bid function

Simulation	Node messages	nRMSD Tslot	nRMSD Scen4
Timeslot	26901	0%	12.55%
Uncontrolled	0	23.70%	22.30%
Scenario 1	4778	11.41%	5.02%
Scenario 2	15204	10.31%	3.78%
Scenario 3	3892	13.86%	7.69%
Scenario 4	52774	10.83%	0%

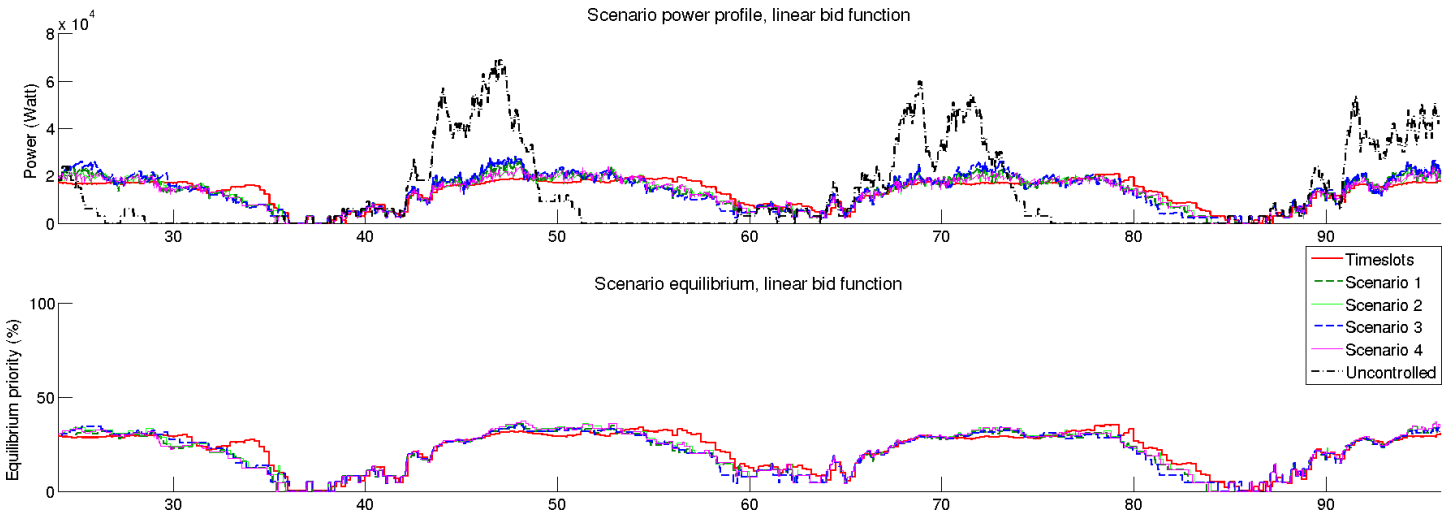

Figure 7.7: Power consumption and equilibrium priority during simulation of different scenarios with 96 (PH)EVs, 3 simulated days, using the linear bid function.

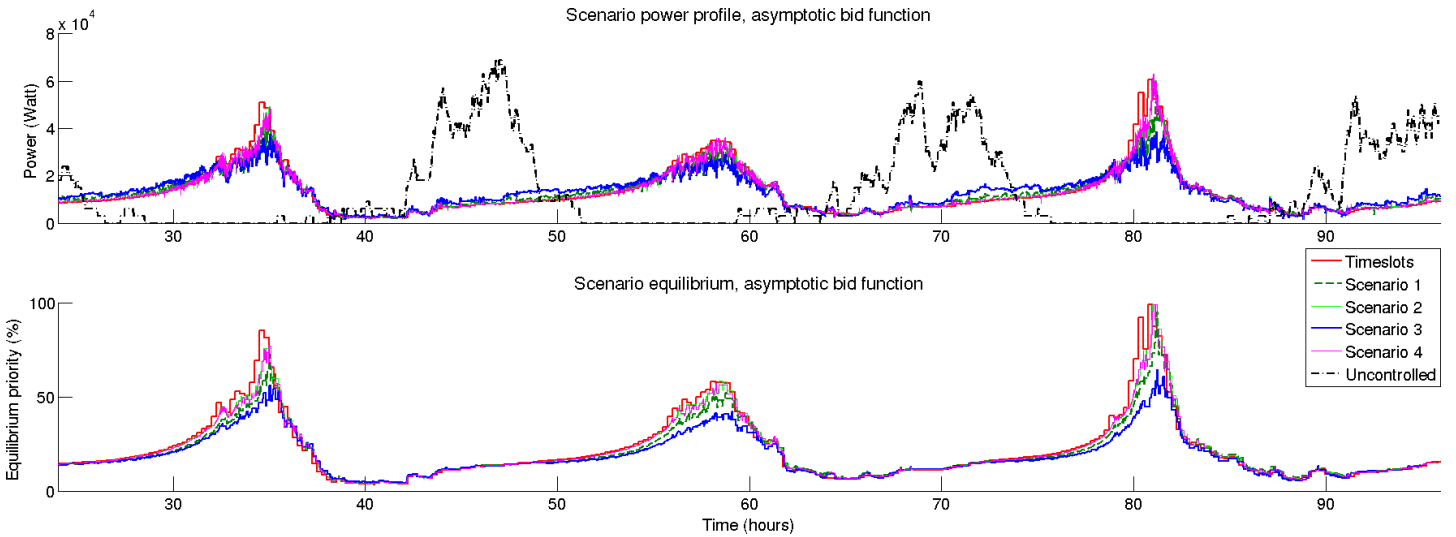

Figure 7.8: Power consumption and equilibrium priority during simulation of different scenarios with 96 (PH)EVs, 3 simulated days, using the asymptotic bid function.

Results

Tables 7.7 and 7.8 show the numerical results in the case of asymptotic and 'linear1' bid functions respectively.

In the uncontrolled case, power peaks occur during the evening and before midnight, when the largest share of the vehicles are connected to a charger. In the controlled scenarios, consumption is centered in the morning and before noon, when most vehicles have their departure time. This is shown on figs. 7.7 and 7.8.

The more a scenario employs aggressive caching of bids and equilibrium priorities, the more its power consumption profile deviates from the benchmark. But the positive effect of the caching is the drastically reduced need for communication between device agents, which can be seen in table 7.7.

In case of scenario 1, with intermediate levels of caching and using the 'linear1' demand function, device agent message count was reduced by almost 70% when compared to the equivalent time slot implementation.

From the results, it is clearly possible to balance coordination optimality (represented by the normalized RMS difference with the time slot system and scenario 4 of the continuous MBC) with communication load (the number of device agent messages) and responsiveness (determined in the parameter sets from table 7.6). But scenario 2's profile is almost identical to that of scenario 4, showing that not much additional gain is achieved by further decreasing the caching thresholds beyond some point.

Scalability

Because the simulations from the previous section were limited to 96 (PH)EVs, the results do not give an an idea about the ability of the algorithms to handle larger clusters. Therefore the number of vehicles is increased while maintaining the same hierarchy ratio for the agent network. The static producer bid was also scaled accordingly.

Figure 7.9 shows the results for the different scenarios, using the asymptotic demand function. It can be seen that scaling performance of the event-based system is similar to a time slot implementation which equals slightly better than linear. Using the linear bid function returned comparable numbers.

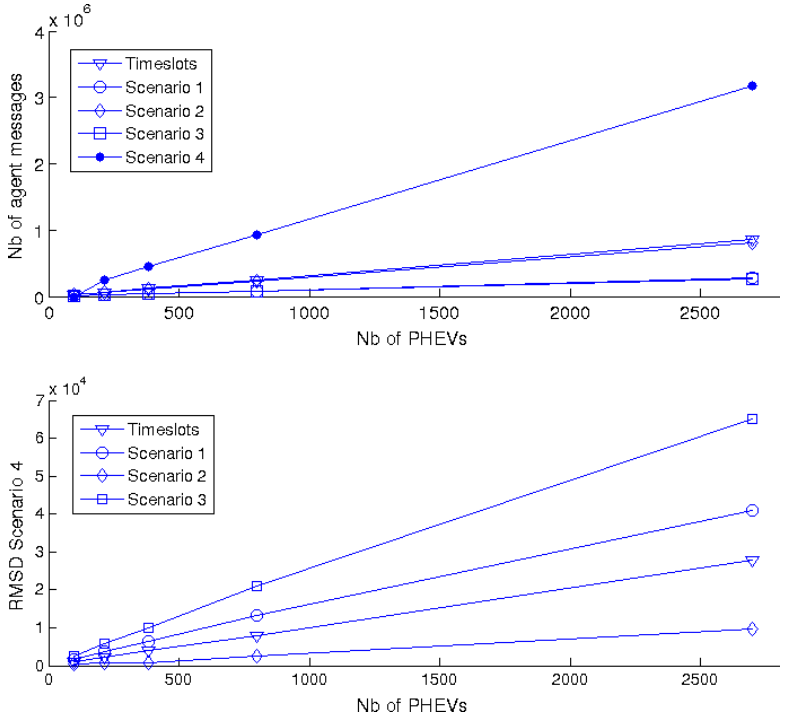

Figure 7.9: Scaling behavior for the different scenarios

7.2.2 Trade-off behavior

To be able to visualize the trade-off between device agent messaging and the optimality of control, a genetic process generates and selects from a population of random caching parameters. Each parameter set is simulated and a Figure-of-Merit for the scenario is determined by the use of a *fitness* function (7.8):

$$\text{FOM} = (\text{RMSD}_{\text{ts}}) * (\text{number of messages}/10000) \tag{7.8}$$

Because the generation and selection of random parameter sets takes a lot of time, again a cluster of 96 (PH)EVs distributed over 4 concentrators is used for these simulations. As the benchmark, scenario 4 was selected this time, because it is the most uncompromising regarding caching parameters.

In fig. 7.10, both evaluation metrics are plotted against each other. Each point represents the outcome of one simulation. The dashed line was added to show a hard “front“; no set exists beyond this border. Note that this is not the same as a full Pareto-front; examination reveals that sets close to the “corner” of

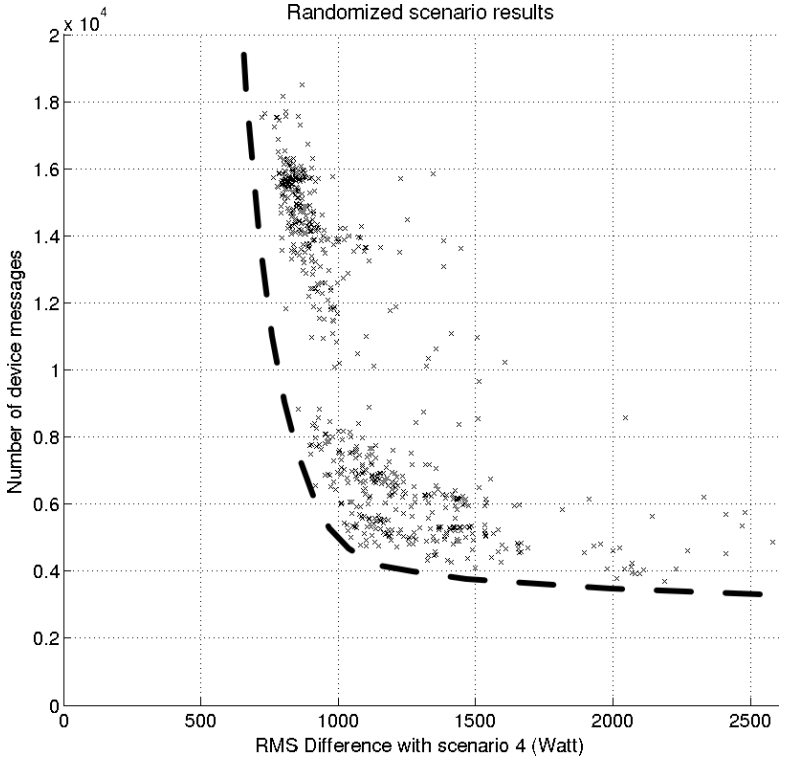

Figure 7.10: Trade-off between coordination accuracy and agent messaging

the front have a low device agent message count and good optimality, but do so by effectively sidestepping the intermediate agent level due the use of very aggressive caching parameters there.

7.3 Conclusion

In this chapter, the ideas and concepts presented in chapters 5 and 6 have been tested in simulations for some basic cases. Section 7.1.1 presented a peak-shaving case where the total power of a cluster was to stay below a predetermined limit. The goal of these simulations is to determine the most suitable demand function when coordinating EVs with the MAS MBC algorithm from section 5.1. It was found that the 'linear2' demand function performed better than its two counterparts, since it leads to less emergency charging and is not oversensitive to the equilibrium priority.

In section 7.1.2, the MAS MBC with planning was used with a ToU cost minimization objective, and an implementation based on the use of time slots was compared with an event driven one. The use of time slots leads to a small loss of flexibility and the appearance of incompletely charged EV batteries. The term *energy deficit* was introduced to account for the subsequent loss in delivered energy. It has also been shown that the use of the 'asymptotic' demand function creates more path deviations than the 'linear' alternatives.

Eventually, in section 7.2, the communication requirements of a time slot based and event driven implementation were compared. The results show the discrepancies a time slot based system implies in the case of coordinated charging, which are hard to avoid without switching to very small time steps. This is where a continuous or event-based system has a clear advantage; it has virtually infinitely small time steps.

However, due to the use of caching in the event based implementation, a trade-off exists between reducing the amount of messages exchanged with EV agents and the optimality of the coordination, when compared to the time slot based results. Nevertheless, as an example of one case, a slightly improved coordination (in this case due to lower cost of charging) can be achieved at 70% less messages when compared to the time slot based implementation.

In the next chapter, we will move to more realistic scenarios, where the EVs are situated in distribution grids. Two business cases will be considered, and the situation where multiple aggregators are active in the same distribution grid is considered.

Chapter 8

Market-setting Applications

Coordinated charging is often believed to be able to reduce the impact on the power system, by limiting peak power or shifting consumption to periods when more generation capacity is available or when it makes more economical sense to do so. The latter is the basis of the business case of aggregators, who operate at the market level. Such market-setting applications form the basis of this chapter.

In short, in this chapter we want to determine what coordinated charging of large groups of EVs does to weak distribution grids. We will use two different objectives at the market level for this. At the technical level, the addition of a voltage droop controller to the chargers is examined as a possible solution for distribution grid problems.

8.1 Problem description

In the preceding chapter, a fleet of electric vehicles is treated as some sort of pool, possibly consisting of geographically dispersed participants. Their physical placement in the grid is not taken into account, which is a valid abstraction at the market level. Therefore, during normal operation, power flows in the grid are defined by the outcome of the different markets (day-ahead, intra-day, balancing).

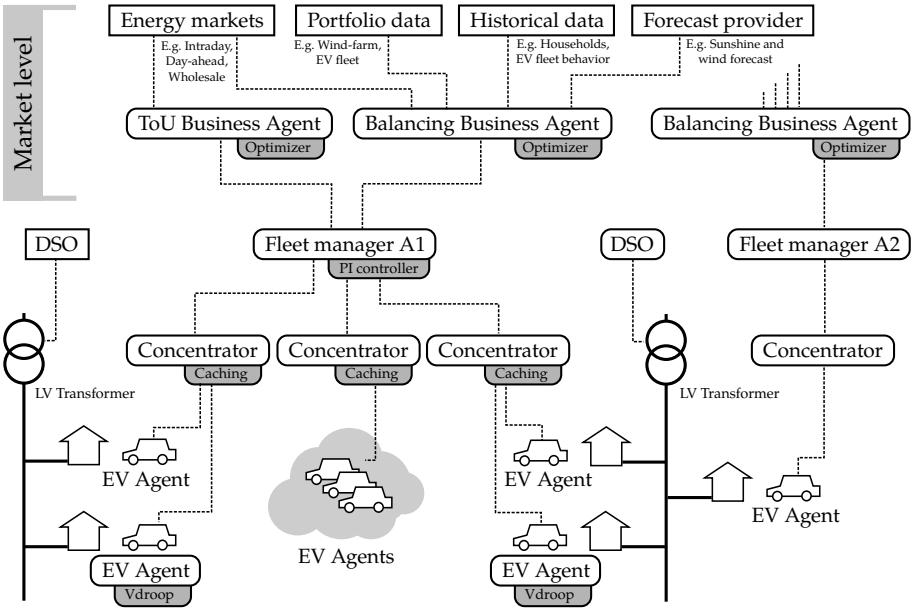

Figure 8.1: Overview of the applications

Impact on grid congestion

However, in reality, charging vehicles are typically concentrated at car parks or dense urban areas. In its current state, the grid infrastructure at these places has, more often than not, not been dimensioned for the additional load imposed by simultaneous charging of EVs. In the long term, wide-spread use and significant integration of EVs could lead to congestion and overloads at these locations [11, 109]. In fact, coordinated charging with objectives at the market level has the potential to make matters worse; e.g. when coordination is based on wholesale Time-of-Use prices, aggregators will prefer to postpone fleet charging to a few points in time where market prices are lowest. Consequently, large amounts of loads will be switched synhronously, correlated to the market situation, contributing to a demand peak and grid congestion.

The effect of two distinct market-level objectives in the form of ToU lowest cost and balancing on the occurrence of grid congestion is one of the aspects studied in this chapter.

Market versus Real-time level

In case of technical violations, the distribution grid cannot maintain exclusive market oriented operation as DSOs will want to take emergency measures to avoid local interruption of power delivery. One way of automating such emergency measures is through the use of voltage droop control, previously discussed in section 3.6.1. There is a link with the growing share of distributed generation in the power system [110]. In some countries, large-scale PV installations are now required to be able to provide grid services to the distribution system operator (for example by providing reactive power to stabilize the voltage). Similarly, small PV installations are required to respond to overfrequency and overvoltage by limiting injected power or temporarily disconnecting [83, 84].

It can be expected that sooner or later, similar norms regarding grid stabilizing behavior will be imposed on EVSE or chargers. This means that the market level operation in coordinated charging can be temporarily suspended at any time. Therefore, also in this chapter, the effect and magnitude of this interdependency between market-level and real-time level is examined.

Multi-aggregator

Another unclear aspect is when multiple competing aggregators are active within the same distribution grid. Situations can occur where one aggregator is responsible for the grid problems that mostly affect another aggregator. Since directly exchanging data about their objectives beforehand could divulge too much strategic information of an aggregator, external and neutrally operated mechanisms to allocate grid capacity between the aggregators are needed, referred to as grid congestion management in section 3.5.2.

In section 3.5.1, the relevant technical details of grid constraints have already been discussed. Next, in section 8.2, a default grid with matching agent structure is defined and in sections 8.3 to 8.5 the coordination strategies are evaluated in a Time-of-Use setting. Then, from section 8.6 onwards, more advanced applications are examined.

8.2 Grid topology and agent structure

When simulating the effects of coordinated charging on the state of the distribution grid, it makes sense to focus on weak grid configurations, where problems are more likely to occur. The question then arises of what specific topology should be used as grid model. From discussions with experts, information on the current state of distribution grids in Flanders is severely lacking. During planning and deployment of new grid segments, DSOs selected appropriate values for the cable sizes and lengths, and individual connection points were spaced out evenly over the phases. Decades later, sections have been added, reconfigured, new connections points have been attached to "random" phases, etc. This makes the occurrence of virtually any situation possible in practice and with the increasing share of PV installations on the roof of households, power quality problems have already started to appear. More information regarding PV and power quality problems can be found in [73].

Nonetheless, indicative simulations and other work [111][112, ch. 3] suggests that power quality problems in the grid due to charging electric vehicles only comes into view at larger penetration levels of over 30-50%, and then mostly in weak grids. Therefore, in the next sections we will focus on a few specific "corner cases" and not on some average grid situation (if that even exists), and look at the impact of coordination strategies in these cases.

8.2.1 Grid topology

Figure 8.2 shows the base topology used in all simulations. A 400 kVA transformer supplies several parallel feeders. Each feeder then supplies a number of household loads, bringing the equivalent transformer load up to 191 households. This is within the limits of the DSO; in a document published by the VREG [113], a maximum occurrence of 220 connections per transformer cabin can be derived. However, there is no mention of the rating of the corresponding transformer. This topology is similar to the one used by [111]. No PV installations were added, since it was found that they do not cause major changes in occurrences of undervoltages due to charging. This can be attributed to the non-coincidence of PV production and EV availability.

One of the feeders, Feeder 0, is linked to a line-segment supplying 38 single-phase household connections. These are alternatingly attached to phases 1 to 3 and spaced apart by distance D2. The distance from the transformer to the first household connection is D1. From each connection point, a cable with length D3 runs from the line to the household's supply terminals. In the simulated model, the other feeders and loads (153 households) connected to the transformer are

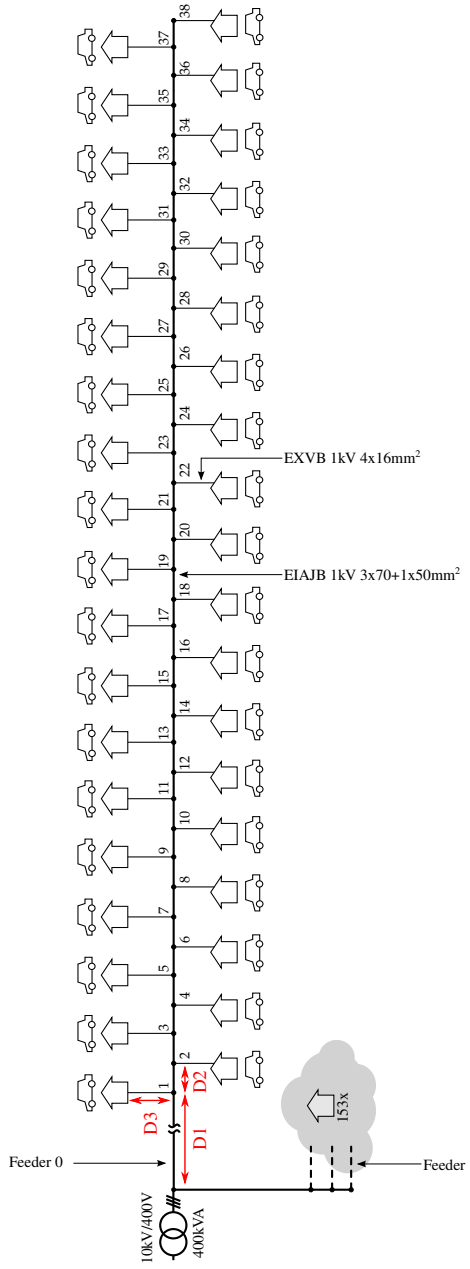

Figure 8.2: Evaluated grid topology

Table 8.1: Variations on the grid topology

Case name		D1	D2	D3	Tot. length
NearTransf **S**hortCable	NS	100 m	15 m	20 m	655 m
NearTransf **L**ongCable	NL	100 m	22 m	20 m	914 m
FarTransf **S**hortCable	FS	250 m	7 m	20 m	509 m
FarTransf **L**ongCable	FL	250 m	15 m	20 m	805 m

lumped together into one single entity (Feeder 1), as their impact is not studied in detail.

Cable parameters are taken from the design specifications of the standard for underground distribution cables, NBN C33-322 [114]. Cable type EIAJB 1 kV 3x70+1x50 mm^2 is used for the main feeder and line (D1,D2), while cable type EXVB 1 kV 4x16 mm^2 is used to connect the household's supply terminals to the main cable (D3).

Table 8.1 shows the variations on this topology that are evaluated in the next sections. Case NS and NL have a relatively short cable (100m) between the transformer and the first household terminal. Case NL and FL represent scenarios with rather long total cable lengths (914 and 805m), due to a longer distance between the household connection points.

8.2.2 Agent structure

The organization of the software agents that represent the charging vehicles is completely independent of the grid topology from the previous section. In our simulations, it is assumed that all agents for vehicles that are physically connected to the same transformer are grouped under a single concentrator agent.

At the same time, for the market operation at the fleet manager to function properly, more flexibility than is provided by the 38 vehicles should be available in the cluster. To that end, the cluster is extended so that, depending on the scenario, a total of 200 or 1 000 vehicle agents takes part in the coordinated charging. These additional agents are not part of the load flow calculations. Figure 8.3 shows the resulting agent topology.

To test additional shares of EVs inside weak distribution grids, additional variations of the agent structure are tested by having multiples of the base topology. These are shown in table 8.2. The suffix after the case number determines the share of agents used in the topology.

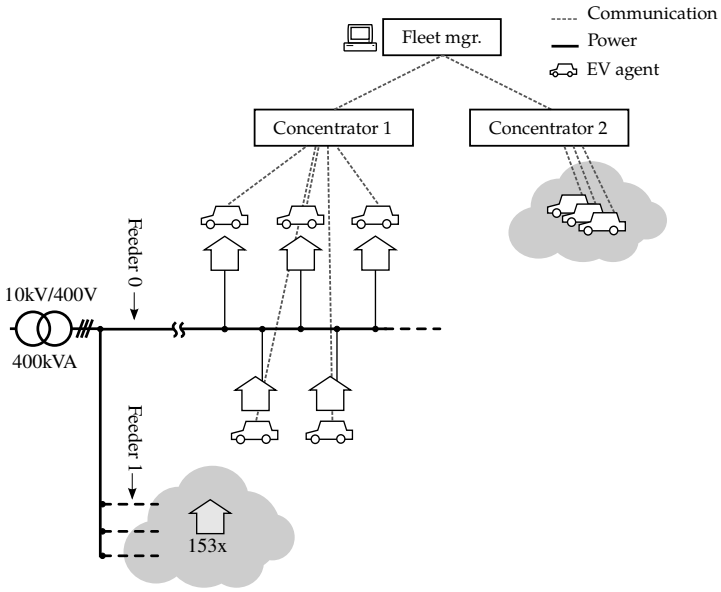

Figure 8.3: Evaluated grid topology, agent structure

Table 8.2: Variations on the agent topology for the ToU scenarios

Case name	EVs inside weak grid
x-38	38
x-114	3x38
x-380	10x38
x-760	20x38

8.3 ToU coordinated charging

In this section, the effect of coordinated charging using market-level objectives on local grid congestion, in the distribution grid scenarios from section 8.2, will be examined.

8.3.1 Optimization problem

As explained before in 7.1.2 and 5.2.2, the objective of the fleet manager during a ToU scenario is to respond on a 24-hour horizon ToU tariff in such a way as to minimize the charging cost of the vehicle fleet. The 24-hour tariff is based

on the wholesale energy price of the hourly BELPEX day-ahead market. It should be noted that using the price profile of a day-ahead market is not fully representative of a future ToU tariff as it could be implemented by utilities. Still, prices on the day-ahead market do reflect real-world peak and off-peak periods on an hourly basis, which is what is needed in these simulations.

The following three algorithms are examined:

- **Uncoordinated** or **dumb** charging: vehicles plug in and start charging upon arrival at their maximum rated power $P_{\max}$.
- **Timeslot:** The MAS MBC implementation based on 15 minute time slots.
- **Event:** The MAS MBC event-based implementation.

8.3.2 Scenario randomization and performance indicators

Because of the seasonal effects of household consumption and tariffs, distribution grid problems are correlated to the time of the year. To limit the influence of the choice of day on the results and get a global picture, randomized sets of scenario parameters are generated and tested. The randomized parameters consist of the day of the year for the tariff, vehicle driving profiles and household load profiles. The latter two are discussed in more detail in section 4.4.1 and 4.4.3.

During each scenario, simulations are run for 8 consecutive days, from which the first day is cut out due to transient behavior at the start of the simulation. Of the remaining week, the following results are recorded and calculated:

- EN 50160 worst voltage magnitude deviations in all phases of *Feeder 0*. According to the standard [70], the 10 minute mean should not drop below 0.9 p.u. for 95% of the week, and never below 0.85 p.u.

  Worst case values matter, because if the EN 50160 norm is exceeded even during only one week of the year, that can be sufficient to mark a grid as inadequate. In practice, in case of suspected voltage problems, a DSO will install measurement equipment for a single full week. On the other hand, there is no benefit for either the consumers or DSO in performing significantly better than what the EN 50160 standard defines.

- EN 50160 worst VUF deviations in all phases of *Feeder 0*. The VUF expresses the unbalance between the phases, as explained in section 3.5.1.

According to the standard, the VUF should remain below 2% for 95% of the week.

- Cost of charging for the whole fleet, for the aggregator.
- Load duration curve of *Feeder 0*; Power at the feeder is recorded every 60 seconds, sorted and stored as a load duration curve, providing a visualization of the capacity utilization of the grid. To save memory, this curve is resampled to 110 points, but in two parts; first a high resolution part for the shortest 1/5th of time lengths and a lower resolution part for the remaining time lengths.
- Number of incompletely charged batteries at departure and the accumulated missing charge in Wh, also referred to as battery energy deficit.

The parameters for the time slot based and event-based MAS MBC implementation are the same as used in sections 7.1.2 and 7.1.2 respectively.

It should also be mentioned that the effects of weekends are not explicitly taken into account, as the randomization of vehicle profiles and tariffs are not aligned. The vehicle profiles do not contain seasonal effects, only weekend behavior. Because the market prices are often lower during the weekend, cost figures of charging therefore have to be considered as indicative only. As we are focusing on trends of distribution grid problems, exact cost calculations are outside the intended scope of the simulations.

8.4 ToU coordinated charging, passive distribution grid

First, a passive grid situation is investigated, meaning that there are no devices or appliances present that implement voltage droop control.

The result of 100 randomized parameter sets for each case and coordination option regarding voltage problems is shown in figs. 8.4 to 8.6. A table with all EN 50160 observations, including minimum and maximum occurrences, can be found in appendix section A.1, tables A.1 to A.8.

8.4.1 Real-time level results

Looking at the household-only (HHOnly) results of figs. 8.4 to 8.6 indicates that the chosen topologies are fine as long as no EVs are introduced. With charging

EVs, the severity of distribution grid problems depends strongly on the grid topology, shown as cases NS, NL, FS and FL. Having the longest cable sections to the loads, case FL leads to the highest amount of voltage magnitude and VUF problems, while case NS experiences the least problems.

However, the observed trend is the same: uncoordinated charging is responsible for a peak in the evening that overlaps with the peak of household loads. Charging coordination based on ToU cost minimization objectives leads to only a little less voltage problems. The reason is that, while the coincidence of household loads and charging has disappeared, all available vehicles are now asked to commence charging at one or two points during the day. This creates a new peak that is in itself sufficient to create voltage problems. To illustrate, fig. 8.8 shows the power through the feeder and the voltage profile at the worst nodes for one specific simulated week inside case FL-38, for the event-driven MAS MBC implementation. The situation has the potential to be a lot worse, were the low wholesale prices to correspond to the household evening peak.

On fig. 8.9, the load duration curves for all 100 simulations for case FL-38 are shown by taking the minimum and maximum power occurrences at each time value. The other cases produce quasi identical graphs, so they are omitted. Again it is clear that the introduction of EVs has a significant impact on the distribution grid load. Coordinated charging according to a ToU objective creates short power peaks that are higher then when uncoordinated charging would be used. This was also observed in [15, p. 104] on a cluster-level, but no load flow analysis was performed.

Unsurprisingly, at least weak grids have difficulty supporting high EV penetration levels, as the voltages regularly drop below 0.9 p.u. for more than 5% of the time, and events where the voltage drops below 0.85 p.u. are quite common. The problems will no doubt turn for the worse in situations with unbalanced phase connections, higher charge currents (such as future 6.6 kW chargers or up) and increasing household loads (e.g. the rise in heat pump installations). In section 3.5.2, ways to overcome grid congestion problems were discussed, such as voltage droop control. The next section, 8.5 considers an active grid scenario, having voltage droop controllers in the EV agents.

There is also a small but consistent difference between the event and time slot based implementations. The event-based version produces a higher peak in the power profile and consequently a worse voltage situation. This is due to the same effect mentioned in the results of 7.1.2: the time slot version has slightly less flexibility, leading to slightly more forced spreading of the charging energy, in turn leading to a lower power peak.

8.4.2 Market-level results

Figure 8.7 shows the cost of charging. Due to technical reasons, the 8 cases were simulated in separate batches, using different random parameter sets, the total cost values between the cases cannot simply be compared. However, within the cases, it is apparent that the cost of coordinated charging for the event-based approach is lower than for the time slot implementation, albeit only with a small but consistent margin of around 1.25%. See table 8.3 for the numeric values. The results were obtained with a cluster of 200 EVs.

As expected, increasing the fleet's share of EVs present inside the distribution grid cases did not have a significant influence on neither the real-time level and market-level results. Therefore, the graphs for cases x-114 have been omitted here, but the full results can be found in appendix A, tables A.1 to A.8.

For the time slot based implementation, an energy deficit can be taken into account in the total cost, according to section 7.1.2, and also shown in table 8.3. Using these cost figures, the procentual gain of using the event-based implementation over the time slot one is slightly more than doubled.

This energy deficit and the related emergency charging statistics are shown in more detail in table A.9. It can be seen that the use of time slots leads to about 1.6% of "missing energy".

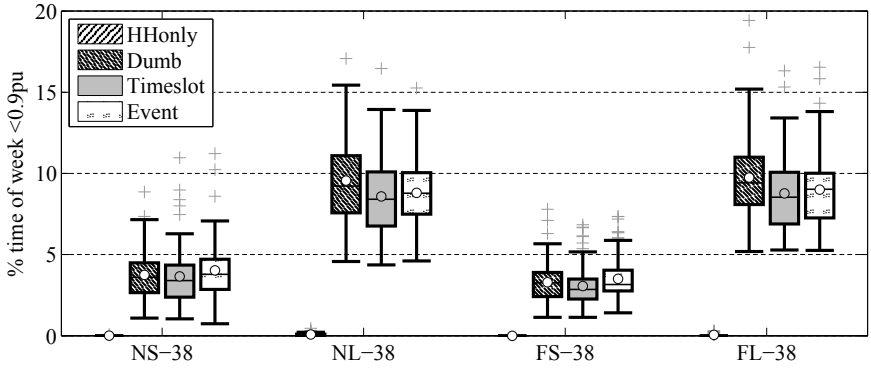

Figure 8.4: EN 50160 voltage magnitude stats (V<0.9pu), passive grid.

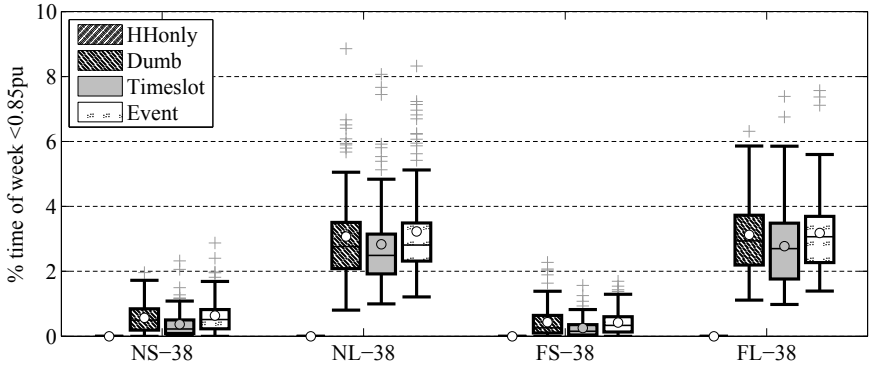

Figure 8.5: EN 50160 voltage magnitude stats (V<0.85pu), passive grid.

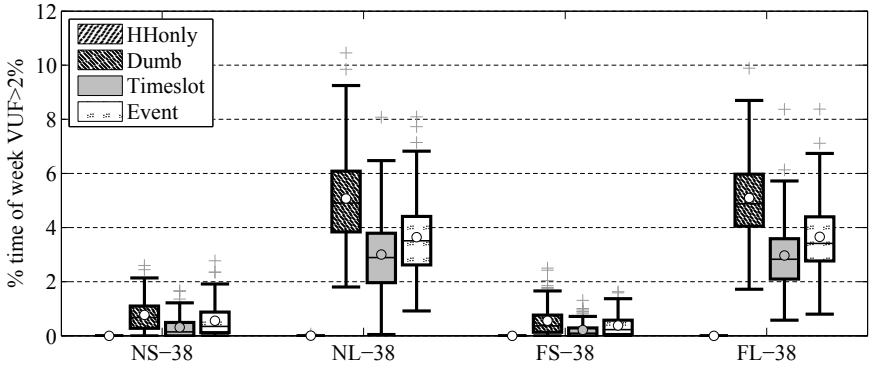

Figure 8.6: EN 50160 VUF stats (VUF>2%), passive grid.

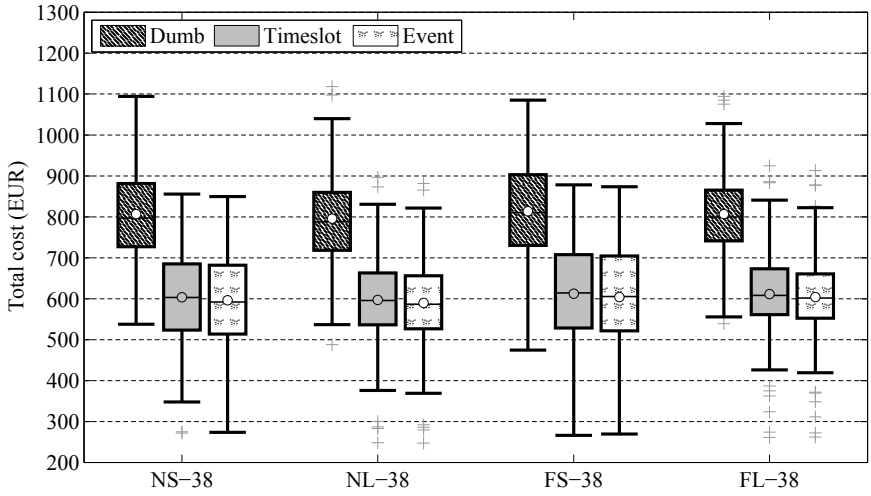

Figure 8.7: Charging cost over 7 days for the ToU aggregator, cluster of 200 EVs, passive distribution grid.

Table 8.3: Charging cost over 7 days for the ToU aggregator, cluster of 200 EVs, passive distribution grid scenarios.

	Dumb	Timeslot		Event	ΔTimeslot/ Event
		w/o E_{deficit}	w. E_{deficit}		
Case NS-38	€805.46	€602.45	€612.48	€595.00	−1.24%
Case NL-38	€795.83	€596.90	€606.87	€589.72	−1.20%
Case FS-38	€814.26	€612.53	€622.50	€604.59	−1.30%
Case FL-38	€806.75	€611.45	€621.43	€603.77	−1.26%
Case NS-114	€792.28	€589.01	€598.79	€580.16	−1.50%
Case NL-114	€823.00	€619.42	€629.42	€611.03	−1.35%
Case FS-114	€816.26	€622.72	€632.54	€614.34	−1.35%
Case FL-114	€819.28	€618.90	€628.81	€610.95	−1.28%

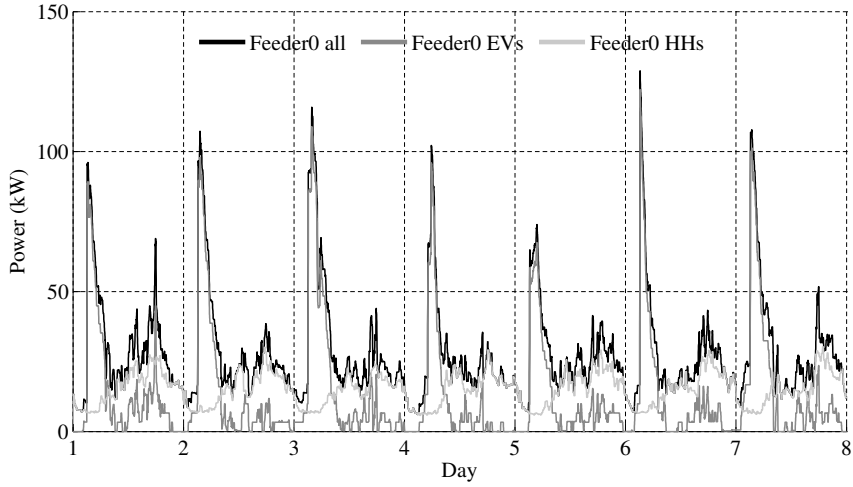

(a)

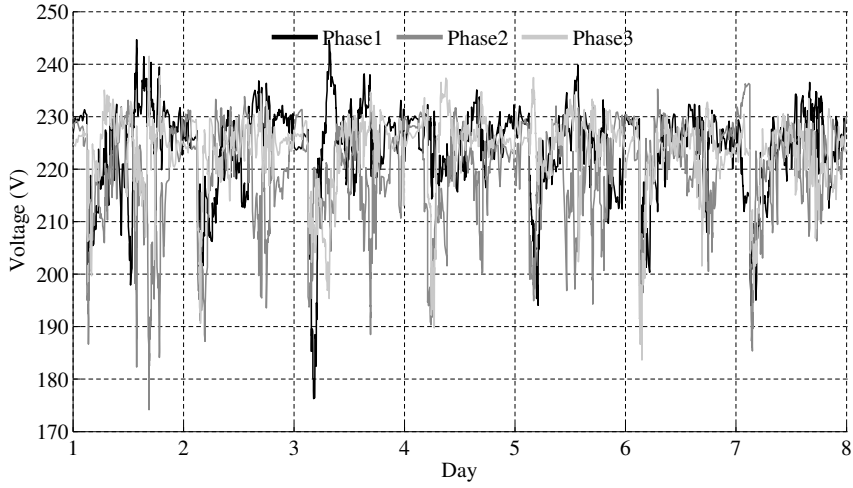

(b)

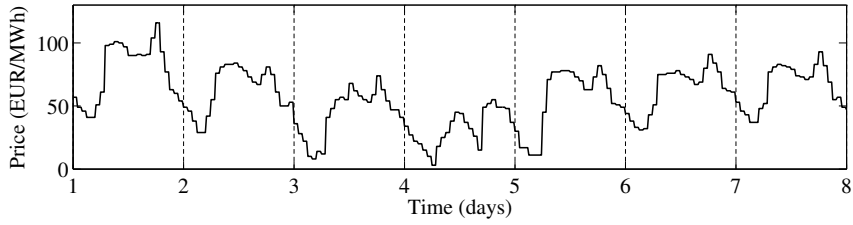

(c)

Figure 8.8: Single simulation instance of case FL-38, passive distribution grid, for the event-based MAS MBC, week starting at day 16; (a) power profiles, (b) voltages in the 3 phases of the Feeder0-line and (c) tariff used for ToU objective.

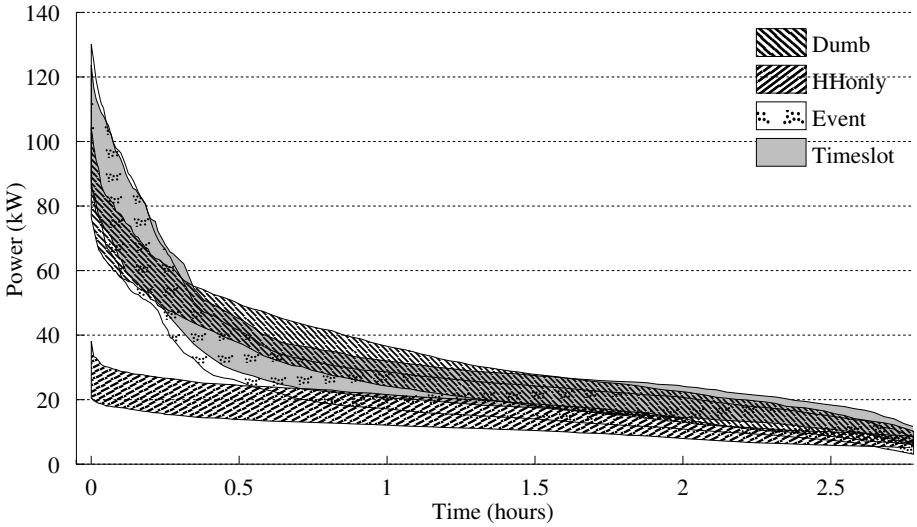

Figure 8.9: Load duration curves of case FL-38, passive distribution grid scenario. The minimum and maximum values that occur during 100 simulations are used to construct the zones for each scenario.

8.5 ToU coordinated charging, active distribution grid

In the previous section and also sections 3.6.1 and 8.1, it was stated that additional grid support functionality could avoid voltage problems in grids with high penetration levels of EVs. This is referred to as an active distribution grid.

8.5.1 Addition of grid support functions

Previously, a link was made to the integration of DER and it was mentioned that in many countries, PV installations are already required by law to respond to grid events [84, sec. 2.13][115]. In its most basic form, such installations simply disconnect from the grid in case the voltage or frequency exceeds a preset threshold value [116, sec. 4.1], in order to avoid islanding. In countries such as Germany, where PV integration levels have reached high levels, legislation now specifies the implementation of a droop mechanism to scale down the power that is injected into the grid [83].

The use of droop control was introduced in section 3.6.1. In this section, agents are added that implement a voltage droop control algorithm. This means that the charger will limit power as soon as the voltage on its connection drops below 0.9 pu. For more details on the implementation, see 4.3.3.

In our evaluation, we want to examine the effect of such droop control enabled vehicle agents inside the grid topologies from section 8.2 and compare the results with the non-droop case of section 8.4.
The EN 50160 statistics are straightforward to compare, but because of the droop control intervention, it can be expected that some vehicles might end up with an incompletely charged battery at departure time t_{dep}, influencing the ToU cost numbers. This effect can be expressed through the energy deficit metric, used in the previous section for the time slot implementation and in 7.1.2, but of course, this number is directly related to the amount of vehicles that can suffer from distribution grid problems. The vehicles outside the load flow simulation (section 8.2.2) will obviously never end up with lost energy.

A distinction between 3 event-based strategies is made; event-based without droop control (Event), event-based with droop control (Event+droop) and event-based with droop control combined with a PI-loop at the fleet manager level (Event+droop+comp). The latter was introduced in section 6.4 and controls the fleet's equilibrium priority with a feedback loop on the quarter hourly accumulated energy. Originally, this method intends to reduce the error introduced by the caching at the cost of an increased number of agent messages,

but should also help to reduce the impact of lost charging energy due to droop at the fleet manager level.

8.5.2 Real-time level results

From figs. 8.11 to 8.13, it is immediately visible that the severity of voltage deviations for the droop enabled agents are reduced. However, because the voltage droop control only activates below 0.9 pu, the measured values for 0.9 pu are still often outside the 5% specifications of the EN 50160 standard. Looking at the 0.85 pu results reveals that such occurrences are entirely solved by the use of the voltage droop controller. By tuning the setpoints of the controller so that it intervenes sooner, the weak grids can be brought into full EN 50160 compliance. This could be done automatically based on forecasts or maybe using a mechanism comparable to 'slow-start' congestion control in the TCP protocol, to find an optimal but adaptive voltage droop controller setting.

Similar to the passive distribution grid case, fig. 8.10 shows the power through Feeder0, this time for both the EVs with and without voltage droop control enabled, and the voltage at the worst nodes of the line. From fig. 8.10c, the voltage droop controller inside the vehicle chargers keeps the voltage deviations in check. This is connected to a change in the power consumed by the EVs, as apparent by fig. 8.10a, where the power profile of the same simulation without droop control is also plotted. Below it, the difference between both profiles is shown. It is visible that initially, power during the peak is lower, but immediately afterwards the lost energy is recovered.

8.5.3 Market-level results

While the droop controller has a positive effect on the voltage problems, it also increases the cost of charging the fleet. Without taking into account the energy deficit at departure time, there is already a small cost increase of 0.6% for the 38-cases, and almost 2% for the 114-cases, where close to 60% of the EVs are situated in weak distribution grids. Taking into account E_{deficit}, this cost increase is doubled.

With the compensation loop, the cost increase can, in the a-cases, be entirely recovered, at the expense of higher requirements to the communication system. The gain seems small, but, since the use of a ToU objective leads to a 'switching behavior', the compensation loop has almost no margin on the equilibrium priority to function properly.

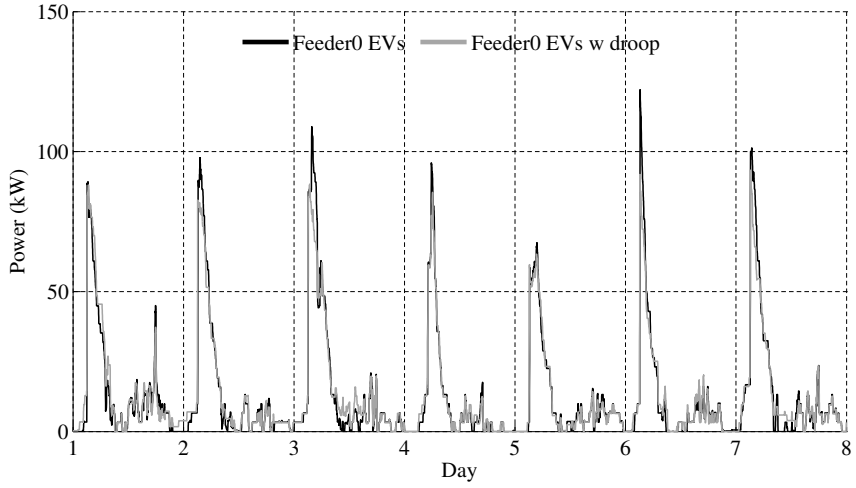

(a)

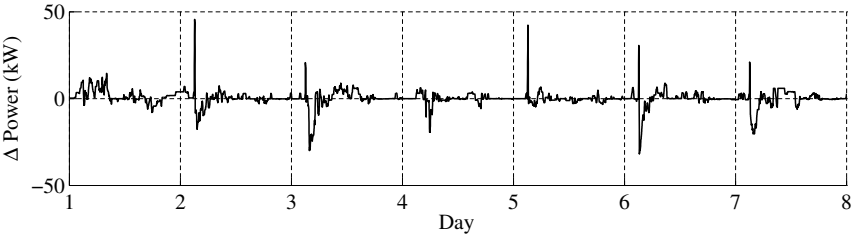

(b)

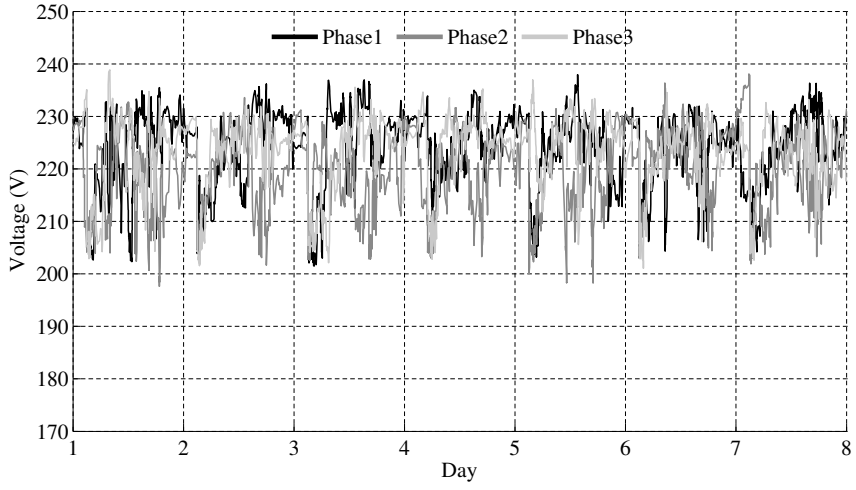

(c)

Figure 8.10: Single simulation instance of case FL-38, both active and passive distribution grid, for the Event-based MAS MBC, week starting at day 16; (a) power profiles for Feeder0, (b) difference between power profiles for EVs with and without droop control and (c) voltage at the worst nodes.

Again, in table A.10, the values regarding the battery deficit and emergency charging are shown. The use of a droop controller clearly leads to an increase in incompletely charged batteries; the cumulative battery deficit volume takes up to 1.15% of the total delivered energy. Comparing table A.9 with table A.10 confirms that the use of a time-slot implementation leads to more occurrences of EVs that depart with incompletely charged batteries and a lower SOC, with respect to the event-based implementation, even if the latter suffers from the activation of droop controllers. Thus, the use of droop control had less negative impact on the market level objective than the implementation of the DR algorithm with the use of time slots instead of event-based.

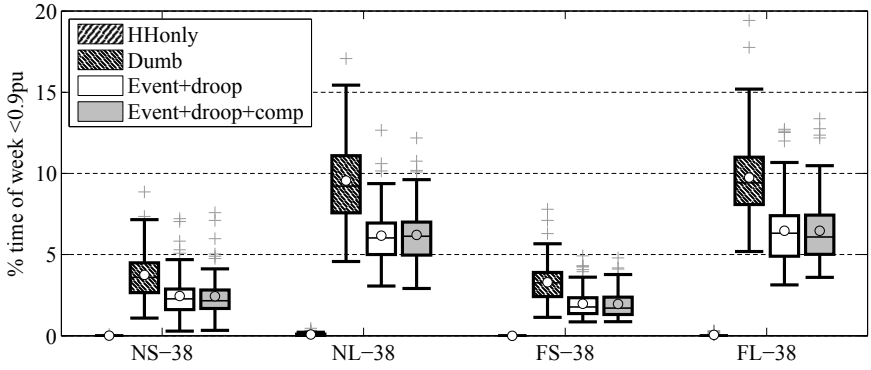

Figure 8.11: EN 50160 voltage magnitude stats (V<0.9pu), active grid.

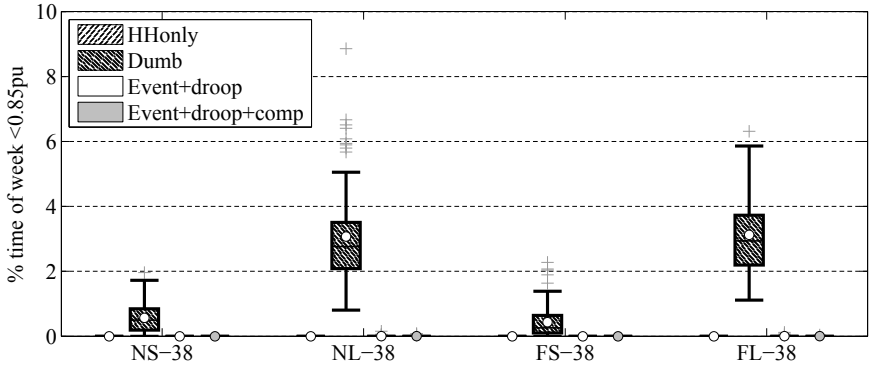

Figure 8.12: EN 50160 voltage magnitude stats (V<0.85pu), active grid.

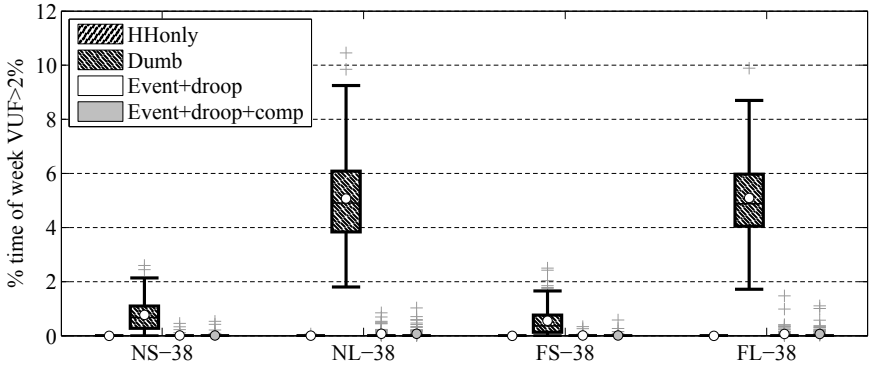

Figure 8.13: EN 50160 VUF stats (VUF>2%), active grid.

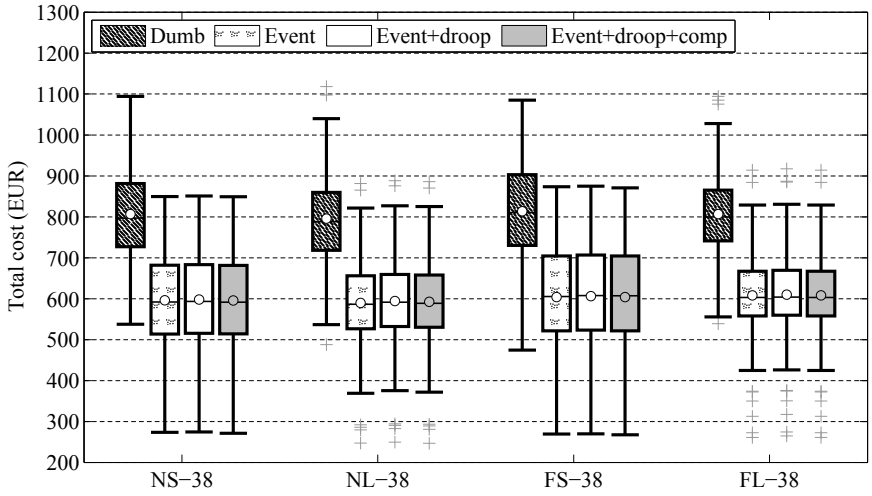

Figure 8.14: Charging cost over 7 days, cluster of 200 EVs.

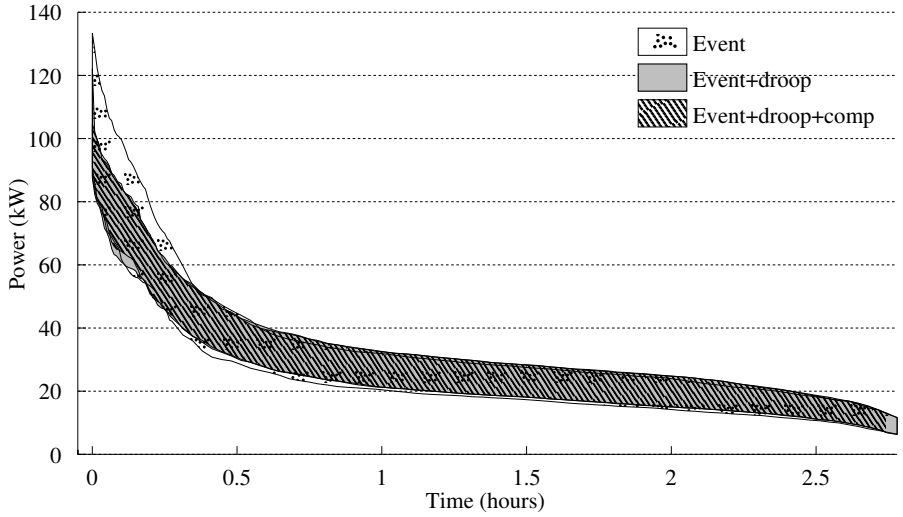

Figure 8.15: Load duration curves of case FL-38, active distribution grid scenarios. The reduction in power peaks, compared to fig. 8.9 due to the use of voltage droop control is apparent.

Table 8.4: Cost of charging over 7 days for the ToU aggregator, passive and active distribution grid scenarios

	Dumb	Event	Evnt+droop		Δdroop	Evnt+droop+comp		Δcomp
			w/o E_{deficit}	w/ E_{deficit}		w/o E_{deficit}	w. E_{deficit}	
Case NS-38	€805.46	€595.00	€596.71	€598.03	+0.28%	€594.48	€595.80	-0.37%
Case NL-38	€795.83	€589.72	€594.25	€600.02	+0.77%	€592.30	€597.96	-0.33%
Case FS-38	€814.26	€604.59	€606.71	€608.20	+0.35%	€604.73	€606.21	-0.33%
Case FL-38	€806.75	€603.77	€609.84	€616.50	+1.00%	€607.94	€614.37	-0.31%
Case NS-114	€792.28	€580.16	€585.32	€589.99	+0.89%	€584.05	€588.72	-0.22%
Case NL-114	€823.00	€611.03	€626.54	€645.26	+2.50%	€625.54	€644.06	-0.16%
Case FS-114	€816.26	€614.34	€620.61	€625.55	+1.02%	€619.37	€624.31	-0.20%
Case FL-114	€819.28	€610.95	€630.91	€653.93	+3.27%	€629.79	€652.49	-0.18%

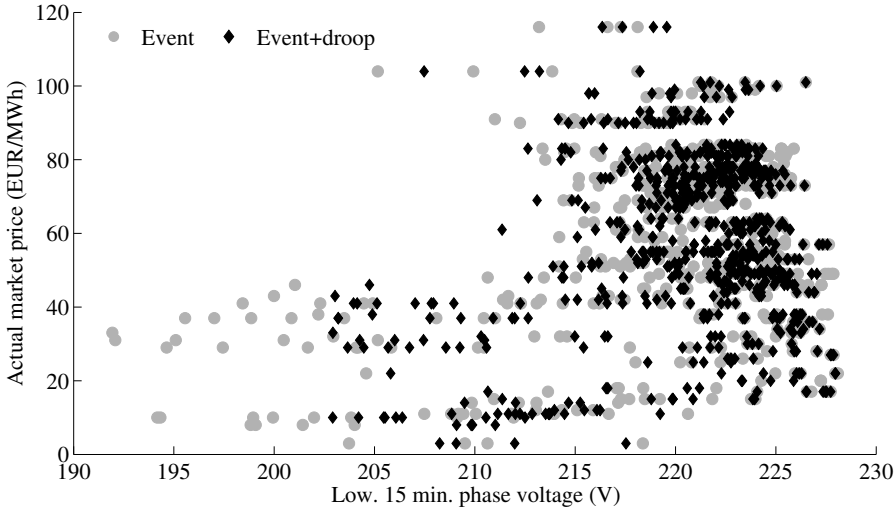

Figure 8.16: Worst phase voltages in Feeder0 versus actual market prices over 7 days, for the MAS MBC algorithm with the ToU-objective, during case FL-38, both active and passive distribution grid. A correlation can be seen between low market prices and the occurrence of voltage dips.

8.5.4 Conclusions on the ToU scenarios

From the results, it is apparent that the Time-of-Use based controlled charging of EVs has the potential to create significant power quality problems, because of the tendency to synchronously switch a large amount of the controlled loads when market prices are low, thereby creating large power peaks. This is illustrated by fig. 8.16.

The effect on the state of the distribution grid can be even worse than when no coordinated charging is used (dumb charging). In fact, there were two mitigating factors in the simulations; the household connection points' phases were alternatingly distributed along the line and the price profiles used by the aggregator kept the power peak of the vehicles out of the household's evening peak. If the latter two were not the case, the EN 50160 results would be even worse.

One could argue that, once the penetration level of electric vehicles reaches a significant share, peak periods will be reflected in the ToU prices, which in turn will favor the spreading of charging load. However, even at high penetration levels, the charging of EVs will remain a small part of the total daily energy

volume and the tariff at the market level will not be dramatically influenced[1]. Furthermore, problems in distribution grids can arise much earlier, due to clustering effects. Additionally, when the share of variable renewable energy sources increases, the wholesale price will become more decorrelated from the instantaneous load. E.g. when wind or solar generation is peaking, electricity prices could be low even though the distribution grids are experiencing high load. Influencing distribution grid congestion through ToU tariffs will need carefully designed tariffs [120, 121].

On the positive side, the use of a simple voltage droop controller can practically solve the encountered power quality issues and can bring the distribution grids back into EN 50160 compliance with some tuning. Figure 8.15 shows the load duration curves of case FL-38 for the event MAS MBC with and without droop, and with compensation. The difference between the droop and no droop case is quite clear.

However, the use of a droop controller has a negative impact on the business case of the aggregator, as the cost of charging goes up and a small number of vehicles do not get their required charge at departure time. But quantitatively speaking, the differences only start to become significant (>2%) when a large share (>50%) of an aggregator's fleet is situated inside weak grids.

[1] According to [117], in 2013, a total of 5.493.472 cars were on the road in Belgium. At ∼50% or 10 kWh of charge per day, and if all vehicles were of the EV type, this amounts to 55 GWh of an average daily total energy demand of 220 GWh [118]. More extensive estimates and information can also be found in [119]

8.6 Balancing case

In the previous sections, the objective for the coordinated charging at the market-level has been the cost of charging for the whole fleet. The outcome of an optimization over a Time-of-Use tariff of the next 24 hours and the constraints of the vehicles results in a charging schedule. While a well-established generic objective, it does not entirely represent the potential of coordinated charging for fleet aggregators.

Alternatively, an aggregator could use the flexibility of a fleet to reduce the uncertainty on his portfolio after day-ahead commitments are made, to limit his exposure to the balancing market. In Europe, balancing services are traded on separate markets than wholesale energy [6]. While the prices for these services are correlated to those of the energy markets, they tend to be more expensive. The responsibility and the costs of balancing are usually attributed to an Access Responsible Party (ARP), which will prefer to reschedule their own generation portfolio rather than being exposed to the balancing market.

For wind farms, for example, wind predictions are used to build estimated production profiles and the required day-ahead nominations. Since the predictions are not perfect, real output will deviate from the day-ahead prediction during the day itself, and without intervention this difference leads to a positive or negative imbalance. By using the energy flexibility of the charging vehicles, an aggregator could try to reduce this wind imbalance.

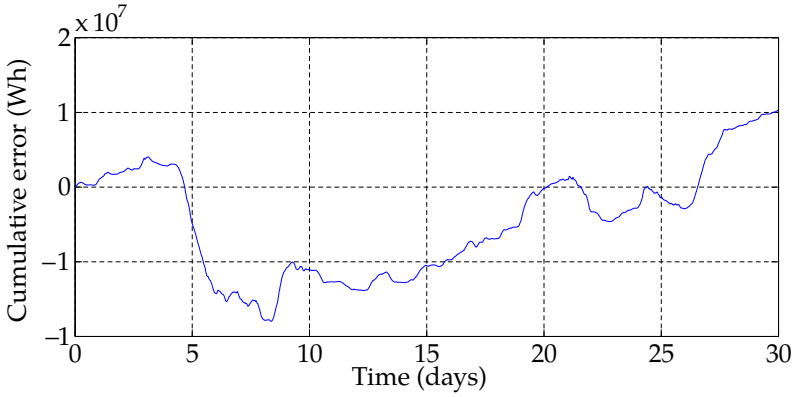

Figure 8.17: Illustration of cumulative wind prediction error over one month.

Wind balancing

The main difficulty in balancing wind with vehicles, however, is that large imbalances require the shifting of a considerable share of the fleet's available flexibility. Because the driving behavior of a fleet has a 24 hour periodicity and remains relatively constant over time, so is the amount of charging energy per day. At the same time, wind prediction errors do not cancel each other out over the course of a day. To illustrate this, the cumulative wind prediction error over the course of one month is shown in Figure 8.17.
Therefore, using all the vehicles' flexibility early in the day means any unexpected imbalance later that day cannot be compensated anymore. A possible solution could consist of incorporating stochastic optimization and intra-day prediction updates to refine the scheduling process.

Nomination induced imbalance

Another source of imbalance lies within the time resolution of the nominations; nominations for the day-ahead market in Belgium require energy values on an hourly basis [122]. However, imbalance volumes are settled on a 15 minute basis. Even if an ARP has predictions on his portfolio with high resolution and accuracy, imbalance will still occur because nominated values are averaged per hour. This is shown in Figure 8.18, where the nominated values represent the same energy as the accurate predictions, but the 1 hour resolution of the nominations allows the 15 minute imbalance to differ from zero.

8.6.1 Optimization problem

The fleet manager could improve the position of the ARP if the charging of the vehicles is controlled in such a manner that aforementioned 15 minute imbalance differences are minimized. Figure 8.19 shows conceptually how the nominated energy's flat power profile can be achieved despite the ramping wind power profile, by using an appropriate EV charging schedule. In the figure there is no forecast error, so the nominated volume E_{nomin} equals the sum of the predicted wind volume E_{wind} and the EV's allocated charging energy over the whole hour. In reality, forecasts are not perfect and there will always be some remaining imbalance, which could be spread out over time using an optimization. Of course, there is a trade-off between focusing on short-term imbalance reduction versus preserving flexibility for still unknown future imbalances.

Equation (8.1) describes the optimization problem. The objective is to minimize the quadratic difference between the energy consumed by the EVs ($E_{\text{EV},t,s}$)

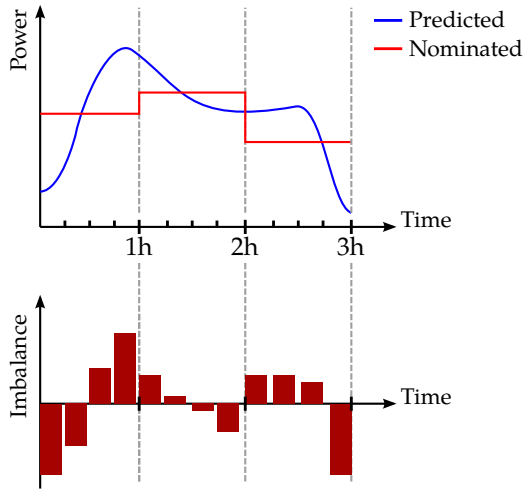

Figure 8.18: Illustration of nomination induced imbalance. The predicted energy equals the nominated on an hourly base (top), but not on a 15 minute base (bottom)

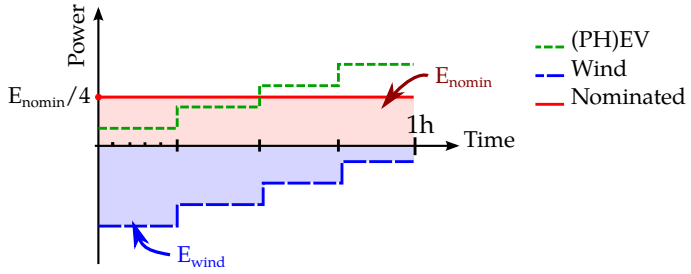

Figure 8.19: Illustration of the balancing objective. The day-ahead nominated energy E_{nomin} contains both the predicted wind and EV energy for that hour. In reality the wind is predicted to ramp according to E_{wind}, leading to an imbalance with the nominated profile on a 15 minute base. However, if there is no wind prediction error, an EV fleet charging schedule exists so that the ARP's power profile still equals the day-ahead nomination.

during the current quarter t, the short term predicted wind energy ($E_{\text{wind},t}$) and part of the nominated energy ($\frac{1}{4}E_{\text{nomin},t/4}$) for the current quarter. A quadratic objective is used so that remaining imbalance is spread as flat as possible over the entire optimization horizon.

$$\min \sum_{t=0}^{t_{\text{horiz}}} \left[\left(\sum_{s=0}^{s_{\text{steps}}} E_{\text{EV},t,s} + E_{\text{wind},t} + \frac{1}{4} E_{\text{nomin},t/4} \right)^2 \right] \tag{8.1}$$

where t_{horiz} is the number of quarter hours inside the optimization's horizon, and s_{steps} the number of steps in the energy constraints graph within a quarter hour.

Additionally, the general constraints related to energy constraints graph optimization apply here as well, see section 5.2.2.

8.6.2 Nomination

The nominated energy $\mathbf{E}_{\text{nomin}}$ consists of a nomination for the EV fleet and the day-ahead wind power prediction with a resolution of 1 hour, for 24 hours. Such nominations have to be determined by the ARP or aggregator, for example from historical records or estimates.

$$E_{\text{nomin},t} = E_{\text{EV,nomin},t} + E_{\text{wind,nomin},t} \tag{8.2}$$

Because the driving behavior of an entire fleet behaves stable and predictable over time, it can be justified to use the power profile of a previous day or week as nomination for the fleet.

When historic energy constraints graphs are used, the amount of flexibility at any given time can be maximized by following an energy path through it according to a fixed ratio of e.g. one half or third in between $\mathbf{E}^{\text{max}}_{\text{aggreg}}$ and $\mathbf{E}^{\text{min}}_{\text{aggreg}}$. Figure 8.20 illustrates such a planned path. The power values that correspond to the path can then be translated to hourly energy values to compose $\mathbf{E}_{\text{EV,nomin}}$. Path deviations will be responsible for not being able to accurately follow this path.

8.6.3 Future fleet constraints

Unfortunately, a problem arises when using real-time energy constraint information from the vehicles. The aggregated energy constraints graph $\mathbf{E}_{\text{aggreg}}$ only contains $\mathbf{E}^{\text{min}}$ and $\mathbf{E}^{\text{max}}$ of the currently active vehicles, not of vehicles

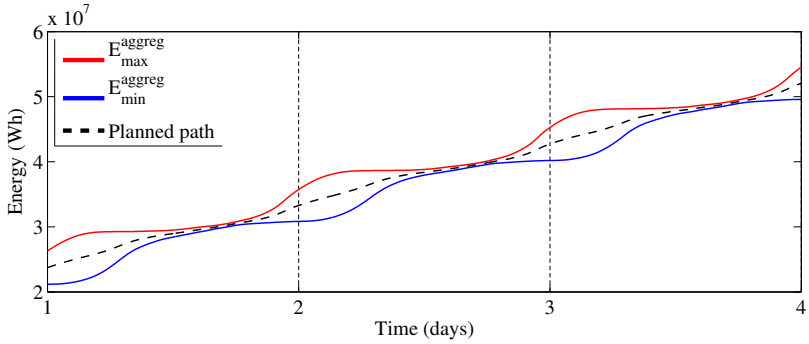

Figure 8.20: Planned EV cluster energy path for determining $\mathbf{E}_{\mathrm{EV,nomin}}$, by plotting a path between $\mathbf{E}^{\mathrm{min}}_{\mathrm{aggreg}}$ and $\mathbf{E}^{\mathrm{max}}_{\mathrm{aggreg}}$

that have yet to arrive. In fact, many vehicles have departure times within 12 hours. This means that only limited flexibility is visible beyond 12 hours. Every time the optimization is performed, new vehicles have arrived and the energy constraints graph's tail rises. To visualize this effect, fig. 8.21 shows consecutive aggregated energy constraints graphs plotted over the historical data. The starting point of each aggregated graph is positioned at approximately the current energy state of the fleet. It can be seen that these graphs flatten out at their t_{horiz}, while ideally they would follow the shape of the historical data.

At the same time, the nominated energy values in $\mathbf{E}_{\mathrm{EV,nomin}}$ already take the energy demand of future charging into account. The result is that the optimization, being quadratically penalized for imbalance, favors to spread out the difference with the nomination and allow imbalance on the short term. Figures 8.22 and 8.23 illustrates this effect. Despite a perfect nomination and sufficient flexibility (fig. 8.23), the "Wind+EV Energy" curve does not coincide with the "Nomination" curve. The net effect is that the aggregator always ends up with a fleet power setting that does not help to reduce imbalance.

Decay-term

There are several ways to handle this complication. An extra decay-term, γ can be added to reduce the influence of long-term information in the objective function of (8.1):

$$\min \sum_{t=0}^{t_{\mathrm{horiz}}} \left[\gamma^{t/t_{\mathrm{horiz}}} \left(\sum_{s=0}^{s_{\mathrm{steps}}} E_{\mathrm{EV},t,s} + E_{\mathrm{wind},t} + \frac{1}{4} E_{\mathrm{nomin},t/4} \right)^2 \right] \tag{8.3}$$

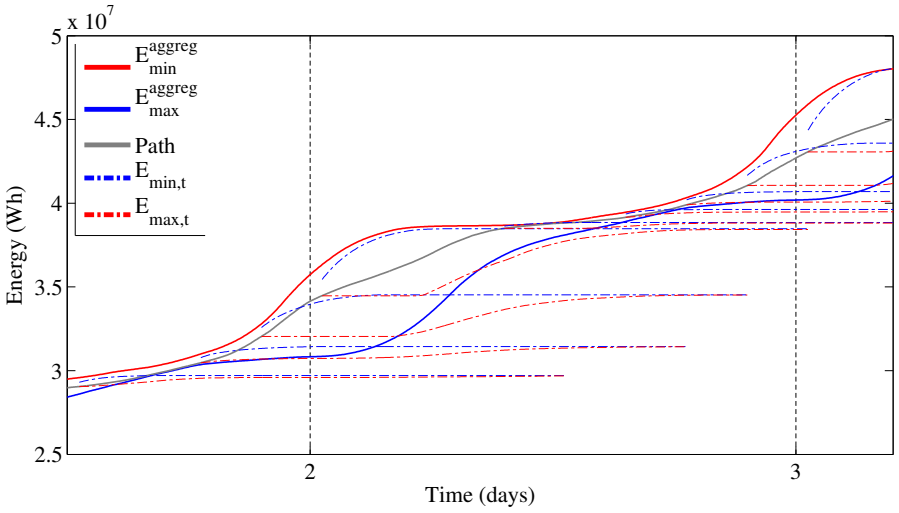

Figure 8.21: Illustration of successive aggregated energy constraints graphs as known to the fleet manager. Thick lines represent historic $\mathbf{E}^{\max}_{\text{aggreg}}$ and $\mathbf{E}^{\min}_{\text{aggreg}}$ data, the gray line in between is the followed path and the dashed lines are real-time energy constraints graphs at the fleet manager. This illustrates that 'real-time' energy constraints data only contains the short term part of the available flexibility.

A $\gamma < 1$ will assign a higher optimization cost to the quarter hour imbalance values that are closest in time. In the limit, a gamma$\rightarrow$0 will mean that the system will be *myopic*, as no information on the future is taken into account. It behaves as the MAS MBC algorithm without planning and minimizes instantaneous imbalance.

However, only so much can be gained by using this method, because the amount of energy nominated e.g. at times >12 hours can happen to be much larger than the energy before it. A more drastic alternative is to reduce the horizon length to 8 hours, but then the ability to consider a fully nominated day is lost.

The decay-term γ could also be used to introduce predicted imbalance-price profiles and try to steer "unavoidable" imbalance towards periods where the probability of low corresponding imbalance price is low.

Historic energy constraints data

A better way to improve the optimization is to modify the energy constraints graphs at the aggregator so that they reflect upcoming EV charging demand.

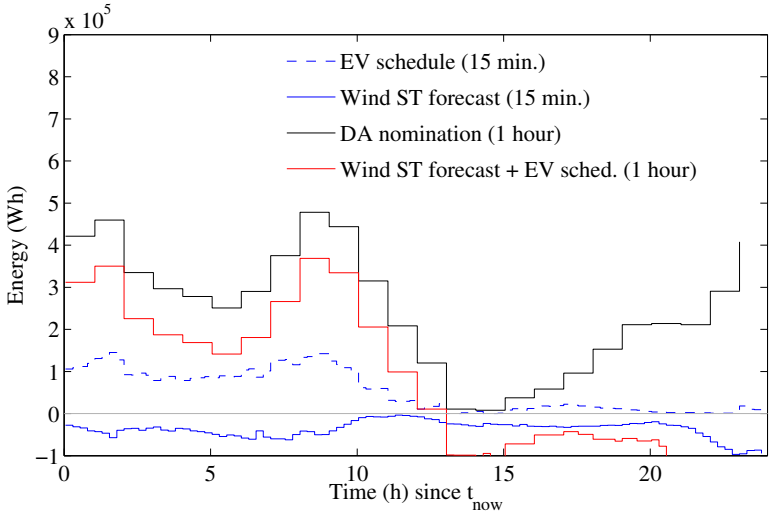

Figure 8.22: Illustration of the outcome of a single balancing objective optimization. Under ideal circumstances, the *Wind Short-Term forecast* together with the *EV scheduled energy* volumes (both on 15 min. basis and the latter being the solution of (8.1)) corresponds to the *Day-ahead nomination*. However, closer to the horizon, the energy constraints shown in fig. 8.23 limit the EV energy that can be scheduled. Due to the quadratic objective, the unavoidable imbalance this creates is spread out over the whole horizon, thus leading to short-term imbalance. Thus, the *Day-ahead nomination* volumes are not met.

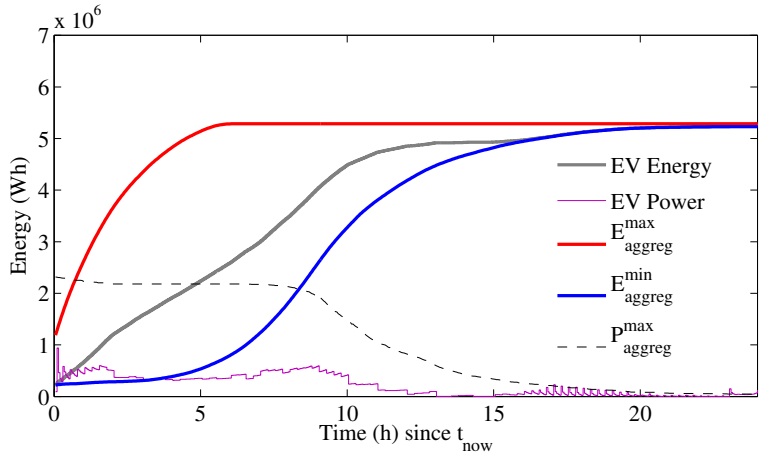

Figure 8.23: Illustration of the outcome of a single balancing objective optimization. Shown are the aggregated energy constraints $\mathbf{E}^{\max}_{\text{aggreg}}$, $\mathbf{E}^{\min}_{\text{aggreg}}$, $\mathbf{P}^{\max}_{\text{aggreg}}$ and optimized path according to the balancing case from (8.1).

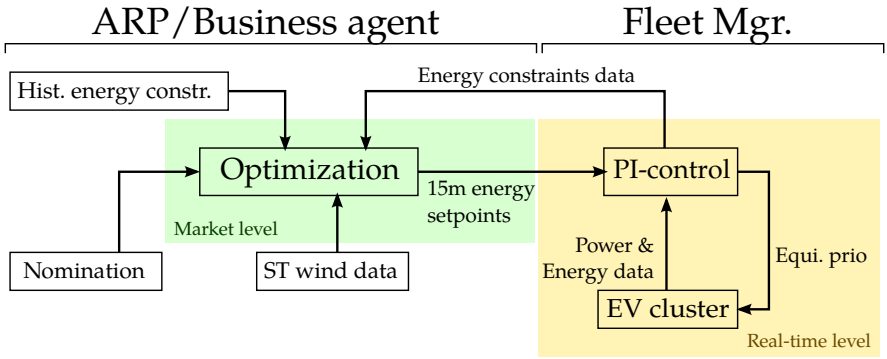

Figure 8.24: Overview of the implemented balancing scenario at the level of the fleet manager and ARP

In the most simple form, one could, similarly to the construction of the fleet nomination $E_{\mathrm{EV,nomin}}$, take historic data for this as a form of prediction. Again, this can be justified by the finding that driving profiles for the aggregated cluster (and therefore charging) do not change significantly from day to day.

A more complicated system could try to combine the aggregated energy constraints from the device agents on the short term with the historic data for the part closer to the horizon of the constraints.

In the balancing case simulations that follow, the thick lines of fig. 8.21 are essentially "cut out" between the appropriate interval, and then replace their aggregated counterparts to obtain the aggregated energy constraints graph.

8.6.4 Scenario and performance indicators

In order to evaluate the benefit of using this objective, a new 'dumb' scenario is added during which the fleet manager only tries to keep the energy consumption as close as possible to the nomination (referred to as *tracking* the nomination with the fleet). All scenarios use the event-based MAS MBC system with PI-loop to coordinate the fleet, but in the 'Tracking' scenario, no optimization to minimize the difference with the nomination using short-term wind data takes place.

An overview of the implemented mechanism is shown in Figure 8.24.

Due to the relatively long simulation time, the need to prepare nomination data for the wind and EVs and an exponentially increasing set of parameters,

a fixed simulation case is chosen for the simulations, in which the wind and vehicle profiles start at day 112 of the year. This was chosen because the first 3 days of the consequent week had relatively little wind imbalance and the last 3 relatively large. To end up with a significant amount of energy flexibility, the EV cluster consists of 1 000 vehicles. Similar to the ToU scenarios, different shares of vehicles can be inside weak distribution grids, following table 8.2.

The main performance indicator consists of the total energy volume of remaining quarter hourly imbalance and the resulting cost. For the latter, real market data on the positive and negative imbalance price from Elia is used. It should be noted that the price data used dates from 2012, because the operating principle of the imbalance settlement was changed from then onwards, while the wind data available is from 2008.

While the total remaining imbalance volume accumulated during a simulation gives a good idea about the performance, it does not tell anything about its distribution during the day. From fig. 8.25, it can be seen that during the first 3 days, nominated and measured wind energy values are reasonably balanced over the course of a day. However, during the last 4 days, the difference between prediction and measured energy exists for the whole period. This is apparent from fig. 8.25b, where the resulting prediction error during each hour of the simulation is shown. Unless the ratio of energy flexibility to wind power is very high, it is difficult to end up without imbalance under such conditions. But the quadratic nature of the objective will favor to spread out the imbalance as much as possible, so that a relatively flat imbalance profile should be obtained in the case of $\gamma = 1$. Therefore, looking solely at the remaining imbalance volume as a measure of performance would not capture the intent of the algorithm's objective.

Because the ability to smoothen or influence the occurrence of imbalance can be very beneficial for an ARP, it makes sense to look at the "variability" of the imbalance profiles. The spectral content of the imbalance profile is obtained by taking the sum of FFTs over a sliding window of 32 profile samples. Then the mean value is subtracted to get rid of the DC component, and the surface under the spectral plot is kept, expressed in kW Hz. The higher this value, the more variability there is on the remaining imbalance's power profile.

To evaluate the effects at the real-time level, the EN 50160 specifications and performance indicators from the ToU case, section 8.3.2, are used here as well.

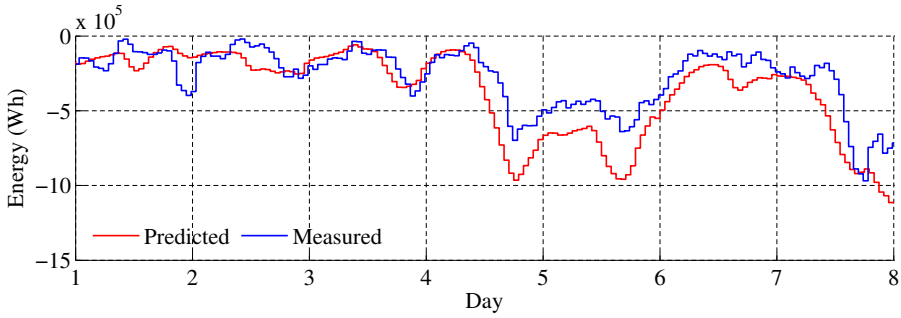

(a)

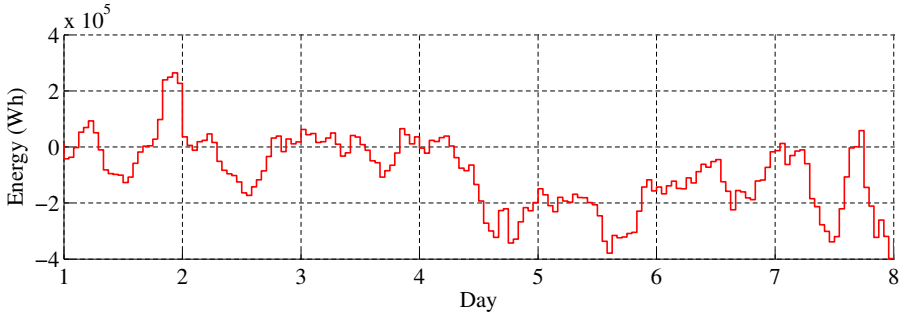

(b)

Figure 8.25: (a) shows predicted and nominated versus measured hourly wind energy for 1.25 MW peak wind power and (b) resulting hourly prediction error over the simulated days

8.7 Balancing case, passive distribution grid

In this section, the balancing case is introduced in the grid scenarios and its variations from section 8.2, without the use of voltage droop control.

8.7.1 Market-level results

In a first simulation, only the behavior at the market level is investigated, disregarding the distribution grid completely. In fig. 8.26a, the 15 minute imbalance volumes are plotted for different values of γ, for a simulation covering the 7 days from fig. 8.25. It is visible that the event-based balancing successfully reduces the amount of imbalance with the nomination. Smaller γ values lead to *myopic* behavior and force the imbalance profile close to zero for as long as possible, until of course the aggregator runs out of short-term flexibility.

In fig. 8.26b, the Fourier transformed imbalance volume is plotted. This figure thus shows its frequency components. In case of the balancing optimization scenarios, it is visible that their imbalance profiles contain less high-frequency components then when no balancing optimization is done. This confirms what can be seen in fig. 8.26a, namely that the case with the balancing optimization for $\gamma = 1$ is able to better spread out the remaining imbalance.

In the above scenario, the wind nominations and measurements introduced in section 4.4.2 were scaled with a factor $W = 0.5$, to obtain a peak wind output of 1.25 MW. Varying ratios of wind and vehicles have also been examined, of which the results are shown in table 8.5 and fig. 8.27.

The improvement in remaining imbalance volume over the tracking case is between 20 and 30%. Smaller γ values act more myopic and lead to slightly less remaining imbalance over 7 days compared to a $\gamma = 1$. However, since the objective of the optimization is related to the quadratic imbalance over the optimization horizon, the conclusion that a myopic algorithm performs better based on the total remaining imbalance would be misleading. It has to be looked at together with the 'spreading' of the remaining imbalance, expressed by the spectral content on the 'V. diff' column of table 8.5.

For larger wind scaling factors and thus larger wind prediction error volumes, the improvement regarding remaining imbalance decreases to 16~21%. A similar effect is observed for the spectral content values. It can be deduced that, based on this balancing method, around 1 to 1.25 MW of wind power can be properly compensated per 1 000 EVs. Higher or lower shares of wind power decrease the efficiency of the system.

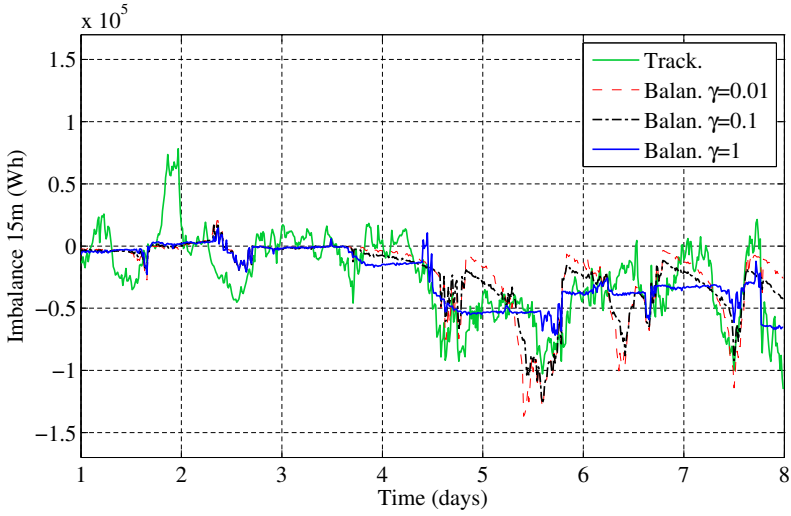

(a)

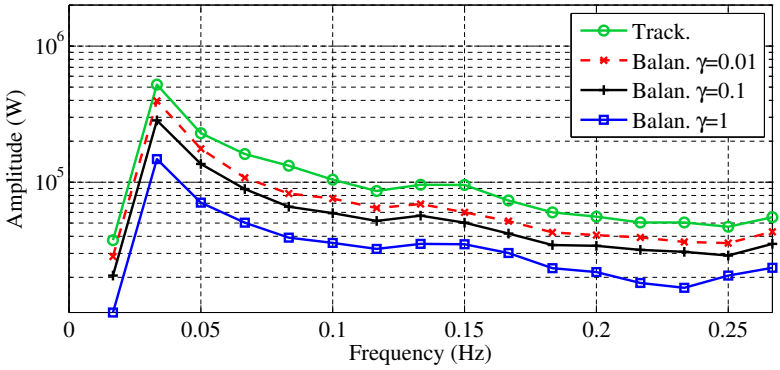

(b)

Figure 8.26: Imbalance rebalancing scenario, 1 000 EVs, $W = 0.5$. For different values of γ and the case without balancing optimization, plot 8.26a shows the power profile as known to the fleet manager, while plot 8.26b shows the spectral plot of the remaining imbalance

Table 8.5: Balancing case simulation results for 7 consecutive days and a cluster 1 000 EVs, for different values of the wind scaling parameter W and decay γ

W=0.05 (0.125 MWp)	Imbal Volume	Imbal Cost	V. diff	Spectr.	S. diff
Tracking nomin.	2.543 MWh	€171.2	0%	2.7 kW Hz	0%
Balancing $\gamma = 1$	2.087 MWh	€128.7	17.9%	2.5 kW Hz	7.4%
Balancing $\gamma = 0.1$	1.988 MWh	€120.9	21.8%	3.1 kW Hz	-14.8%
Balancing $\gamma = 0.01$	1.967 MWh	€117.1	22.7%	3.5 kW Hz	-29.6%
W=0.2 (0.5 MWp)	Imbal Volume	Imbal Cost	V. diff	Spectr.	S. diff
Tracking nomin.	8.633 MWh	€580.3	0%	9.3 kW Hz	0%
Balancing $\gamma = 1$	6.832 MWh	€434.3	20.7%	3.3 kW Hz	64.5%
Balancing $\gamma = 0.1$	6.322 MWh	€397.8	26.8%	6.2 kW Hz	33.3%
Balancing $\gamma = 0.01$	6.131 MWh	€379.7	28.9%	8.0 kW Hz	14.0%
W=0.5 (1.25 MWp)	Imbal Volume	Imbal Cost	V. diff	Spectr.	S. diff
Tracking nomin.	21.056 MWh	€1413	0%	23.2 kW Hz	0%
Balancing $\gamma = 1$	16.680 MWh	€1091	20.8%	7.6 kW Hz	67.2%
Balancing $\gamma = 0.1$	15.775 MWh	€1014	25.1%	13.2 kW Hz	43.1%
Balancing $\gamma = 0.01$	15.313 MWh	€989.4	27.3%	16.9 kW Hz	27.2%
W=0.7 (1.75 MWp)	Imbal Volume	Imbal Cost	V. diff	Spectr.	S. diff
Tracking nomin.	29.364 MWh	€1970	0%	32.5 kW Hz	0%
Balancing $\gamma = 1$	23.888 MWh	€1570	18.6%	12.2 kW Hz	62.5%
Balancing $\gamma = 0.1$	22.860 MWh	€1471	22.1%	18.9 kW Hz	41.2%
Balancing $\gamma = 0.01$	22.216 MWh	€1443	24.3%	23.8 kW Hz	23.8%
W=1.0 (2.5 MWp)	Imbal Volume	Imbal Cost	V. diff	Spectr.	S. diff
Tracking nomin.	41.830 MWh	€2806	0%	46.4 kW Hz	0%
Balancing $\gamma = 1$	35.112 MWh	€2324	16.1%	20.8 kW Hz	55.2%
Balancing $\gamma = 0.1$	33.762 MWh	€2186	19.3%	29.2 kW Hz	37.1%
Balancing $\gamma = 0.01$	33.141 MWh	€2150	20.8%	34.9 kW Hz	24.8%

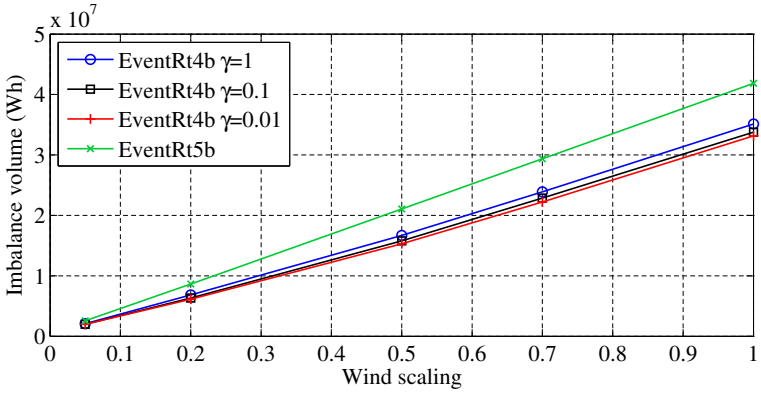

Figure 8.27: Total accumulated imbalance over 7 days in function of the wind scaling parameter W and decay γ

8.7.2 Real-time level results

For the effects at the distribution level, the different cases and its variations again come into play. From the tested parameters in the previous section, we keep the wind scaling of $W = 0.5$ since this parameter led to the best performance at the market level, and a γ of 1, as this is the most generic application.

The EN 50160 results of the passive distribution grid scenarios are grouped together with the active distribution grid scenarios in figs. 8.28a to 8.28c, to improve clarity and avoid duplication. These plots show the results for the FL case. Compared to the ToU results, the problems are a lot less worse, but voltages still drop below 0.85 pu.

The household-only results have been omitted, since there were never voltage problems and the outcome is the same as in sections 8.4 and 8.5.

8.8 Balancing case, active distribution grid

In the simulations in the previous section, the concept of the balancing case was demonstrated in a setting where the state of the local grid was not taken into account. In this section, we continue with the parameters $W = 0.5$, $\gamma = 1$ and in the FL-grid with droop enabled agents.

8.8.1 Real-time level results

As expected, figs. 8.28a to 8.28c show that the use of voltage droop control reduces the limited remaining voltage problems to below the EN 50160 specifications.

Since the tracking scenario already tries to follow the nomination, which is a smooth path through the aggregated energy constraints graph for the EVs, the reduction in voltage deviations are relatively small when voltage droop controllers are introduced, in comparison to the balancing case. This is also captured in the load duration curve for case FL-760 in fig. 8.33, where the plot for the tracking cases shows less power peaks.

8.8.2 Market level results

The amount of vehicles that is affected by droop is supposed to influence the business case at the market level. It would follow that moving from case FL-38 to FL-760 will increase the remaining imbalance, as less and less peak flexibility is available to the fleet manager. Figure 8.29 shows that the imbalance volume is constant for case FL-38 and FL-114, having respectively ~4% and ~21% of the EVs inside of a weak grid.

For case FL-380, with 38% of the fleet inside the weak distribution grids, a small increase of 2.4% in the imbalance volume is noticeable, and finally, for the case FL-760 with 76% of the EVs located inside the constrained grids, the observed increase in imbalance volume is 10.3%. During the latter, the 'dumb' tracking scenario also suffered slightly with a minor 0.95% increase. The resulting energy paths for case FL-760 are also shown in fig. B.1.

On fig. 8.30, the average amount of time left before departure, Δt_{dep}, that remains when emergency charging activates for all vehicles, over the course of 7 days, is shown. According to the plot, with an increasing share of vehicles inside weak grids, EVs enter emergency charging earlier. But at the same time, the amount of vehicles that enters emergency charging decreases. This is shown

on fig. 8.31 and the explanation lies in the compensation by the fleet manager; when EVs start to droop their power consumption, the equilibrium priority is lowered to compensate the energy loss at the market level, as visible on fig. 8.32. A lower priority ensures that vehicles that would otherwise enter emergency charging later on, already commence or speed up their charging. Thus the use of emergency charging decreases.

An exception to the above trend is tracking scenario, where in the FL-760 case, the compensation loop tries to suppress an accumulating energy deficit in order to follow an outdated EV nomination. Initially, due to the voltage droop controllers' activation, the fleet manager compensates by lowering the equilibrium priority to get more vehicles to charge. Later on, these batteries still need to get charged, but the fleet manager desperately tries to follow the nomination, which does not take this into account. With a large share of EVs in weak grids, this overwhelms the limited compensation and equilibrium priority shoots up, as shown in fig. B.2.

Appendix table A.12 lists the exact numbers of the emergency charging results during the balancing scenario.

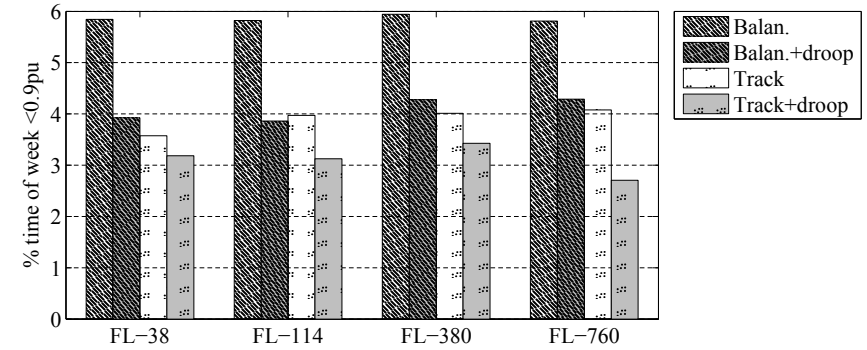

(a)

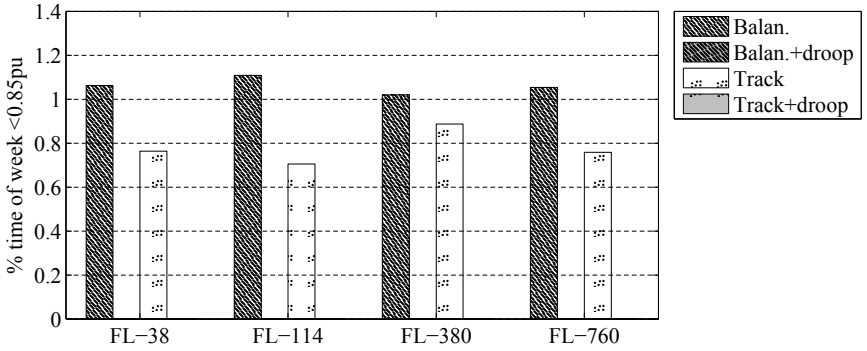

(b)

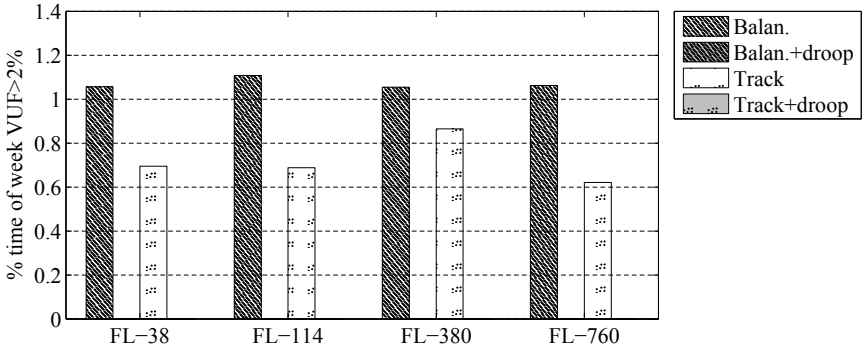

(c)

Figure 8.28: EN 50160 voltage magnitude stats for the single-aggregator balancing scenarios; (a) V<0.9pu, (b) V<0.85pu and (c) VUF>2%

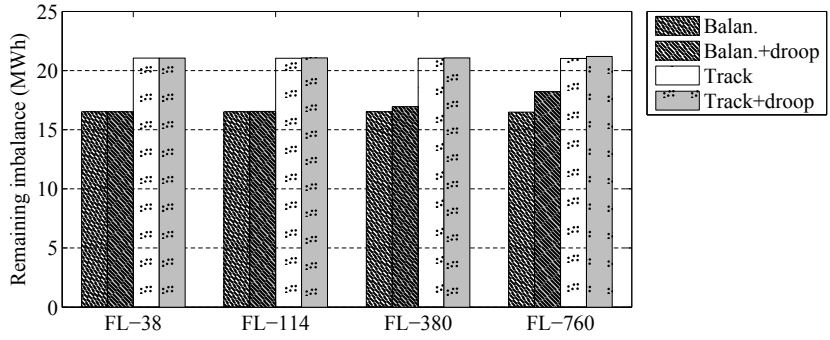

Figure 8.29: Total remaining imbalance after 7 days, for different shares of EVs in weak distribution grids. At larger shares, an effect on the remaining imbalance is noticeable, as the aggregator fails to compensate the activation of the droop controllers.

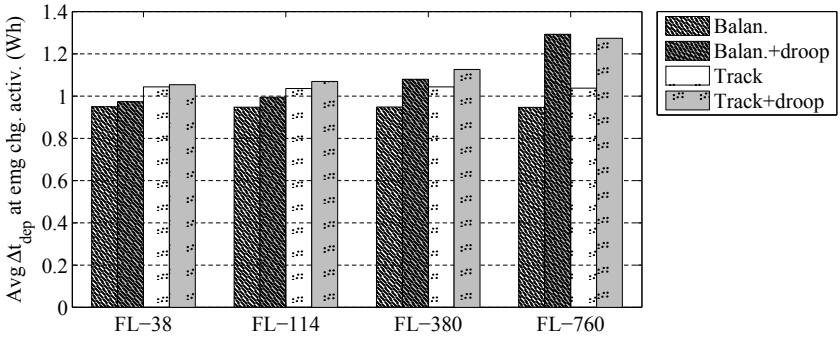

Figure 8.30: Average time-till-departure Δt_{dep} when emergency charging activates during the balancing case, for different shares of EVs in weak distribution grids.

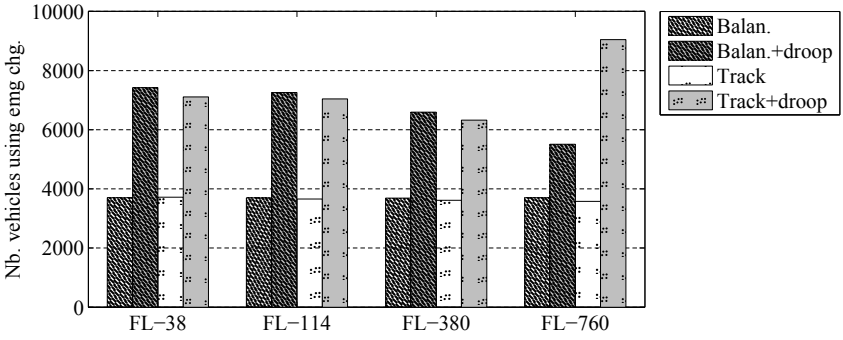

Figure 8.31: Number of occurrences of EVs using emergency charging during the balancing scenario. In general, higher shares of EVs situated in weak grids lead to a reduction in the use of emergency charging.

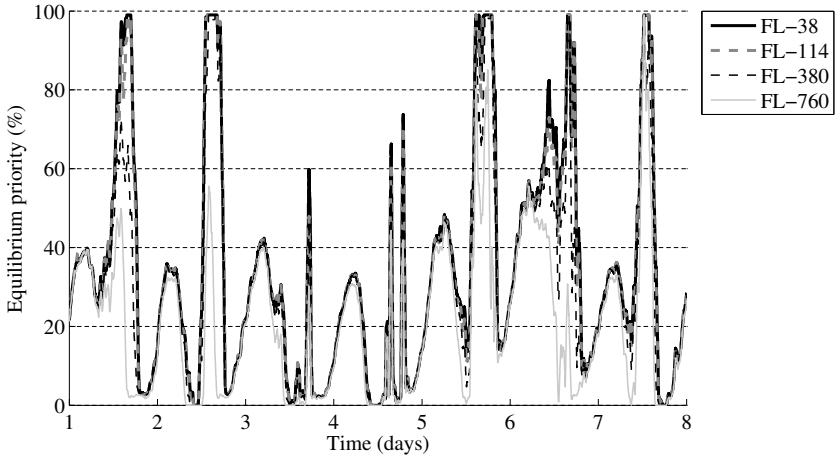

Figure 8.32: Equilibrium priority during the balancing optimization scenarios, active distribution grid cases. Increasing shares of EVs situated in weak grids lead to a decrease in the equilibrium priority.

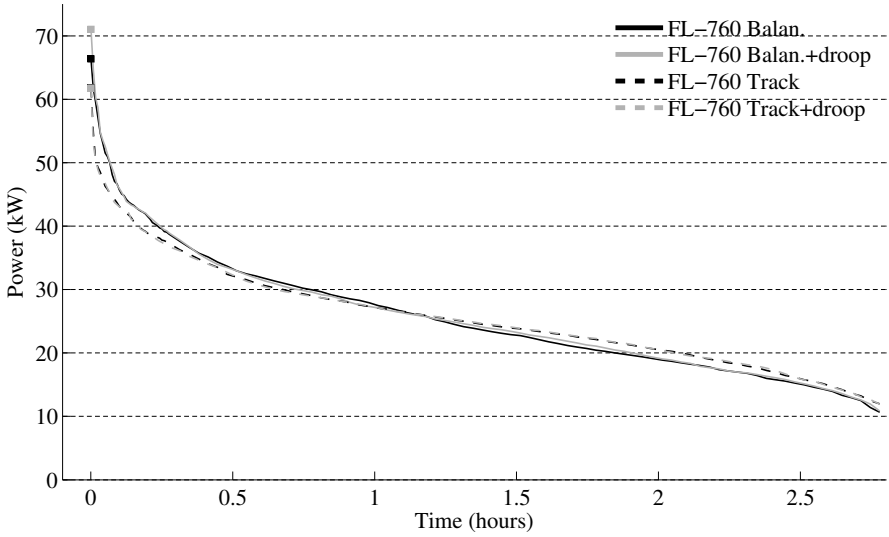

Figure 8.33: Load duration curve for the FL-760 balancing scenario, for feeder0. The use of a voltage droop controller in the balancing optimization case leads to less and smaller power peaks. For the tracking scenario, which tries to accurately follow the day-ahead nominated EV energy, there is practically no gain.

8.8.3 Conclusions on the balancing scenarios

From the results of the simulations using the balancing scenario, we can draw a few conclusions:

- The balancing concept was successfully tested on a portfolio consisting of wind generation and charging EVs. The optimization reduces both the imbalance that originates from the hourly discretization of the day-ahead nomination, and the imbalance that exists because of imperfect wind speed predictions. Using short-term information on the wind production, the imbalance can also be intentionally spread in time. This can be beneficial for the aggregator, as the remaining imbalance could be then be countered by other generation units in its portfolio.
- The use of the balancing objective puts less load on the grid compared to the ToU objective, because flexibility of the EVs is intentionally spread out when creating the nomination of the charging energy and therefore not enabled all at once.
- Voltage droop controllers inside EV chargers are successful in mitigating weak grid constraints. Some tuning of its parameters may be needed to find a setting where the grid state at all nodes is within the EN 50160 specifications during all the time.
- Unless a very large share of EVs of a coordinated charging fleet manager is located inside weak grids, the business case is practically unaffected by the addition of local voltage droop control, using the coordination system that was implemented in this work. That means being event-based for fast response and having a compensation loop at the fleet manager. The combination of both ensures that, when droop controllers activate, the equilibrium priority is changed quickly so that flexibility of other vehicles is used to compensate the loss in expected energy over time.

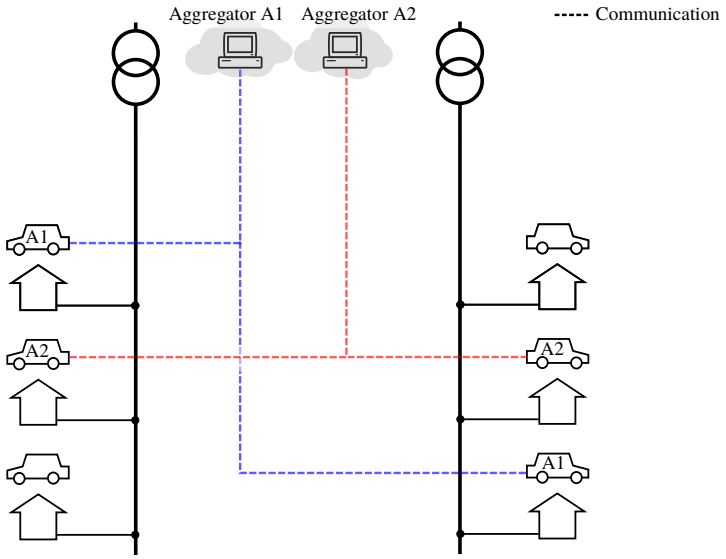

Figure 8.34: Multi-aggregator grid situation. Two aggregators, A1 and A2, control a number of charging EVs that are connected to the same distribution grid transformer.

8.9 Multi-aggregator case

In many cases, when studying coordinated charging of EVs, there is only a single fleet manager or aggregator. However, if the business case of using the energy flexibility of vehicles takes off, it can be anticipated that multiple competing services will become available. This leads to the question what problems can arise if multiple aggregators are active within the same distribution grid, as illustrated by fig. 8.34.

In case of problems, is there a need for additional congestion management mechanisms, to ensure that capacity inside individual grids is allocated to the aggregator's objective that has the highest value, or is the use of a voltage droop controller that intervenes when problems arise sufficient?

The advantage of a voltage droop controller lies in its simplicity of operation and the fact that it does not rely on communication with external actors. More complex grid congestion management systems, briefly touched upon in section 3.5.3, assign an active role to the DSO, that must perform ahead-of-time capacity allocation and/or check iteratively whether all aggregators' schedules are feasible (advance capacity allocation). This would be required for every grid segment wherein aggregators are active. Or, a DSO could set up dynamic ToU

network tariffs based on location and projected network load.

8.9.1 ToU scenario

Since the use of a ToU objective implies that aggregators use the same actual market prices, a multi-aggregator version of the ToU scenario of section 8.3 will not perform any different than its single-aggregator counterpart. Therefore, the simulations and results have been omitted.

However, in case one aggregator is serving mostly customers that are located at the beginning of a line and the other aggregator mainly ones at the end, the latter will be at a disadvantage. A similar situation will occur if the phase connections are heavily correlated with the aggregator assignment. The only way to enforce absolute fairness between the EVs in such case is to resort to congestion management mechanisms, such as discussed in section 3.5.3.

8.9.2 Balancing scenario

During the balancing case, different aggregators can base their optimizations on different predictions or portfolios, and the expected results are not as straightforward to derive as in the ToU cases.

For our simulations, both aggregators will be using an identical portfolio, again consisting of a fleet of 1 000 EVs combined with 1.25 MW of peak wind generation. To have a realistic case that represents wind generation in a geographically shared region, the wind predictions should at least be correlated, which is taken care of by adding one day of difference for the second aggregator. Figure 8.35 shows the resulting wind predictions for both aggregators in the simulations.

To ensure that aggregators each have the same fleet size, the total amount of vehicles in the simulations has to be doubled. But to ensure that aggregator A1 is still assigned the same EVs as during the single-aggregator cases, the simulator framework has to assign the EV driving profiles after the complete agent structure has been set up and each agent's membership to a specific aggregator has been determined. For the additional 1 000 EVs that are assigned to aggregator A2, new historic energy constraints data is derived, identical in purpose as in section 8.6.3.

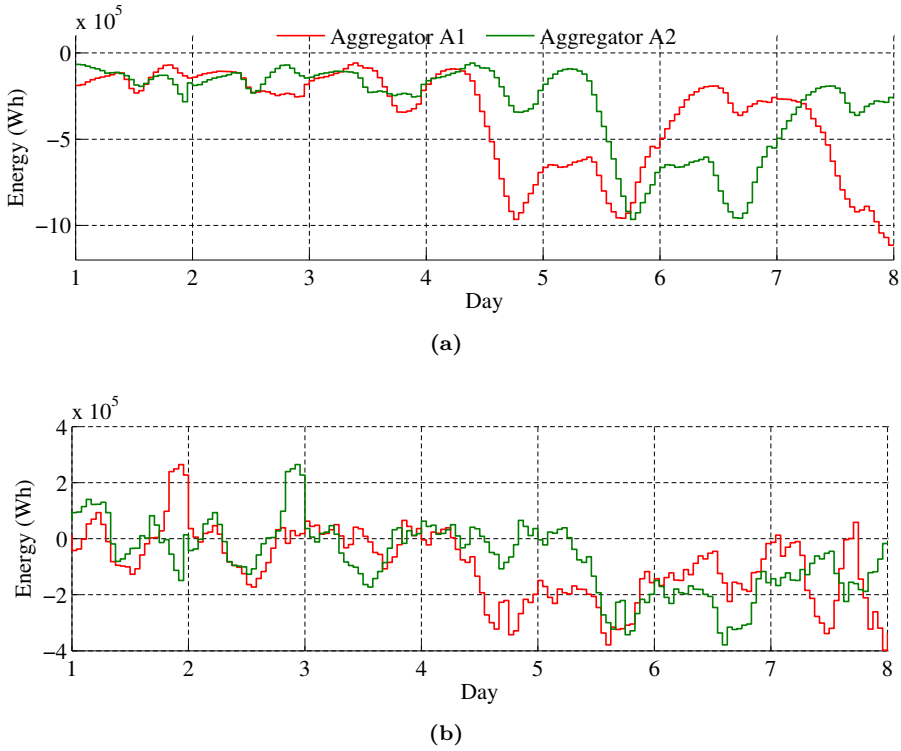

Figure 8.35: Nominated hourly wind energy for both aggregators, with a peak wind power of 1.25 MW on (a) and resulting hourly imbalance on (b).

8.10 Multi-aggregator case with active distribution grid

Again, different cases represent varying shares of vehicles that are inside the weak distribution grids. Case FL-38 has been left out, since at less than 4% of EVs inside a weak grid, the effects during the balancing scenario are practically zero, as previously shown in fig. 8.28 for the voltage deviations and in fig. 8.29 for the remaining imbalance volume.

8.10.1 Real-time level results

On figs. 8.36a to 8.36c, the EN 50160 results are plotted for cases x-114, x-380 and x-760 (respectively with 114, 380 and 760/1 000 EVs inside weak distribution grids). Compared to the single-aggregator scenario, the severity of the voltage deviations is a lot less. This can be entirely attributed to the reduced coincidence of the objectives of both aggregators: the wind profiles differ by one day, and the EVs are divided 50/50 between the two aggregators.

8.10.2 Market level results

The total remaining imbalance for both aggregators after one simulated week is shown in fig. 8.37. Just as with the single aggregator case in fig. 8.29, the imbalance volume is only affected by the droop controllers at high shares of EVs in weak grids. It should be mentioned that absolute volume of aggregator A2 is lower because its wind profile starts one day earlier than that of A1, thereby avoiding a day with large prediction error. This is due to the choice of scenario, and it is not relevant to compare the remaining imbalance volumes of A1 and A2 directly.

On figs. 8.39a and 8.39b, the equilibrium priority during the 7 days for the A1 and A2 fleets are shown. As was the case with the single aggregator scenario, more vehicles enabling voltage droop lead to a lower equilibrium priority. This is clearly visible in the evening of day 5, where both aggregators suffer from a large wind mismatch. Overall, this leads to a decreasing number of EVs that need to enable emergency charging, as visible from fig. 8.38. However, droop control increases the need for emergency charging.

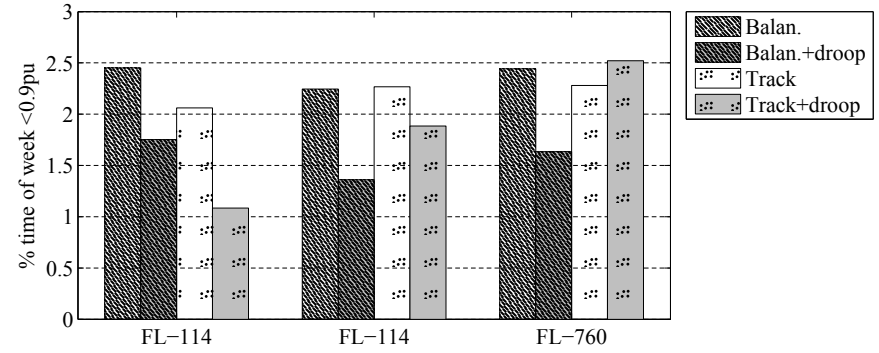

(a)

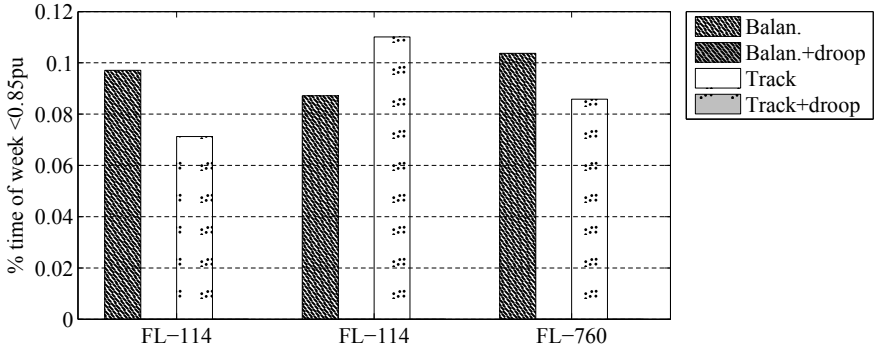

(b)

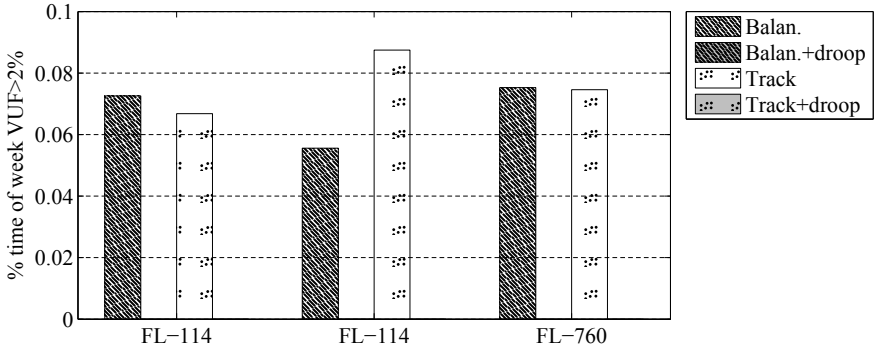

(c)

Figure 8.36: EN 50160 voltage magnitude stats for the multi-aggregator balancing scenarios; (a) V<0.9pu, (b) V<0.85pu and (c) VUF>2%

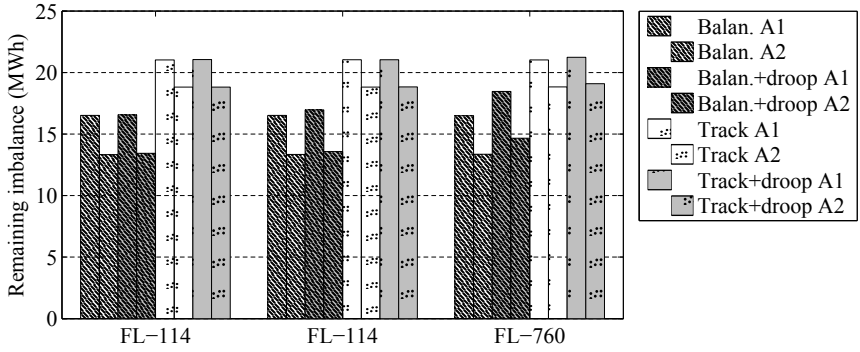

Figure 8.37: Total remaining imbalance after 7 days. Left side of bar represents aggregator A1, right side aggregator A2

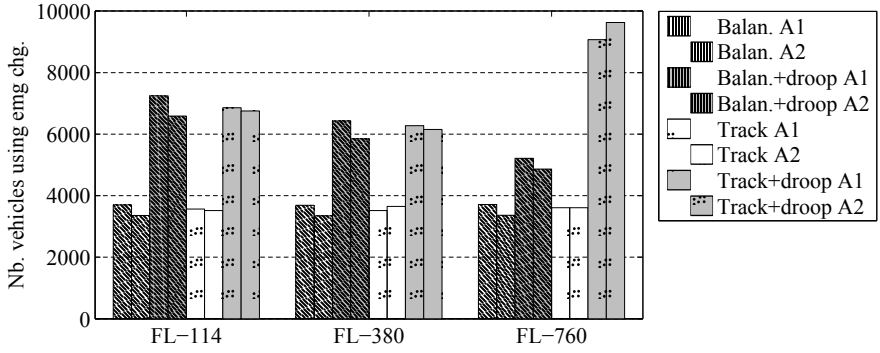

Figure 8.38: Number of vehicles using emergency charging over 7 days. Left side of bar represents aggregator A1, right side aggregator A2

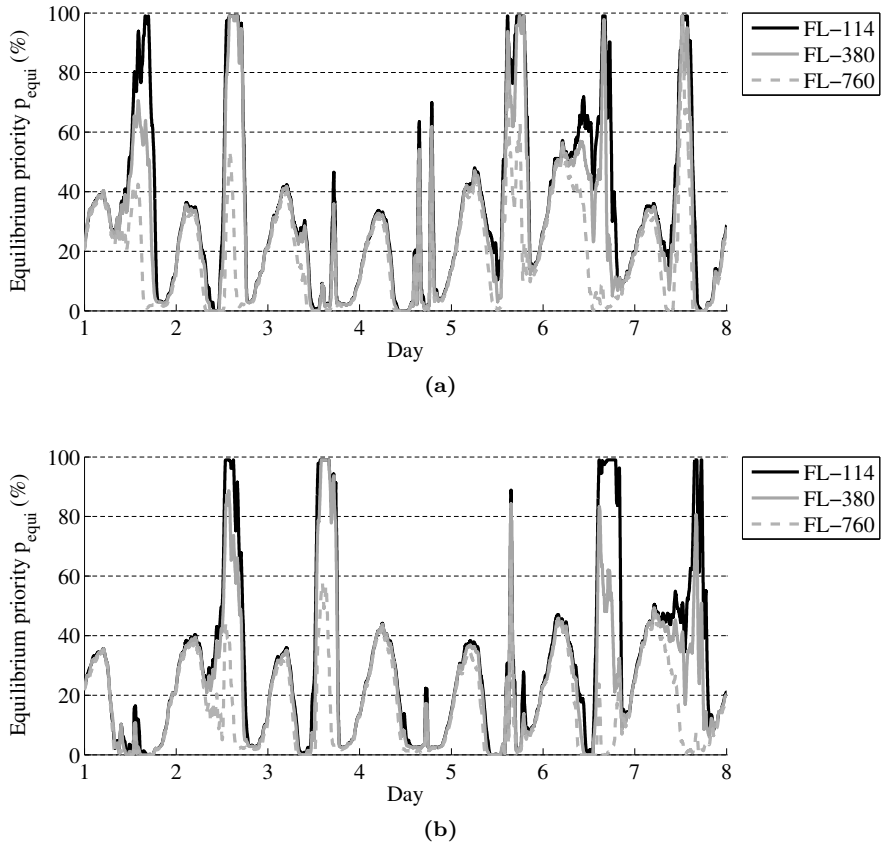

Figure 8.39: Equilibrium priority for (a) aggregator A1 and (b) A2 during the balancing with droop simulations

8.10.3 Conclusions on the multi-aggregator scenarios

From the results, it can be concluded that settings where two aggregators are active within the same part of the distribution grid do not show problematic behavior. This is due to the fact that the wind profiles are not the same for both aggregators, so that access to EVs' flexibility in one distribution grid is spread out and less voltage deviations appear. Therefore, in the worst case, voltage deviations would be similar to those of the single-aggregator case. After the single-aggregator results, this may now look as a logical outcome.

But, with these results in mind, and based on the implemented DR algorithm with voltage droop controllers inside the presented grid configurations, the necessity of additional grid congestion management mechanisms can be questioned. The complexity introduced by such solutions, computationally and from a responsibility perspective, are hard to justify with the amount of gains that can be achieved.

It was however assumed that the EVs were evenly assigned to both aggregators. In the situation where one aggregator controls all the EVs at the beginning of a grid and the other all the EVs towards the end of the line, the latter will be subjected to more droop activations and be at a disadvantage compared to the other aggregator. But again, the limited energy deficits this causes might not warrant the deployment of grid congestion management mechanisms (e.g. capacity markets in cooperation with the DSO, section 3.5.3).

Chapter 9

Conclusions and Future Work

In this dissertation, the problem of performing Demand Response by means of steering a fleet of charging Electric Vehicles (EVs) was approached from practical, real-world considerations. An existing agent based algorithm, rooted in market-based control was expanded and adapted to operate in an event-driven environment. For evaluation purposes, a simulation framework was developed in Java and MATLAB, allowing to simulate both the market objectives of an aggregator and the technical constraints at the level of the distribution where the EVs and residential loads are located.

In this chapter, the conclusions of each chapter are synthesized, then the contributions of this work are listed and finally directions for future work are indicated.

9.1 Summary of the chapters

In chapter 2, the situation surrounding and the standardization of electric vehicle charging in Europe has been discussed. The IEC 62196-2 Type 2 connector is quickly becoming the default solution for AC charging up to 32 A. However, due to the limitations of typical residential electrical installations, charging EVs at home using a single phase connection is limited to 16 A or 3.3 kW, unless dedicated wiring is added.

Since compatibility issues regarding the charging connections are now gradually being resolved, attention is shifting towards enabling high-level communication between EVs and external services. At the moment, IEC 62196-1 allows for

simple signaling from and to the vehicle to determine and change the charging power, but more advanced solutions are essential to allow EVs to participate in large-scale Demand Response (DR) systems. The upcoming IEC 15118 will address this kind of applications.

Since the topic of Demand Response gained renewed interest in recent years, a lot of research focuses on the optimization and coordination of demand response clusters. In chapter 3, a selected number of relevant algorithms from literature for the optimization and coordination of demand response clusters is discussed and classified. Depending on the way the optimization is performed, a distinction is made between distributed, centralized and aggregate & dispatch algorithms.

> *Distributed* algorithms perform part of the optimization process of allocating energy over the cluster at the participating devices themselves. The computational complexity is spread out over the demand response cluster, typically using an iterative process where information is communicated between the participants.
>
> In *centralized* algorithms, a central actor collects information from the DR devices, such as individual constraints and deadlines or comfort settings. Using the collected data, and possibly predictions or stochastic functions, the central coordinator performs a single optimization that returns an optimal schedule satisfying all the constraints at once. Inherently, this makes centralized algorithms the least scalable, as the optimization process quickly becomes intractable and the communication to a single point poses a potential bottleneck.
>
> *Aggregate & dispatch* algorithms decouple the optimization of the objective and the dispatch of its outcome, thus alternatively the term 'dispatching mechanism' is equally fitting. An aggregate and dispatch mechanism allows information from and to the central entity to be aggregated, reducing the complexity of the optimization and improving scalability, but carrying certain compromises or constraints regarding the optimality of the results.

In a DR system, there is a collection of users with their own objectives (minimizing energy cost or losses, maximizing comfort, etc.) that compete or cooperate with each other and an aggregator. Since the actors involved are capable of taking autonomous decisions in the DR cluster, they can be represented by agents inside a multi-agent system (MAS).

The second part of chapter 3 focuses on grid congestion problems and mitigating solutions. In weak or overloaded distribution grids, power quality problems will appear, usually in the form of under/over-voltages. In this work, grid congestion problems are described along the EN 50160 standard.

Besides increasing the transfer capacity, a Distribution System Operator (DSO) can address congestion problems by steering the active power flow, e.g. with DR and voltage droop control.

One specific type of aggregate & dispatch algorithm, referred to as Market Based Control (MBC) is rooted in the theory of microeconomics. In an ideal market setting, each economic agent decides on a quantity of resources that is small compared to the total volume traded in the market. Thus individual transactions have no influence on the unit price of the resource. Additionally, all agents respond to the same price, which corresponds to the point where the amount of resources sought by buying agents equals the amount produced by the selling agents. In economics, this is known as a general equilibrium market.

In PowerMatcher, appliances in a DR cluster are represented by software agents. They control a local process (such as heating water or charging an EV battery), but compete for resources (being electric power) on an equilibrium market with other agents. Device agents assemble demand curves representing their willingness to pay and consume, taking into account the specific constraints of the controlled device. Demand functions are sent upwards and an auctioneer agent performs a matching process with producing agents. An equilibrium price is communicated back to the agents, that proceed by consuming or producing.

This agent-based market based control process is referred to as MAS MBC. Because of the aggregation of demand curves and the low complexity involved in building a device's demand curve, the algorithm is scalable to large amounts of vehicles. Furthermore, since operation only depends on the exchange of demand functions and price, any kind of device can be integrated in the cluster, as long as it can be represented by a demand function.

The lack of scheduling functionality of the MAS MBC has been addressed with the addition of energy constraints graphs and the application to charging of EVs detailed in chapter 5. A major pitfall of the method is the risk of *path deviations*, which occur due to the application of a heuristic in the demand functions, and lead to a suboptimal dispatch of the aggregated power of the fleet to the individual EVs.

To address the separation of market-level and real-time level objectives, chapter 6 describes the modifications and additions to the MAS MBC.

1. *Dual coordination* by splitting the auctioneer agent in an asynchronous part, the fleet manager, and a synchronous part, controlled by a market operator agent. Energy setpoints are passed from the business agent to the fleet manager to coordinate the EV cluster. Optionally, the fleet manager implements a PI loop by steering the equilibrium priority in function of

the error between the business agent's energy targets and the expected consumption of the cluster.

2. *Event-based interaction* between the agents, for fast communication of constraints and equilibrium priorities.

3. *Caching* of constraints and equilibrium priorities, and *estimation* of the EVs' energy state by the concentrator agents.

The additions have been designed primarily for use with DR clusters consisting of EVs only, and in chapter 7 the event-driven MAS MBC (RT-MAS MBC) is applied in a few scenarios to evaluate EV demand functions, compare the performance of the event-driven versus a time slot based implementation, and assess the impact on the amount of communication with the device agents.

From the results of the simulations in chapter 7, the use of time slots leads to a small loss of DR flexibility compared to the event-driven implementation and the appearance of incompletely charged EV batteries, in a scenario with a Time-of-Use cost minimization objective. The term energy deficit was introduced to account for the subsequent loss in delivered energy. It has also been shown that the use of the 'asymptotic' demand function creates more path deviations than the 'linear' alternatives.

In another scenario, the results show the discrepancies (response speed and communication, energy loss) that a time slot based system implies in the case of coordinated charging, which are hard to avoid without switching to very small time steps. This is where a continuous or event-driven system has a clear advantage; it has virtually infinitely small time steps.

Due to the use of caching in the event-driven implementation, a trade-off exists between reducing the amount of messages exchanged with EV agents and the optimality of the coordination, when compared to the time slot based results. Nevertheless, in one case, a slightly improved coordination (a lower cost of charging) was achieved at 70% less messages when compared to the time slot based implementation. It is expected that similar results can also be achieved under different settings, e.g with more EVs or other market-level objectives.

In chapter 8, scenarios encompassing both market-level objectives and distribution grid effects are considered, meaning that the physical location of the charging EVs in the grid is taken into account, together with the effects of voltage droop controllers inside the chargers. The latter is referred to as active distribution grid cases. Four 'weak grid' topologies are defined according to the distance between the household nodes and to the distribution grid transformer. The results regarding undervoltage and phase unbalance are evaluated according to the EN 50160 standard.

In a first series of simulations, a single aggregator is responsible for the charging of all EVs that are present inside the simulated distribution grids. When a cost minimization objective based on a Time-of-Use tariff is used at the business agent, DR of EVs creates significant power quality problems. The tendency to synchronously switch a large amount of the controlled loads when market prices are low creates large power peaks at one or two points during the day, and is responsible for the occurrence of severe undervoltage events. The effect on the state of the distribution grid with coordinated charging can be even worse than when no coordinated charging is used (dumb charging).

On the positive side, the use of a simple voltage droop controller embedded in the EV chargers can solve power quality issues and bring the distribution grids back into EN 50160 compliance with some tuning.

An alternative objective for the business agent consists of the balancing of a wind generation and EV portfolio. Day-ahead nominations contain predicted wind output and EV consumption, of which the latter is based on a preferred operating path. During the day itself, an optimization takes the nomination and updated wind information to steer EV charging in an effort to spread remaining imbalance and thereby minimizing exposure to the imbalance market. The simulations show that such objective puts a lot less stress on the distribution grid compared to the ToU case, as EVs are more gradually charged over time.

It was also shown that the use of voltage droop controllers alone embedded in the EVs proves very effective in reducing grid congestion problems. Only when large shares of the cluster of EVs (>40%) are located within weak grids would the business case of the aggregator become negatively affected by the activation of the droop.

The step to a scenario where multiple aggregators control charging EVs that are connected to the same transformer is made in section 8.9. In case of the ToU objective, the worst case corresponds to a single-aggregator scenario. Because each aggregator's EVs are equally and alternatingly distributed over the phases, no major effect has been measured on the business case.
For the balancing optimization case, results are very similar to the single-aggregator scenario. Due to the fact that the wind profiles are not the same for both aggregators, access to EVs' flexibility in one distribution grid is spread out and less voltage deviations appear. Under worst case conditions however, they would be equal to the single-aggregator case.

9.2 Conclusions regarding the research objectives

The main contributions, in the light of the challenges stated in section 1.4, can be summarized as follows:

- An agent-based Demand Response algorithm was adapted and extended in order to address the separation between market-level objectives and technical objectives. Both work at different levels; the market operation level is responsible for the business case of a fleet of EVs and operates synchronous with the energy markets. The real-time operation level uses the setpoints determined by the business case and uses an event-driven architecture to efficiently dispatch constraints from and control signals to the charging EVs.
- It has been shown that the event-driven approach allows for a quick response and reduced amount of communication with the EVs, compared to a time slot based implementation, and that the optimality of control can be traded off for a further reduction in communication with the EVs.
- The effect of using market-level objectives on congestion in weak distribution grids has been examined. Especially the use of ToU cost minimization objectives has a negative effect on the occurrence of undervoltages, with respect to the EN 50160 standard. Synchronization of large amounts of controllable loads is to be avoided in DR.
- Besides a ToU cost minimization objective, it has been shown that a cluster of fast-responding EVs can be used to limit an aggregator's exposure to the balancing market. An optimization at the market level determines setpoints for the fleet such that the remaining imbalance between predicted and nominated wind output and more recent short-term predictions is spread out in time. This can be beneficial for the aggregator, as the remaining imbalance could be then be countered by other generation units in its portfolio.
- A straightforward and common way of mitigating grid congestion is the use of a voltage droop controller. While fast, inexpensive and able to act independently from any central coordinator, its activation will intervene in the schedule intended by the business case. In literature, the overruling of the market operation level by technical objectives is often presented as a major challenge to be addressed. The results in chapter 8 show that, unless very large shares of the EV fleet are located inside such weak grids, the effects of the activation of voltage droop controllers on the business case remains relatively modest. This is due to the limited amount of

scheduled energy that is 'lost' and the possibility to compensate for it by other EVs present in the DR cluster.

- Additionally, situations where multiple aggregators are active within the same distribution grid were also looked at. Based on the assumptions made and using the presented DR algorithm, it can be stated that the use of voltage droop controllers only is already effective in mitigating grid congestion problems without significantly disturbing the aggregators' business cases. The need for additional grid congestion management algorithms, such as a capacity market in cooperation with the DSO, might better be reserved to a few corner cases, e.g. where increasing the transfer capacity of the grid is (economically or otherwise) infeasible.

9.3 Future work

- The simulated weak distribution grids are of a synthetic nature, being constructed to find a point where, given a realistic number of households, problems would appear due to the addition of a high number of charging EVs. To further support the conclusions regarding the value of voltage droop controllers and grid congestion management, new simulations in actually existing settings and 'corner case' distribution grids are recommended. These could include unbalanced phase connections, residential PV installations, and penetration levels of EVs less than 100%. An interesting development is the increasing use of residential heat pumps, which, on top of charging EVs in weak grids might be tipping point for what is physically feasible. However, the focus should remain on evaluating solutions that are economically feasible and technically implementable, as they have to compete with the relatively straightforward approach of upgrading grid infrastructure instead.

- In the presented work, attention was always towards the application of coordinated charging of EVs, which have a large amount of flexibility and no power profile constraints to speak of. To make the DR algorithm suitable for non-EV clusters, the suitability of some of the adaptations and extensions should be evaluated. For example, in case of heat pumps, the energy constraints graph ($E_{\max}$, $E_{\min}$) is not a very good way to represent its flexibility, and for devices where only the start point can be shifted, other solutions should be found.

- Another approach, related to the previous point, is the application of the techniques that were introduced in the event-driven MAS MBC algorithm on other aggregate & dispatch algorithms, such as the state bin modeling

for heat pumps by [60]. At the level of the business agent, advanced learning methods can also reduce the dependency on accurate descriptions of future flexibility, such as energy constraints graphs.

- It might be relevant to examine and devise ways to make DR algorithms more resilient to communication-related failures (accidental or with malicious intent, such as a Denial-of-Service attack). In the MAS MBC algorithm implemented this work, agents will continue charging at the last known good value, and switch to emergency charging when needed. One way to ensure a more graceful failure-mode could be to provide equilibrium priorities to device agents according to a complete schedule, instead of just sending the actual equilibrium priority.

Appendix A

Extended Load Flow Results

A.1 ToU scenario load flow results

This section contains the detailed results from section 8.3.

A.1.1 Cases x-38

Table A.1: ToU simulation results for 7 consecutive days, 200 (PH)EVs, Case NS-38

Dumb	Average	Min	Max
t(<0.9)	3.78%	1.08%	8.86%
t(<0.85)	0.56%	0.00%	1.96%
VUF	0.77%	0.00%	2.60%
Event	Average	Min	Max
t(<0.9)	4.00%	0.74%	11.22%
t(<0.85)	0.64%	0.00%	2.87%
VUF	0.56%	0.00%	2.77%
Event+droop	Average	Min	Max
t(<0.9)	2.44%	0.28%	7.21%
t(<0.85)	0.00%	0.00%	0.00%
VUF	0.01%	0.00%	0.45%
Event+droop+feedback	Average	Min	Max
t(<0.9)	2.43%	0.33%	7.59%
t(<0.85)	0.00%	0.00%	0.00%
VUF	0.01%	0.00%	0.53%
HHOnly	Average	Min	Max
t(<0.9)	0.00%	0.00%	0.09%
t(<0.85)	0.00%	0.00%	0.00%
VUF	0.00%	0.00%	0.00%
Timeslot	Average	Min	Max
t(<0.9)	3.64%	1.04%	10.96%
t(<0.85)	0.37%	0.00%	2.32%
VUF	0.32%	0.00%	1.66%

Table A.2: ToU simulation results for 7 consecutive days, 200 (PH)EVs, Case NL-38

Dumb	Average	Min	Max
t(<0.9)	9.56%	4.57%	17.08%
t(<0.85)	3.07%	0.81%	8.86%
VUF	5.07%	1.80%	10.45%
Event	Average	Min	Max
t(<0.9)	8.80%	4.60%	15.26%
t(<0.85)	3.23%	1.21%	8.33%
VUF	3.56%	0.91%	8.09%
Event+droop	Average	Min	Max
t(<0.9)	6.17%	3.06%	12.67%
t(<0.85)	0.00%	0.00%	0.15%
VUF	0.07%	0.00%	0.85%
Event+droop+feedback	Average	Min	Max
t(<0.9)	6.21%	2.92%	12.18%
t(<0.85)	0.00%	0.00%	0.09%
VUF	0.08%	0.00%	1.03%
HHOnly	Average	Min	Max
t(<0.9)	0.08%	0.00%	0.46%
t(<0.85)	0.00%	0.00%	0.00%
VUF	0.00%	0.00%	0.07%
Timeslot	Average	Min	Max
t(<0.9)	8.58%	4.36%	16.47%
t(<0.85)	2.83%	1.00%	8.07%
VUF	3.00%	0.05%	8.08%

Table A.3: ToU simulation results for 7 consecutive days, 200 (PH)EVs, Case FS-38

Dumb	Average	Min	Max
t(<0.9)	3.28%	1.14%	7.79%
t(<0.85)	0.43%	0.00%	2.28%
VUF	0.56%	0.00%	2.50%
Event	Average	Min	Max
t(<0.9)	3.51%	1.41%	7.35%
t(<0.85)	0.42%	0.00%	1.69%
VUF	0.38%	0.00%	1.63%
Event+droop	Average	Min	Max
t(<0.9)	1.97%	0.86%	4.92%
t(<0.85)	0.00%	0.00%	0.00%
VUF	0.01%	0.00%	0.34%
Event+droop+feedback	Average	Min	Max
t(<0.9)	1.96%	0.86%	4.79%
t(<0.85)	0.00%	0.00%	0.00%
VUF	0.01%	0.00%	0.58%
HHOnly	Average	Min	Max
t(<0.9)	0.00%	0.00%	0.00%
t(<0.85)	0.00%	0.00%	0.00%
VUF	0.00%	0.00%	0.00%
Timeslot	Average	Min	Max
t(<0.9)	3.05%	1.13%	6.84%
t(<0.85)	0.25%	0.00%	1.57%
VUF	0.21%	0.00%	1.31%

Table A.4: ToU simulation results for 7 consecutive days, 200 (PH)EVs, Case FL-38

Dumb	Average	Min	Max
t(<0.9)	9.75%	5.19%	19.42%
t(<0.85)	3.12%	1.12%	6.31%
VUF	5.09%	1.72%	9.89%
Event	Average	Min	Max
t(<0.9)	9.00%	5.25%	16.55%
t(<0.85)	3.18%	1.39%	7.57%
VUF	3.66%	0.800%	8.38%
Event+droop	Average	Min	Max
t(<0.9)	6.47%	3.13%	12.72%
t(<0.85)	0.00%	0.00%	0.12%
VUF	0.06%	0.00%	1.48%
Event+droop+feedback	Average	Min	Max
t(<0.9)	6.46%	3.59%	13.37%
t(<0.85)	0.00%	0.00%	0.04%
VUF	0.07%	0.00%	1.11%
HHOnly	Average	Min	Max
t(<0.9)	0.05%	0.00%	0.30%
t(<0.85)	0.00%	0.00%	0.00%
VUF	0.00%	0.00%	0.00%
Timeslot	Average	Min	Max
t(<0.9)	8.77%	5.28%	16.32%
t(<0.85)	2.77%	0.98%	7.39%
VUF	2.97%	0.57%	8.37%

A.1.2 Cases x-114

Table A.5: ToU simulation results for 7 consecutive days, 200 (PH)EVs, Case NS-114

Dumb	Average	Min	Max
t(<0.9)	3.83%	1.46%	9.66%
t(<0.85)	0.53%	0.00%	3.32%
VUF	0.72%	0.00%	2.99%
Event	Average	Min	Max
t(<0.9)	4.13%	1.54%	9.07%
t(<0.85)	0.58%	0.00%	2.44%
VUF	0.53%	0.00%	2.18%
Event+droop	Average	Min	Max
t(<0.9)	2.49%	0.52%	6.07%
t(<0.85)	0.00%	0.00%	0.00%
VUF	0.01%	0.00%	0.33%
Event+droop+feedback	Average	Min	Max
t(<0.9)	2.50%	0.65%	6.06%
t(<0.85)	0.00%	0.00%	0.00%
VUF	0.01%	0.00%	0.40%
HHOnly	Average	Min	Max
t(<0.9)	0.00%	0.00%	0.09%
t(<0.85)	0.00%	0.00%	0.00%
VUF	0.00%	0.00%	0.00%
Timeslot	Average	Min	Max
t(<0.9)	3.70%	1.19%	8.61%
t(<0.85)	0.36%	0.00%	1.88%
VUF	0.29%	0.00%	1.61%

Table A.6: ToU simulation results for 7 consecutive days, 200 (PH)EVs, Case NL-114

Dumb	Average	Min	Max
t(<0.9)	9.73%	5.38%	16.99%
t(<0.85)	3.27%	1.03%	9.07%
VUF	3.66%	0.72%	7.44%
Event	Average	Min	Max
t(<0.9)	6.19%	2.63%	13.10%
t(<0.85)	0.00%	0.00%	0.09%
VUF	0.06%	0.00%	1.32%
Event+droop	Average	Min	Max
t(<0.9)	6.26%	2.42%	12.88%
t(<0.85)	0.00%	0.00%	0.08%
VUF	0.06%	0.00%	1.32%
Event+droop+feedback	Average	Min	Max
t(<0.9)	6.26%	2.42%	12.88%
t(<0.85)	0.00%	0.00%	0.08%
VUF	0.06%	0.00%	1.32%
HHOnly	Average	Min	Max
t(<0.9)	0.06%	0.00%	0.46%
t(<0.85)	0.00%	0.00%	0.00%
VUF	0.00%	0.00%	0.07%
Timeslot	Average	Min	Max
t(<0.9)	8.67%	4.28%	17.29%
t(<0.85)	2.79%	0.16%	7.81%
VUF	2.97%	0.28%	7.59%

Table A.7: ToU simulation results for 7 consecutive days, 200 (PH)EVs, Case FS-114

Dumb	Average	Min	Max
t(<0.9)	3.23%	1.26%	8.17%
t(<0.85)	0.41%	0.00%	2.61%
VUF	0.54%	0.00%	2.53%
Event	Average	Min	Max
t(<0.9)	3.48%	1.55%	8.28%
t(<0.85)	0.40%	0.00%	1.64%
VUF	0.37%	0.00%	2.23%
Event+droop	Average	Min	Max
t(<0.9)	1.99%	0.78%	6.20%
t(<0.85)	0.00%	0.00%	0.00%
VUF	0.00%	0.00%	0.16%
Event+droop+feedback	Average	Min	Max
t(<0.9)	2.02%	0.69%	5.60%
t(<0.85)	0.00%	0.00%	0.00%
VUF	0.00%	0.00%	0.19%
HHOnly	Average	Min	Max
t(<0.9)	0.00%	0.00%	0.00%
t(<0.85)	0.00%	0.00%	0.00%
VUF	0.00%	0.00%	0.00%
Timeslot	Average	Min	Max
t(<0.9)	3.10%	0.83%	7.14%
t(<0.85)	0.25%	0.00%	1.30%
VUF	0.21%	0.00%	1.77%

Table A.8: ToU simulation results for 7 consecutive days, 200 (PH)EVs, Case FL-114

Dumb	Average	Min	Max
t(<0.9)	10.02%	5.37%	21.63%
t(<0.85)	3.22%	0.76%	10.78%
VUF	5.07%	1.91%	10.75%
Event	Average	Min	Max
t(<0.9)	8.97%	4.30%	16.73%
t(<0.85)	3.30%	1.01%	8.71%
VUF	3.66%	0.48%	9.47%
Event+droop	Average	Min	Max
t(<0.9)	6.36%	3.44%	17.58%
t(<0.85)	0.00%	0.00%	0.03%
VUF	0.09%	0.00%	1.67%
Event+droop+feedback	Average	Min	Max
t(<0.9)	6.39%	3.09%	16.95%
t(<0.85)	0.00%	0.00%	0.07%
VUF	0.10%	0.00%	1.38%
HHOnly	Average	Min	Max
t(<0.9)	0.05%	0.00%	0.30%
t(<0.85)	0.00%	0.00%	0.00%
VUF	0.00%	0.00%	0.00%
Timeslot	Average	Min	Max
t(<0.9)	8.81%	4.57%	16.07%
t(<0.85)	2.88%	0.44%	8.49%
VUF	3.02%	0.37%	7.67%

A.1.3 ToU scenarios emergency charging statistics

Table A.9: Emergency charging statistics for the passive grid scenarios, after 7 days for the ToU aggregator, cluster of 200 EVs, 100 randomized simulations.

(a) Avg. percentage of received/requested energy at t_{dep} for EVs that used emergency charging.

	Event	Timeslot
Case NS-38	100%	93.71%
Case NL-38	100%	93.67%
Case FS-38	100%	93.55%
Case FL-38	100%	93.46%

(b) Avg. nb. of EVs that had an incompletely charged battery at t_{dep}.

	Event	Timeslot
Case NS-38	0	418.24
Case NL-38	0	415.28
Case FS-38	0	411.59
Case FL-38	0	418.24

(c) Average amount of cumulative battery deficit energy in total delivered energy.

	Event	Timeslot
Case NS-38	0.00%	1.64%
Case NL-38	0.00%	1.63%
Case FS-38	0.00%	1.63%
Case FL-38	0.00%	1.64%

Table A.10: Emergency charging statistics for the active grid scenarios, after 7 days for the ToU aggregator, cluster of 200 EVs, 100 randomized simulations.

(a) Average percentage of received/requested energy at t_{dep} for EVs that used emergency charging.

	Event	Event+droop	Event+droop+comp
Case NS-38	100%	96.96%	96.98%
Case NL-38	100%	93.23%	93.25%
Case FS-38	100%	97.58%	97.53%
Case FL-38	100%	93.36%	93.46%

(b) Average number of EVs that had a battery deficit at t_{dep}.

	Event	Event+droop	Event+droop+comp
Case NS-38	0	50.02	50.04
Case NL-38	0	86.98	85.13
Case FS-38	0	65.30	63.44
Case FL-38	0	109.70	108.28

(c) Average amount of cumulative battery deficit energy in total delivered energy.

	Event	Event+droop	Event+droop+comp
Case NS-38	0.00%	0.24%	0.24%
Case NL-38	0.00%	0.96%	0.93%
Case FS-38	0.00%	0.24%	0.24%
Case FL-38	0.00%	1.18%	1.15%

A.2 Balancing case, single aggregator

This section has the detailed results from the simulation from section 8.6.

Table A.11: Balancing case EN50160 simulation results for 7 consecutive days, 1 000 EVs, Case FL

FL-38	Balan.	Balan.+droop	Track.	Track.+droop
t(V<0.9pu)	5,84%	3,92%	3,57%	3,18%
t(V<0.85pu)	1,06%	0,00%	0,76%	0,00%
t(VUF>2%)	1,05%	0,00%	0,70%	0,00%
FL-114	Balan.	Balan.+droop	Track.	Track.+droop
t(V<0.9pu)	5,82%	3,86%	3,97%	3,13%
t(V<0.85pu)	1,11%	0,00%	0,71%	0,00%
t(VUF>2%)	1,11%	0,00%	0,69%	0,00%
FL-380	Balan.	Balan.+droop	Track.	Track.+droop
t(V<0.9pu)	5,94%	4,27%	4,01%	3,43%
t(V<0.85pu)	1,02%	0,00%	0,89%	0,00%
t(VUF>2%)	1,05%	0,00%	0,86%	0,00%
FL-760	Balan.	Balan.+droop	Track.	Track.+droop
t(V<0.9pu)	5,81%	4,29%	4,08%	2,71%
t(V<0.85pu)	1,05%	0,00%	0,76%	0,00%
t(VUF>2%)	1,06%	0,00%	6,21%	0,00%

Table A.12: Balancing case emergency charging results for simulations spanning 7 consecutive days, 1 000 EVs, Case FL

FL-38	Balan.	Balan.+droop	Track.	Track.+droop
Avg Δt_{dep} when emg chg activates	0,95 h	0,97 h	1,04 h	1,05 h
Avg ΔE_{req} when emg chg activates	3 097,9 Wh	3 135,3 Wh	3 404,0 Wh	3 403,7 Wh
Σ occur. of emg chg activations	3 700	7 421	3 720	7 111
Σ_i occur. of ${}^i\Delta E_{\text{req}} > 0$ at ${}^i t_{\text{dep}}$	3 699	3 710	3 719	3 555
Total energy after 7 days	61.25 MWh	61.25 MWh	61.49 MWh	61.50 MWh
FL-114	Balan.	Balan.+droop	Track.	Track.+droop
Avg Δt_{dep} when emg chg activates	0,95 h	0,99 h	1,04 h	1,07 h
Avg ΔE_{req} when emg chg activates	3 093,9 Wh	3 175,7 Wh	3 378,3 Wh	3 438,5 Wh
Σ occur. of emg chg activations	3 696	7 255	3 655	7 041
Σ_i occur. of ${}^i\Delta E_{\text{req}} > 0$ at ${}^i t_{\text{dep}}$	3 695	3 627	3 654	3 520
Total energy after 7 days	61.24 MWh	61.26 MWh	61.53 MWh	51.48 MWh
FL-380	Balan.	Balan.+droop	Track.	Track.+droop
Avg Δt_{dep} when emg chg activates	0,95	1,08	1,04	1,13
Avg ΔE_{req} when emg chg activates	3 095,9 Wh	3 320,0 Wh	3 404,9 Wh	3 463,5 Wh
Σ occur. of emg chg activations	3 689	6 595	3 614	6 327
Σ_i occur. of ${}^i\Delta E_{\text{req}} > 0$ at ${}^i t_{\text{dep}}$	3 688	3 297	3 613	3 163
Total energy after 7 days	61.25 MWh	61.41 MWh	61.50 MWh	61.46 MWh
FL-760	Balan.	Balan.+droop	Track.	Track.+droop
Avg Δt_{dep} when emg chg activates	0,95	1,29	1,04	1,27
Avg ΔE_{req} when emg chg activates	3 090,2 Wh	3 656,1 Wh	3 384,5 Wh	3 793,4 Wh
Σ occur. of emg chg activations	3 698	5 507	3 576	9 047
Σ_i occur. of ${}^i\Delta E_{\text{req}} > 0$ at ${}^i t_{\text{dep}}$	3 697	2 753	3 575	4 523
Total energy after 7 days	61.25 MWh	61.69 MWh	61.51 MWh	61.41 MWh

Appendix B

Balancing case

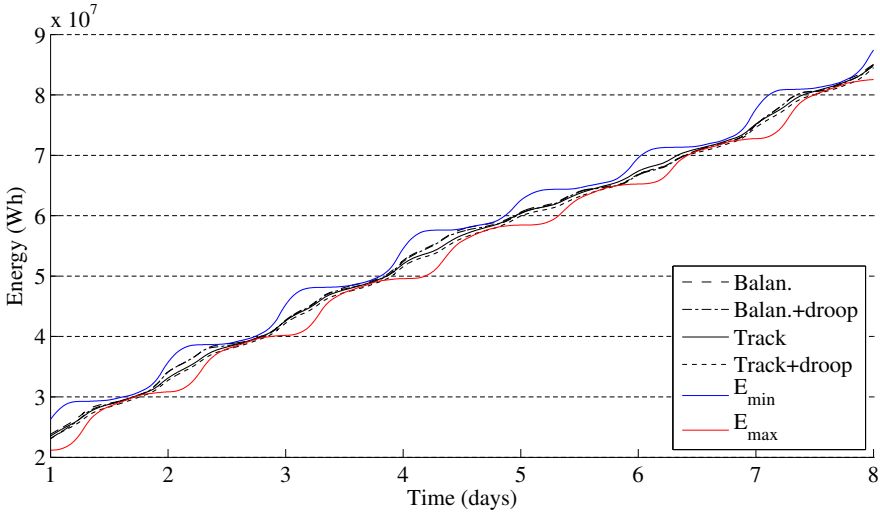

Figure B.1: Energy consumption path for case4d, for the different algorithms, and positioned within the theoretical $E_{\min}$ and $E_{\max}$ boundaries. Because of the different paths followed, the total energy at the end of the graph is slightly different for each algorithm, but it is apparent that approximately the same amount of energy is used every day.

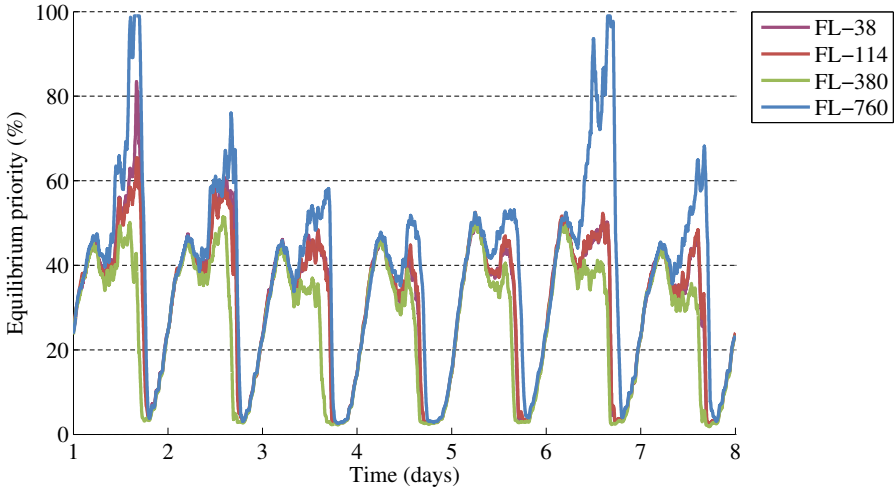

Figure B.2: Equilibrium priority during the tracking scenarios, active distribution grid cases. In general, increasing shares of EVs situated in weak grids leads to a decrease in the equilibrium priority, except for the case FL-760. This is explained in section 8.8.2.

Bibliography

[1] IEA, *The IEA World Energy Outlook 2011.*, 2011.

[2] M. H. Albadi and E. F. El-Saadany, "A summary of demand response in electricity markets," *Electric Power Systems Research*, vol. 78, no. 11, pp. 1989–1996, 2008. [Online]. Available: http://www.sciencedirect.com/science/article/pii/S0378779608001272

[3] ——, "Demand Response in Electricity Markets: An Overview," in *2007 IEEE Power Engineering Society General Meeting*. IEEE, Jun. 2007, pp. 1–5. [Online]. Available: http://ieeexplore.ieee.org/lpdocs/epic03/wrapper.htm?arnumber=4275494

[4] Ontario Ministry of Energy, "Smart Meters and Time-of-Use Prices." [Online]. Available: http://www.energy.gov.on.ca/en/smart-meters-and-tou-prices/

[5] DNO Energie, "Onbalanssturing." [Online]. Available: http://www.dnoenergie.nl/

[6] M. Baritaud, "Securing Power during the Transition," p. 47, 2012. [Online]. Available: http://www.iea.org/publications/insights/SecuringPowerTransition_Secondeedition_WEB.pdf

[7] S. Barker, A. Mishra, D. Irwin, P. Shenoy, and J. Albrecht, "SmartCap: Flattening peak electricity demand in smart homes," in *2012 IEEE International Conference on Pervasive Computing and Communications*. IEEE, Mar. 2012, pp. 67–75. [Online]. Available: http://ieeexplore.ieee.org/lpdocs/epic03/wrapper.htm?arnumber=6199851

[8] Elia, "Ancillary services." [Online]. Available: http://www.elia.be/en/suppliers/purchasing-categories/energy-purchases/Ancillary-services

[9] O. Ma, N. Alkadi, P. Cappers, P. Denholm, J. Dudley, S. Goli, M. Hummon, S. Kiliccote, J. MacDonald, N. Matson, D. Olsen, C. Rose, M. D. Sohn, M. Starke, B. Kirby, and M. O'Malley, "Demand Response for Ancillary Services," *IEEE Transactions on Smart Grid*, vol. 4, no. 4, pp. 1988–1995, Dec. 2013. [Online]. Available: http://ieeexplore.ieee.org/lpdocs/epic03/wrapper.htm?arnumber=6630115

[10] G. Strbac, "Demand side management: Benefits and challenges," *Energy Policy*, vol. 36, no. 12, pp. 4419–4426, Dec. 2008. [Online]. Available: http://www.bis.gov.uk/assets/foresight/docs/energy/demand-side-management-benefits-and-challenges.pdfhttp://linkinghub.elsevier.com/retrieve/pii/S0301421508004606

[11] K. Clement-Nyns, E. Haesen, and J. Driesen, "The Impact of Charging Plug-In Hybrid Electric Vehicles on a Residential Distribution Grid," *IEEE Transactions on Power Systems*, vol. 25, no. 1, pp. 371–380, Feb. 2010. [Online]. Available: http://ieeexplore.ieee.org/lpdocs/epic03/wrapper.htm?arnumber=5356176

[12] S. Shao, M. Pipattanasomporn, and S. Rahman, "Grid Integration of Electric Vehicles and Demand Response With Customer Choice," *IEEE Transactions on Smart Grid*, vol. 3, no. 1, pp. 543–550, Mar. 2012. [Online]. Available: http://ieeexplore.ieee.org/lpdocs/epic03/wrapper.htm?arnumber=6140943

[13] P. Bach Andersen, J. Hu, and K. Heussen, "Coordination strategies for distribution grid congestion management in a multi-actor, multi-objective setting," in *2012 3rd IEEE PES Innovative Smart Grid Technologies Europe (ISGT Europe)*. IEEE, Oct. 2012, pp. 1–8. [Online]. Available: http://ieeexplore.ieee.org/lpdocs/epic03/wrapper.htm?arnumber=6465853

[14] R. Garcia-Valle and J. a. A. Peças Lopes, Eds., *Electric Vehicle Integration into Modern Power Networks*. New York, NY: Springer New York, 2013. [Online]. Available: http://www.springerlink.com/index/10.1007/978-1-4614-0134-6

[15] R. Verzijlbergh, "The Power of Electric Vehicles - Exploring the Value of Flexible Electricity Demand in a Multi-Actor Context," 2013.

[16] K. De Craemer and G. Deconinck, "Analysis of state-of-the-art smart metering communication standards," *Proceedings of the 5th Young Researchers Symposium*, 2010.

[17] K. De Craemer, G. Deconinck, and M. Stifter, "Protocols for Automatic Meter Reading," in *IEEE Industrial Communication Technology Handbook, Second Edition*. CRC Press, 2014, ch. 60.

[18] "iMinds SPARC project page," 2012. [Online]. Available: http://www.iminds.be/en/research/overview-projects/p/detail/sparc-2

[19] K. De Craemer, S. Vandael, B. Claessens, and G. Deconinck, "An Event-Driven Dual Coordination Mechanism for Demand Side Management of PHEVs," *IEEE Transactions on Smart Grid*, pp. 1–10, 2013. [Online]. Available: http://ieeexplore.ieee.org/lpdocs/epic03/wrapper.htm?arnumber=6565418

[20] K. De Craemer and G. Deconinck, "Balancing Trade-offs in Coordinated PHEV Charging with Continuous Market-based Control," in *Proceedings of the Third IEEE PES Innovative Smart Grid Technologies (ISGT) Europe Conference*, 2012.

[21] J. Gomez and M. Morcos, "Impact of EV battery chargers on the power quality of distribution systems," *IEEE Transactions on Power Delivery*, vol. 18, no. 3, pp. 975–981, Jul. 2003. [Online]. Available: http://ieeexplore.ieee.org/lpdocs/epic03/wrapper.htm?arnumber=1208386

[22] Panasonic, "Lithium Ion Batteries Technical Handbook," p. 29, 2007. [Online]. Available: http://industrial.panasonic.com/www-data/pdf/ACI4000/ACI4000PE5.pdf

[23] H. Seljeseth, T. Henning, and T. Solvang, "Measurements of network impact from electric vehicles during slow and fast charging," in *22nd International Conference on Electricity Distribution*, 2013.

[24] A. Kapoor, "Charging algorithms of lithium-ion batteries: An overview," in *2012 7th IEEE Conference on Industrial Electronics and Applications (ICIEA)*. IEEE, Jul. 2012, pp. 1567–1572. [Online]. Available: http://ieeexplore.ieee.org/lpdocs/epic03/wrapper.htm?arnumber=6360973

[25] K. Clement-Nyns, E. Haesen, and J. Driesen, "The impact of vehicle-to-grid on the distribution grid," *Electric Power Systems Research*, vol. 81, no. 1, pp. 185–192, 2011. [Online]. Available: http://www.sciencedirect.com/science/article/pii/S0378779610002063

[26] J. Tomić and W. Kempton, "Using fleets of electric-drive vehicles for grid support," *Journal of Power Sources*, vol. 168, no. 2, pp. 459–468, 2007. [Online]. Available: http://www.sciencedirect.com/science/article/pii/S0378775307005575

[27] W. Kempton and T. Kubo, "Electric-drive vehicles for peak power in Japan," *Energy Policy*, vol. 28, no. 1, pp. 9–18, 2000. [Online]. Available: http://www.sciencedirect.com/science/article/pii/S0301421599000786

[28] M. E. Chehaly, O. Saadeh, C. Martinez, and G. Joos, "Advantages and applications of vehicle to grid mode of operation in plug-in hybrid electric vehicles," in *2009 IEEE Electrical Power & Energy Conference (EPEC)*. IEEE, Oct. 2009, pp. 1–6. [Online]. Available: http://ieeexplore.ieee.org/lpdocs/epic03/wrapper.htm?arnumber=5420958

[29] S. B. Peterson, J. Apt, and J. F. Whitacre, "Lithium-ion battery cell degradation resulting from realistic vehicle and vehicle-to-grid utilization," *Journal of Power Sources*, vol. 195, no. 8, pp. 2385–2392, 2010.

[30] P. N. Vovos, A. E. Kiprakis, A. R. Wallace, and G. P. Harrison, "Centralized and Distributed Voltage Control: Impact on Distributed Generation Penetration," *IEEE Transactions on Power Systems*, vol. 22, no. 1, pp. 476–483, Feb. 2007. [Online]. Available: http://ieeexplore.ieee.org/lpdocs/epic03/wrapper.htm?arnumber=4077146

[31] European Commission, "M468 - Standardisation mandate to CEN, CENELEC and ETSI concerning the charging of electric vehicles." 2010. [Online]. Available: http://ec.europa.eu/energy/gas_electricity/smartgrids/doc/2010_06_04_mandate_m468_en.pdf

[32] IEC Technical Committee 23, "IEC 62196 ed2.0: Plugs, socket-outlets, vehicle connectors and vehicle inlets - Conductive charging of electric vehicles," Geneva, 2011.

[33] IEC Technical Committee 69, "IEC 61851 ed2.0: Electric vehicle conductive charging system," Geneva, 2010.

[34] Mennekes, "Charging socket with or without shutter," 2012. [Online]. Available: http://www.mennekes.de/uploads/media/Type2_with_Shutter_01.pdf

[35] D. Herron, "European Parliament Considers Legislation To Kill CHAdeMO Electric Car Chargers," 2013. [Online]. Available: http://www.plugincars.com/european-parliament-mulling-legislation-would-terminate-chademo-127927.html

[36] J. Pokrzywa, "SAE's J1772 'combo connector' for AC and DC charging advances with IEEE's help," 2011. [Online]. Available: http://ev.sae.org/article/10128

[37] S. Ruthe, J. Schmutzler, C. Rehtanz, and C. Wietfeld, "Study on V2G Protocols against the Background of Demand Side Management," *IBIS – Interoperability in Business Information Systems*, pp. 33–44, 2011.

[38] A. Mathoy, "Definition and implementation of a global EV charging infrastructure," 2008.

[39] C. Lewandowski, S. Gröning, J. Schmutzler, and C. Wietfeld, "Performance Evaluation of PLC over the IEC 61851 Control Pilot Signal," in *5th Workshop on Power Line Communications*, 2011. [Online]. Available: http://www.isplc.org/docsearch/Proceedings/2011/pdf/Lewandowski.pdf

[40] J. S. Johansen, "Fast-Charging Electric Vehicles using AC," 2013.

[41] "Open Charge Alliance," 2013. [Online]. Available: http://www.openchargealliance.org/

[42] Enexis, "Wat is OSCP?" 2013. [Online]. Available: http://www.smartcharging.nl/wp-content/uploads/2013/11/Presentatie-OSCP-Nederlands.pptx

[43] P2030.1 Working Group, "IEEE P2030.1 Draft Guide for Electric-Sourced Transportation Infrastructure," 2013. [Online]. Available: http://grouper.ieee.org/groups/scc21/2030.1/2030.1_index.html

[44] J. S. John, "REstore: Balancing Europe's Wind and Solar With EVs, Cold Storage," 2012. [Online]. Available: http://www.greentechmedia.com/articles/read/restore-balances-european-load-with-evs-cold-storage

[45] M. J. Wooldridge, *Introduction to Multiagent Systems*. New York, NY, USA: John Wiley & Sons, Inc., 2001.

[46] N. Gatsis and G. B. Giannakis, "Residential Load Control: Distributed Scheduling and Convergence With Lost AMI Messages," *IEEE Transactions on Smart Grid*, vol. 3, no. 2, pp. 770–786, Jun. 2012. [Online]. Available: http://ieeexplore.ieee.org/lpdocs/epic03/wrapper.htm?arnumber=6168820

[47] ——, "Cooperative multi-residence demand response scheduling," in *2011 45th Annual Conference on Information Sciences and Systems*. IEEE, Mar. 2011, pp. 1–6. [Online]. Available: http://ieeexplore.ieee.org/lpdocs/epic03/wrapper.htm?arnumber=5766245

[48] ——, "Residential demand response with interruptible tasks: Duality and algorithms," in *IEEE Conference on Decision and Control and European*

Control Conference. IEEE, Dec. 2011, pp. 1–6. [Online]. Available: http://ieeexplore.ieee.org/lpdocs/epic03/wrapper.htm?arnumber=6161103

[49] Z. Fan, "A Distributed Demand Response Algorithm and Its Application to PHEV Charging in Smart Grids," *IEEE Transactions on Smart Grid*, vol. 3, no. 3, pp. 1280–1290, Sep. 2012. [Online]. Available: http://ieeexplore.ieee.org/stamp/stamp.jsp?tp=&arnumber=6168819&isnumber=5446437http://ieeexplore.ieee.org/lpdocs/epic03/wrapper.htm?arnumber=6168819

[50] S. Weckx, J. Driesen, and R. D'hulst, "Optimal real-time pricing for unbalanced distribution grids with network constraints," in *2013 IEEE Power & Energy Society General Meeting*. IEEE, Jul. 2013, pp. 1–5. [Online]. Available: http://ieeexplore.ieee.org/lpdocs/epic03/wrapper.htm?arnumber=6672657

[51] S. Boyd, N. Parikh, E. Chu, B. Peleato, and J. Eckstein, "Distributed Optimization and Statistical Learning via the Alternating Direction Method of Multipliers," *Found. Trends Mach. Learn.*, vol. 3, no. 1, pp. 1–122, 2011. [Online]. Available: http://dx.doi.org/10.1561/2200000016

[52] A.-H. Mohsenian-Rad, V. W. S. Wong, J. Jatskevich, R. Schober, and A. Leon-Garcia, "Autonomous Demand-Side Management Based on Game-Theoretic Energy Consumption Scheduling for the Future Smart Grid," *IEEE Transactions on Smart Grid*, vol. 1, no. 3, pp. 320–331, Dec. 2010. [Online]. Available: http://ieeexplore.ieee.org/lpdocs/epic03/wrapper.htm?arnumber=5628271

[53] R. N. Anderson, A. Boulanger, W. B. Powell, and W. Scott, "Adaptive Stochastic Control for the Smart Grid," *Proceedings of the IEEE*, vol. 99, no. 6, pp. 1098–1115, Jun. 2011. [Online]. Available: http://ieeexplore.ieee.org/lpdocs/epic03/wrapper.htm?arnumber=5768096

[54] V. W. Wong, "An approximate dynamic programming approach for coordinated charging control at vehicle-to-grid aggregator," in *2011 IEEE International Conference on Smart Grid Communications (SmartGridComm)*. IEEE, Oct. 2011, pp. 279–284. [Online]. Available: http://ieeexplore.ieee.org/lpdocs/epic03/wrapper.htm?arnumber=6102333

[55] V. Robu, S. Stein, E. Gerding, D. Parkes, A. Rogers, and N. Jennings, "An Online Mechanism for Multi-Speed Electric Vehicle Charging," in *Second International Conference on Auctions, Market Mechanisms and Their Applications (AMMA'11)*, vol. 80, 2012, pp. 100–112. [Online]. Available: http://eprints.soton.ac.uk/272424/

[56] E. H. Gerding, V. Robu, S. Stein, D. C. Parkes, A. Rogers, and N. R. Jennings, "Online Mechanism Design for Electric Vehicle Charging," in *The 10th International Conference on Autonomous Agents and Multiagent Systems - Volume 2*, ser. AAMAS '11. Richland, SC: International Foundation for Autonomous Agents and Multiagent Systems, 2011, pp. 811–818. [Online]. Available: http://dl.acm.org/citation.cfm?id=2031678.2031733

[57] S. Mathieu, D. Ernst, and Q. Louveaux, "An efficient algorithm for the provision of a day-ahead modulation service by a load aggregator," in *IEEE PES ISGT Europe 2013*. IEEE, Oct. 2013, pp. 1–5. [Online]. Available: http://orbi.ulg.ac.be/handle/2268/149295

[58] M. D. Galus, R. La Fauci, and G. Andersson, "Investigating PHEV wind balancing capabilities using heuristics and model predictive control," in *IEEE PES General Meeting*. IEEE, Jul. 2010, pp. 1–8. [Online]. Available: http://ieeexplore.ieee.org/lpdocs/epic03/wrapper.htm?arnumber=5589267

[59] B. Biegel, P. Andersen, T. S. Pedersen, K. M. Nielsen, J. Stoustrup, and L. H. Hansen, "Smart grid dispatch strategy for on/off demand-side devices," in *Control Conference (ECC), 2013 European*. IEEE, 2013, pp. 2541–2548.

[60] S. Koch, J. L. Mathieu, and D. S. Callaway, "Modeling and Control of Aggregated Heterogeneous Thermostatically Controlled Loads for Ancillary Services," in *Proceedings of the 17th Power Systems Computation Conference (PSCC)*, Stockholm, Sweden, 2011.

[61] K. Kok, "The PowerMatcher: Smart Coordination for the Smart Electricity Grid," Ph.D. dissertation, Vrije Universitit Amsterdam, 2013.

[62] M. Maenhoudt, "Stratagic Behavior in Power Wholesale Electricity Markets," Ph.D. dissertation, KU Leuven, 2014.

[63] BELPEX, "Belgian Power Exchange," 2013. [Online]. Available: www.belpex.be

[64] K. Kok, K. Warmer, and R. Kamphuis, "PowerMatcher: multiagent control in the electricity infrastructure," in *AAMAS '05: Proceedings of the 4th int. joint conf. on Autonomous Agents and Multiagent Systems, volume industry track*, New York, 2005, pp. 75–82. [Online]. Available: http://dl.acm.org/citation.cfm?id=1082807

[65] "PowerMatcher," 2013. [Online]. Available: http://www.powermatcher.net/

[66] V. Krishna, *Auction Theory*. Academic Press, 2002.

[67] J. K. Kok, M. J. J. Scheepers, and I. G. Kamphuis, "Intelligence in electricity networks for embedding renewables and distributed generation," in *Intelligent infrastructures*. Springer, 2010, pp. 179–209.

[68] R. Kamphuis, B. Roossien, M. Eijgelaar, H. de Heer, J. van de Velde, and A. van den Noort, "Real-time trade dispatch of a commercial VPP with residential customers in the PowerMatching City SmartGrid living lab," in *22nd International Conference and Exhibition on Electricity Distribution (CIRED 2013)*. Institution of Engineering and Technology, 2013, pp. 0309–0309. [Online]. Available: http://digital-library.theiet.org/content/conferences/10.1049/cp.2013.0666

[69] J. Jargstorf, K. Vanthournout, T. De Rybel, and D. Van Hertem, "Effect of Demand Response on transformer lifetime expectation," in *2012 3rd IEEE PES Innovative Smart Grid Technologies Europe (ISGT Europe)*. Berlin: IEEE, Oct. 2012, pp. 1–8. [Online]. Available: https://lirias.kuleuven.be/handle/123456789/361257http://ieeexplore.ieee.org/lpdocs/epic03/wrapper.htm?arnumber=6465805

[70] CENELEC, "EN 50160 - Voltage Characteristics of Electricity Supplied by Public Electricity Networks, July 2010," 2010.

[71] P. Pillay and M. Manyage, "Definitions of voltage unbalance," *IEEE Power Engineering Review*, vol. 21, no. 5, pp. 50–51, May 2001. [Online]. Available: http://ieeexplore.ieee.org/lpdocs/epic03/wrapper.htm?arnumber=920965

[72] M. Liu, C. Canizares, and W. Huang, "Reactive Power and Voltage Control in Distribution Systems With Limited Switching Operations," *IEEE Transactions on Power Systems*, vol. 24, no. 2, pp. 889–899, May 2009. [Online]. Available: http://ieeexplore.ieee.org/lpdocs/epic03/wrapper.htm?arnumber=4808225

[73] C. Gonzalez, J. Geuns, S. Weckx, T. Wijnhoven, P. Vingerhoets, T. De Rybel, and J. Driesen, "LV distribution network feeders in Belgium and power quality issues due to increasing PV penetration levels," in *2012 3rd IEEE PES Innovative Smart Grid Technologies Europe (ISGT Europe)*. IEEE, Oct. 2012, pp. 1–8. [Online]. Available: http://ieeexplore.ieee.org/lpdocs/epic03/wrapper.htm?arnumber=6465624

[74] N. Efkarpidis, C. Gonzalez, T. Wijnhoven, D. V. Dommelen, T. D. Rybel, and J. Driesen, "Technical Assessment of On-Load Tap-Changers in Flemish LV Distribution Grids," in *International Workshop on Integration of Solar Power into Power Systems*, 2013.

[75] J. C.P Kester, P. Heskes J.M, J. (Sjaak) Kaandorp, J. (Sjef) Cobben, G. Schoonenberg, D. Malyna, E. De Jong, B. Wargers, and A. (Ton) Dalmeijer, "A smart MV/LV-station that improves power quality, reliability and substation load profile," in *20th International Conference on Electricity Distribution*, no. 0776, 2009, pp. 8–11.

[76] B. Biegel, P. Andersen, J. Stoustrup, and J. D. Bendtsen, "Congestion management in a smart grid via shadow prices," in *8th IFAC Symposium on Power Plant and Power System Control*, 2012, pp. 518–523.

[77] O. Sundstrom and C. Binding, "Flexible Charging Optimization for Electric Vehicles Considering Distribution Grid Constraints," *IEEE Transactions on Smart Grid*, vol. 3, no. 1, pp. 26–37, Mar. 2012. [Online]. Available: http://ieeexplore.ieee.org/lpdocs/epic03/wrapper.htm?arnumber=6112699

[78] N. O'Connell, Q. Wu, J. Ø stergaard, A. H. Nielsen, S. T. Cha, and Y. Ding, "Day-ahead tariffs for the alleviation of distribution grid congestion from electric vehicles," *Electric Power Systems Research*, vol. 92, pp. 106–114, 2012.

[79] E. Sortomme and M. A. El-Sharkawi, "Optimal Scheduling of Vehicle-to-Grid Energy and Ancillary Services," *IEEE Transactions on Smart Grid*, vol. 3, no. 1, pp. 351–359, Mar. 2012. [Online]. Available: http://ieeexplore.ieee.org/lpdocs/epic03/wrapper.htm?arnumber=6021358

[80] J. Jargstorf and M. Wickert, "Offer of secondary reserve with a pool of electric vehicles on the German market," *Energy Policy*, vol. 62, pp. 185–195, Nov. 2013. [Online]. Available: http://linkinghub.elsevier.com/retrieve/pii/S0301421513005958

[81] ENTSO-E, "ENTSO-E Operation Handbook - Policy 1: Load-Frequency Control and Performance," 2004. [Online]. Available: https://www.entsoe.eu/publications/system-operations-reports/operation-handbook/

[82] S.-L. Andersson, A. Elofsson, M. Galus, L. Göransson, S. Karlsson, F. Johnsson, and G. Andersson, "Plug-in hybrid electric vehicles as regulating power providers: Case studies of Sweden and Germany," *Energy Policy*, vol. 38, no. 6, pp. 2751–2762, Jun. 2010. [Online]. Available: http://linkinghub.elsevier.com/retrieve/pii/S0301421510000121

[83] DIN VDE Std. VDE-AR-N 4105, "Erzeugungsanlagen am Niederspannungsnetz, Technische Mindestanfor- derungen für Anschluss und Parallelbetrieb von Erzeugungsanlagen am Niederspannungsnetz," 2011.

[84] Synergrid C10/11, "Specifieke technische voorschriften voor decentrale productie-installaties die in parallel werken met het distributienet," 2012. [Online]. Available: http://www.synergrid.be/download.cfm?fileId=C10-11_NL_120604.pdf

[85] T. Loix, "Participation of inverter-connected distributed energy resources in grid voltage control," Ph.D. dissertation, KU Leuven, 2011.

[86] S. Vandael, N. Boucké, R. Claes, K. Clement, S. De Breucker, T. Holvoet, and G. Deconinck, "Gedistribueerde coordinatie en sturing van plug-in hybride elektrische voertuigen in een smart grid," Master's thesis, KU Leuven, 2009.

[87] D. Weyns and T. Holvoet, "A Formal Model for Situated Multi-Agent Systems," *Fundamenta Informaticae - Multiagent Systems (FAMAS'03)*, vol. 63, no. 2-3, pp. 125–158, 2004.

[88] IBM, "IBM Ilog CPLEX," 2010. [Online]. Available: http://pic.dhe.ibm.com/infocenter/cosinfoc/v12r2/topic/ilog.odms.cplex.help/Content/Optimization/Documentation/CPLEX/_pubskel/CPLEX1131.html

[89] J. Löfberg, "Yalmip," 2013. [Online]. Available: http://users.isy.liu.se/johanl/yalmip/

[90] J. Tant, F. Geth, D. Six, P. Tant, and J. Driesen, "Multiobjective Battery Storage to Improve PV Integration in Residential Distribution Grids," *IEEE Transactions on Sustainable Energy*, vol. 4, no. 1, pp. 182–191, Jan. 2013. [Online]. Available: http://ieeexplore.ieee.org/lpdocs/epic03/wrapper.htm?arnumber=6305498

[91] C. Cheng and D. Shirmohammadi, "A three-phase power flow method for real-time distribution system analysis," *IEEE Transactions on Power Systems*, vol. 10, no. 2, pp. 671–679, May 1995. [Online]. Available: http://ieeexplore.ieee.org/lpdocs/epic03/wrapper.htm?arnumber=387902

[92] "Oral communication with Jef Beerten," 2013.

[93] J. Van Roy, N. Leemput, S. De Breucker, F. Geth, T. Peter, and J. Driesen, "An Availability Analysis and Energy Consumption Model for a Flemish Fleet of Electric Vehicles," in *European Electric Vehicle Congress (EEVC)*, Brussels, 2011, p. 12.

[94] A. F. Raab, M. Ellingsen, and A. Walsh., "Mobile Energy Resources in Gridsof Electricity - WP 1 Task 1.6 Deliverable D1.4 - Learning from EV FIeld Tests," Tech. Rep., 2011. [Online]. Available: http://www.ev-merge.eu/images/stories/uploads/MERGE_WP1_D1.4_Final.pdf

[95] A. J. Brand and K. Kok, "Aanbodvoorspeller Duurzame Energie." [Online]. Available: https://www.ecn.nl/avde/

[96] A. J. Brand, "Wind Power Forecasting Method AVDE," in *China Global Wind Power 2008*. Bejing, China: ECN, 2008. [Online]. Available: http://www.ecn.nl/docs/library/report/2009/m09048.pdf

[97] Nordex, "Nordex N100 (2.5 Megawatt)." [Online]. Available: http://www.nordex-online.com/en/produkte-service/wind-turbines/n100-25-mw.html

[98] ——, "Datenblatt N80/2500 (2.5 MW)," 2009. [Online]. Available: http://www.nordex-online.com/en/produkte-service/wind-turbines/n80-25-mw/product-data-sheet-n80-25mw.html

[99] Elia, "Nominations: principles and methods," 2012. [Online]. Available: http://www.elia.be/en/products-and-services/~/media/files/Elia/Products-and-services/ProductSheets/E-Evenwicht/E3_E_E-Nomination.pdf

[100] B. Dupont, P. Vingerhoets, P. Tant, K. Vanthournout, W. Cardinaels, T. De Rybel, E. Peeters, and R. Belmans, "LINEAR breakthrough project: Large-scale implementation of smart grid technologies in distribution grids," in *2012 3rd IEEE PES Innovative Smart Grid Technologies Europe (ISGT Europe)*. IEEE, Oct. 2012, pp. 1–8. [Online]. Available: http://ieeexplore.ieee.org/lpdocs/epic03/wrapper.htm?arnumber=6465708

[101] F. Bliek, A. van den Noort, B. Roossien, R. Kamphuis, J. de Wit, J. van der Velde, and M. Eijgelaar, "PowerMatching City, a living lab smart grid demonstration," in *2010 IEEE PES Innovative Smart Grid Technologies Conference Europe (ISGT Europe)*. IEEE, Oct. 2010, pp. 1–8. [Online]. Available: http://ieeexplore.ieee.org/lpdocs/epic03/wrapper.htm?arnumber=5638863

[102] S. Vandael, B. Claessens, M. Hommelberg, T. Holvoet, and G. Deconinck, "A Scalable Three-Step Approach for Demand Side Management of Plug-in Hybrid Vehicles," *IEEE Transactions on Smart Grid*, vol. 4, no. 2, pp. 720–728, Jun. 2013. [Online]. Available: http://ieeexplore.ieee.org/lpdocs/epic03/wrapper.htm?arnumber=6363501

[103] D. Pudjianto, C. Ramsay, and G. Strbac, "Virtual power plant and system integration of distributed energy resources," *IET Renewable Power Generation*, vol. 1, no. 1, p. 10, 2007. [Online]. Available: http://www.fenix-project.org/http://digital-library.theiet.org/content/journals/10.1049/iet-rpg_20060023

[104] C. Kieny, B. Berseneff, N. Hadjsaid, Y. Besanger, and J. Maire, "On the concept and the interest of virtual power plant: Some results from the European project Fenix," in *2009 IEEE Power & Energy Society General Meeting*. IEEE, Jul. 2009, pp. 1–6. [Online]. Available: http://ieeexplore.ieee.org/lpdocs/epic03/wrapper.htm?arnumber=5275526

[105] G. Mühl, L. Fiege, and P. Pietzuch, *Distributed Event-Based Systems*. Secaucus, NJ, USA: Springer-Verlag New York, Inc., 2006.

[106] L. Fiege, M. Gero, and F. C. Gärtner, "Modular Event-Based Systems," *The Knowledge Engineering Review*, vol. 17, pp. 359–388, 2006.

[107] M. Hommelberg, B. van der Velde, C. Warmer, I. Kamphuis, and J. Kok, "A novel architecture for real-time operation of multi-agent based coordination of demand and supply," in *2008 IEEE Power and Energy Society General Meeting - Conversion and Delivery of Electrical Energy in the 21st Century*. IEEE, Jul. 2008, pp. 1–5. [Online]. Available: http://ieeexplore.ieee.org/lpdocs/epic03/wrapper.htm?arnumber=4596531

[108] L. Lamport, "Time, clocks, and the ordering of events in a distributed system," *Communications of the ACM*, vol. 21, no. 7, pp. 558–565, Jul. 1978. [Online]. Available: http://portal.acm.org/citation.cfm?doid=359545.359563

[109] S. Rezaee, E. Farjah, and B. Khorramdel, "Probabilistic Analysis of Plug-In Electric Vehicles Impact on Electrical Grid Through Homes and Parking Lots," *IEEE Transactions on Sustainable Energy*, vol. 4, no. 4, pp. 1024–1033, Oct. 2013. [Online]. Available: http://ieeexplore.ieee.org/lpdocs/epic03/wrapper.htm?arnumber=6545377

[110] VREG, "Evolutie van het aantal zonnepanelen en hun vermogen," 2014. [Online]. Available: http://www.vreg.be/sites/default/files/uploads/201402_evolutie_van_het_aantal_zonnepanelen_en_hun_vermogen_.pdf

[111] N. Leemput, F. Geth, J. Van Roy, A. Delnooz, J. Büscher, and J. Driesen, "Impact of Electric Vehicle On-Board Single-Phase Charging Strategies on a Flemish Residential Grid," *IEEE Transactions on Smart Grid*.

[112] K. Clement-Nyns, "Impact of Plug-in Hybrid Electric Vehicles on the Electricity System," PhD Thesis, KU Leuven, 2010. [Online]. Available: https://lirias.kuleuven.be/bitstream/123456789/275627/1/K

[113] VREG, "RAPP-2013-06 - De kwaliteit van de dienstverlening van de elektriciteitsdistributienetbeheerders in het Vlaamse Gewest in 2012," Tech. Rep., 2013. [Online]. Available: http://www.vreg.be/sites/default/files/rapporten/rapp-2013-06_4.pdf

[114] NBN, "C33-322 - Kabels Voor Ondergrondse Aanleg, met Synthetische Isolatie en Versterkte Mantel (Type 1kV)," 1975.

[115] DIN VDE Std. 0126-1-1, "Selbstätige Schaltstelle zwischen einer netzparallelen Eigenerzeugeranlage und dem öffentlichen Niederspannungsnetz," 2006.

[116] IEA, "Evaluation of islanding detection methods for photovoltaic utility- interactive power systems," 2002. [Online]. Available: http://apache.solarch.ch/pdfinter/solar/pdf/PVPSTask509.pdf

[117] FOD Economie, "Verkeer en vervoer - Grootte van het voertuigenpark 2013," 2013. [Online]. Available: http://statbel.fgov.be/nl/modules/publications/statistiques/verkeer_vervoer/evolution_du_parc_de_vehicules_2013.jsp

[118] Elia, "Load figures of 2013," 2013. [Online]. Available: http://www.elia.be/en/grid-data/data-download

[119] A. Shakoor and M. Aunedi, "G4V D3.1: Report on the economic and environmental impacts of large-scale introduction of EV/PHEV including the analysis of alternative market and regulatory structures," Tech. Rep., 2011. [Online]. Available: http://g4v.eu/datas/reports/G4V_WP3_D3_1_economic_and_environmental_impact.pdf

[120] S. Shao, T. Zhang, M. Pipattanasomporn, and S. Rahman, "Impact of TOU rates on distribution load shapes in a smart grid with PHEV penetration," in *IEEE PES T&D 2010*. IEEE, 2010, pp. 1–6. [Online]. Available: http://ieeexplore.ieee.org/lpdocs/epic03/wrapper.htm?arnumber=5484336

[121] B. Dupont, C. D. Jonghe, L. Olmos, and R. Belmans, "Demand response with locational dynamic pricing to support the integration of renewables," *Energy Policy*, vol. 67, pp. 344–354, 2014. [Online]. Available: http://www.sciencedirect.com/science/article/pii/S0301421513013220

[122] Elia, "Nominated capacity: Belgium - Netherlands," 2014. [Online]. Available: http://www.elia.be/en/grid-data/interconnections/nominated-capacity-bel-neth

List of publications

All publications are available at `https://www.esat.kuleuven.be/electa/`

Articles in international reviewed journals

K. De Craemer, S. Vandael, B. Claessens, G. Deconinck, "An Event-Driven Dual Coordination Mechanism for Demand Side Management of PHEVs," IEEE Transactions on Smart Grid, vol.5, no.2, pp.751-760, March 2014

Book chapters

K. De Craemer, S. Vandael, B. Claessens and G. Deconinck, "Integration of Distribution Grid Constraints in an Event-driven Control Strategy for Plug-in Electric Vehicles in a Multi-aggregator Setting," in Plug-In Electric Vehicles in Smart Grid: Management and Control Strategies, Springer, *under review.*

K. De Craemer, G. Deconinck, and M. Stifter, "Protocols for Automatic Meter Reading," in IEEE Industrial Communication Technology Handbook, Second Edition, CRC Press, 2014, ch. 60.

International conference papers

B. Claessens, S. Vandael, F. Ruelens, K. De Craemer, B. Beusen, "Peak Shaving of a Heterogeneous Cluster of Residential Flexibility Carriers using Reinforcement Learning." in Innovative Smart Grid Technologies (ISGT2013), Copenhagen, 6-9 October 2013

K. De Craemer, G. Deconinck, "Integrated Demand Side Management of PHEVs using Event-Driven Dual Coordination," in Fourth International Workshop on Agent Technologies for Energy Systems (ATES2013), Minnesota, 6 May 2013

K. De Craemer, G. Deconinck, "Balancing Trade-offs in Coordinated PHEV

Charging With Continuous Market-based Control," in IEEE PES Innovative Smart Grid Technologies (ISGT2012), Berlin, 15-17 October 2012 , ISSN 2165-4816

K. De Craemer, G. Deconinck, "A multi-agent system for continuous market-based coordinated PHEV charging in a smart grid." in Third International Workshop on Agent Technologies for Energy System (ATES2012), Valencia, 4-8 June 2012

M. Strobbe, K. Mets, M. Tahon, M. Tilman, F. Spiessens, J. Gheerardyn, K. De Craemer, S. Vandael, K. Geebelen, B. Lagaisse, B. Claessens, C. Develder, "Smart and secure charging of electric vehicles in public parking spaces," in 4th International Conference on Innovation for Sustainable Production (i-SUP2012), Bruges, Belgium, 6-9 May 2012

G. Deconinck, B. Delvaux, K. De Craemer, Z. Qiu, R. Belmans, "Smart meters from the angles of consumer protection and public service obligations," in International Conference on Intelligent System Applications to Power Systems, Hersonissos (Crete), Greece, 25-28 September 2011

S. Vandael, K. De Craemer, N. Boucké, T. Holvoet, G. Deconinck, "Decentralized coordination of plug-in hybrid vehicles for imbalance reduction in a Smart Grid," in International Conference on Autonomous Agents and Multiagent Systems (AAMAS2012), pp. 803-810, Taipei, 2-6 May 2011

G. Deconinck, H. Joachain, F. Klopfert, L. Holzemer, K. De Craemer, Z. Qiu, K. Bachus, M. Hudon, "An approach towards socially acceptable energy saving policies via monetary instruments on the smart meter infrastructure," in Third International Conference on Infrastructure Systems and Services: Next Generation Infrastructure Systems for Eco-Cities (INFRA), 11-13 November 2010

K. De Craemer, G. Deconinck, "Analysis of State-of-the-art Smart Metering Communication Standards," in Young Researchers Symposium (YRS), Leuven, 29-30 March 2010

FACULTY OF ENGINEERING SCIENCE
DEPARTMENT OF ELECTRICAL ENGINEERING
ELECTA
Kasteelpark Arenberg 10
B-3001 Heverlee
klaas.decraemer@esat.kuleuven.be
https://www.esat.kuleuven.be/electa/